DE-FC26-07NT43096

Computational Modeling and Assessment Of Nanocoatings for Ultra Supercritical Boilers

Task 4 Technical Report

Fireside Corrosion Testing

March 31, 2010

Electric Power Research Institute
Project Managers—David W. Gandy, John P. Shingledecker
davgandy@epri.com, jshingledecker@epri.com

Principal Investigators
Southwest Research Institute
Foster Wheeler North America
Applied Films

CITATIONS

This document was prepared by

Foster Wheeler North America Corp.
12 Peach Tree Hill Rd.
Livingston, NJ 07039

Principal Investigator
M. Gagliano
H. Agarwal
G. Stanko

CONTENTS

1 **INTRODUCTION 1**
Fireside Corrosion 1
Waterwalls 1
Superheater/Reheaters 2
Objective 3

2 **NANOSTRUCTURED COATINGS 1**
Nanocoatings Coupon Specimens 1
Precharacterization of Nanocoating Materials 1
A1 (Figure 2.2) 4
A2 (Figure 2.3) 4
A3 (Figure 2.4) 4
A4 (Figure 2.5) 8
A5 (Figure 2.6) 8
B1 (Figure 2.7) 8
B2 (Figure 2.8) 8
B3 (Figure 2.9) 8
B4 (Figure 2.10) 14
B5 (Figure 2.11) 14
B6 (Figure 2.12) 14
B7 (Figure 2.13) 14

3 **EXPERIMENTAL AND APPROACH 1**
100 Hour Preliminary Screen Tests 1
1000 Hour Corrosion Tests 2
Synthetic Flue Gas 2
Synthetic Fuel Ash 3
Corrosion Testing 4
Post Exposure Evaluation 4

4 **RESULTS – 100 HOUR SCREENING TEST 1**
Macroscopic Evaluation 1
Waterwall Conditions 1
Superheater/Reheater Conditions 1
Microscopic Evaluation 11
Conclusions 11

5 **RESULTS – 1000 HOUR CORROSION TESTS 1**
Macroscopic Evaluation. 1
Waterwall Conditions 2
Superheater/Reheater Conditions 2

Microscopic Evaluation 2
Waterwall Conditions 2
Superheater/Reheater Conditions 2
Post Exposure Characterization 3
A1 (Figures 5-1 and 5-11) 3
A2 (Figures 5-2 and 5-12) 3
A3 (Figures 5-3 and 5-13) 4
A4 (Figures 5-4 and 5-14) 4
A5 (Figure 5-15) 5
B1 (Figures 5-5 and 5-16) 5
B2 (Figures 5-6 and 5-17) 5
B3 (Figures 5-7 and 5-18) 5
B4 (Figures 5-8 and 5-19) 6
B5 (Figures 5-9 and 5-20) 6
B6 (Figures 5-10 and 5-21) 7
B7 (Figure 5-22) 7

***6* SUMMARY AND CONCLUSIONS 1**

***7* REFERENCES 1**

***A* APPENDIX 1**
Macroscopic Appearance of the Pre and Post-Exposed Coupons 1

LIST OF FIGURES

FIGURE 2-1 Representative Photograph of the Nanocoating Samples in the As-Supplied Condition on a 304 Substrate Coupon (A4 is on a 91 Substrate). 2
FIGURE 2-2 As-received Nanocoating A1 on 91 Substrate Material (Top Left), 304 Substrate Material (Top Right), and Haynes 230 Substrate Material (Bottom). 5
FIGURE 2-3 As-received Nanocoating A2 on 91 Substrate Material (Top Left), 304 Substrate Material (Top Right), and Haynes 230 Substrate Material (Bottom). 6
FIGURE 2-4 As-received Nanocoating A3 on 91 Substrate Material (Top Left), 304 Substrate Material (Top Right), and Haynes 230 Substrate Material (Bottom). 7
FIGURE 2-5 As-received Nanocoating A4 on 91 Substrate Material (Top) and 304 Substrate Material (Bottom). 9
FIGURE 2-6 As-received Nanocoating A5 on 304 Substrate Material (Top) and Haynes 230 Substrate Material (Bottom). 10
FIGURE 2-7 As-Received Nanocoating B1 on 91 Substrate Material (Top) and 304 Substrate Material (Bottom). 11
FIGURE 2-8 As-received Nanocoating B2 on 91 Substrate Material (Top) and 304 Substrate Material (Bottom). 12
FIGURE 2-9 As-received Nanocoating B3 on 91 Substrate Material (Top) and 304 Substrate Material (Bottom). 13
FIGURE 2-10 As-received Nanocoating B4 on 91 Substrate Material (Top Left), 304 Substrate Material (Top Right), and Haynes 230 Substrate Material (Bottom). 15
FIGURE 2-11 As-received Nanocoating B5 on 91 Substrate Material (Top) and 304 Substrate Material (Bottom). 16
FIGURE 2-12 As-received Nanocoating B6 on 304 Substrate Material (Top) and Haynes 230 Substrate Material (Bottom). 17
FIGURE 2-13 As-received Nanocoating B7 on 304 Substrate Material (Top) and Haynes 230 Substrate Material (Bottom). 18
FIGURE 4-1 Representative Photograph Showing the Nanocoating and Uncoated Control Samples in the As-supplied Condition, Prior to Performing the Screening Test Under Synthetic Waterwall Conditions. Duplicate Samples Were Removed after 50 Hours. 2
FIGURE 4-2 Representative Photograph Showing the Nanocoating and Uncoated Control Samples in the As-supplied Condition, Prior to Performing the Screening Test under Synthetic Superheater/Reheater Conditions. 3
FIGURE 4-3 Screening Test Samples Following 100 Hours of Exposure to Aggressive Waterwall Conditions. Note that the Uppermost Portion of the Samples Were Not Coated with Deposits. 4
FIGURE 4-4 Stereomicrographs of Nanocoating Samples B1 (Top) and B3 (Bottom) in the Region Not Covered with Deposit after 100 Hours of Exposure to Aggressive Waterwall Conditions. Note the High Number Density of Crack and Fissures on Sample B1. 5
FIGURE 4-5 Stereomicrographs of Nanocoating Samples B4 (Top) and B5 (Bottom) in the Region Not Covered with Deposit after 100 Hours of Exposure to Aggressive Waterwall Conditions. Several Cracks and Fissures are Present in Coating Sample B4. 6
FIGURE 4-6 Screening Test Samples Following 100 Hours of Exposure to Aggressive Superheater/Reheater Conditions. As with the Waterwall Materials, the Uppermost Portion of the Samples were Not Coated with Deposits. 7
FIGURE 4-7 Stereomicrographs of Nanocoating Samples B1 (Top) and B3 (Bottom) after 100 hrs of Exposure to Aggressive SH/RH Conditions. Numerous Cracks and Fissures Created a Crazed Appearance in the Area Not Covered with Deposits on B1. 8

FIGURE 4-8 Stereomicrographs of Nanocoating Samples B4 (Top) and B5 (Bottom) after 100 hrs of Exposure to Aggressive SH/RH Conditions. B4 Contains Several, Relatively Straight Cracks and Fissures in the Region Not Covered with Deposits. 9
FIGURE 4-9 Stereomicrographs of Nanocoating Samples B6 (Top) and B7 (Bottom) after 100 hrs of Exposure to Aggressive SH/RH Conditions. Scattered Cracks are Apparent in the Region Not Covered with Deposits on Coating B6..... 10
FIGURE 4-10 Representative Backscatter SEM Images of Nanocoating B1 in the As-received Condition (Top Left); Exposed for 100hr to Aggressive Waterwall Conditions on 91 Substrate (Top Right); Exposed for 100 hrs to Aggressive Superheater Conditions on 91 Substrate (Bottom Left) and 304 Substrate (Bottom Right)..... 12
FIGURE 4-11 Representative Backscatter SEM Images of Nanocoating B3 in the As-received Condition (Top Left); Exposed for 100hr to Aggressive Waterwall Conditions on 91 Substrate (Top Right); Exposed for 100 hrs to Aggressive Superheater Conditions on 91 Substrate (Bottom Left) and 304 Substrate (Bottom Right)..... 13
FIGURE 4-12 Representative Backscatter SEM Images of Nanocoating B4 in the As-received Condition (Top Left); Exposed for 100hr to Aggressive Waterwall Conditions on 91 Substrate (Top Right); Exposed for 100 hrs to Aggressive Superheater Conditions on 91 Substrate (Bottom Left) and 304 Substrate (Bottom Right)..... 14
FIGURE 4-13 Representative Backscatter SEM Images of Nanocoating B5 in the As-received Condition (Top Left); Exposed for 100hr to Aggressive Waterwall Conditions on 91 Substrate (Top Right); Exposed for 100 hrs to Aggressive Superheater Conditions on 91 Substrate (Bottom Left) and 304 Substrate (Bottom Right)..... 15
FIGURE 4-14 Representative Backscatter SEM Images of Nanocoating B6 in the As-received Condition on 304 Substrate (Top Left) and Haynes 230 Substrate ((Top Right); Exposed for 100 hrs to Aggressive Superheater Conditions on 304 Substrate (Bottom) 16
FIGURE 4-15 Representative Backscatter SEM Images of Nanocoating B7 in the As-received Condition on 304 Substrate (Top Left) and Haynes 230 Substrate ((Top Right); Exposed for 100 hrs to Aggressive Superheater Conditions on 304 Substrate (Bottom 17
FIGURE 5-1 Representative Backscatter SEM Images of Nanocoating A1 on 91 Substrate Material in the As-received Condition (Top Left); after 1000 hrs at 850ºF (Top Right); after 1000 hrs at 975ºF (Bottom Left); after 1000 hrs at 1100ºF (Bottom Right)..... 8
FIGURE 5-2 Representative Backscatter SEM Images of Nanocoating A1 on 91 Substrate Material in the As-received Condition (Top Left); after 1000 hrs at 850ºF (Top Right); after 1000 hrs at 975ºF (Bottom Left); after 1000 hrs at 1100ºF (Bottom Right)..... 9
FIGURE 5-3 Representative Backscatter SEM Images of Nanocoating A3 on 91 Substrate Material in the As-received Condition (Top Left); after 1000 hrs at 850ºF (Top Right); after 1000 hrs at 975ºF(Bottom Left); after 1000 hrs at 1100ºF (Bottom Right)..... 10
FIGURE 5-4 Representative Backscatter SEM Images of Nanocoating A4 on 304 Substrate Material in the As-received Condition (Top Left); after 600 hrs at 850ºF (Top Right); after 600 hrs at 975ºF (Bottom Left); after 600 hrs at 1100ºF (Bottom Right)..... 11
FIGURE 5-5 Representative Backscatter SEM Images of Nanocoating B1 on 91 Substrate Material in the As-received Condition (Top Left); after 600 hrs at 850ºF (Top Right); after 600 hrs at 975ºF (Bottom Left); after 1000 hrs at 1100ºF (Bottom Right)..... 12
FIGURE 5-6 Representative Backscatter SEM Images of Nanocoating B2 on 91 Substrate Material in the As-received Condition (Top Left); after 1000 hrs at 850ºF (Top Right); after 1000 hrs at 975ºF (Bottom Left); after 1000 hrs at 1100ºF (Bottom Right)..... 13
FIGURE 5-7 Representative Backscatter SEM Images of Nanocoating B3 on 91 Substrate Material in the As-received Condition (Top Left); after 1000 hrs at 850ºF (Top Right); after 1000 hrs at 975ºF (Bottom Left); after 1000 hrs at 1100ºF (Bottom Right)..... 14

FIGURE 5-8 Representative Backscatter SEM Images of Nanocoating B4 on 91 Substrate Material in the As-received Condition (Top Left); after 600 hrs at 850ºF (Top Right); after 600 hrs at 975ºF (Bottom Left); after 1000 hrs at 1100ºF (Bottom Right) 15
FIGURE 5-9 Representative Backscatter SEM Images of Nanocoating B5 on 91 Substrate Material in the As-received Condition (Top Left); after 600 hrs at 850ºF (Top Right); after 1000 hrs at 975ºF (Bottom Left); after 1000 hrs at 1100ºF (Bottom Right) 16
FIGURE 5-10 Representative Backscatter SEM Images of Nanocoating B6 on Haynes 230 Substrate Material in the As-received Condition (Top Left); after 600 hrs at 850ºF (Top Right); after 1000 hrs at 975ºF (Bottom Left); after 1000 hrs at 1100ºF (Bottom Right) 17
FIGURE 5-11 Representative Backscatter SEM Images of Nanocoating A1 on 304 Substrate Material in the As-received Condition (Top Left); after 600 hrs of Exposure to SH/RH Conditions at 1100ºF (Top Right); after 600 hrs of Exposure to SH/RH Conditions at 1300ºF (Bottom Left); after 600 hrs of Exposure to SH/RH Conditions at 1500ºF (Bottom Right) 18
FIGURE 5-12 Representative Backscatter SEM Images of Nanocoating A2 on 304 Substrate Material in the As-received Condition (Top Left); after 600 hrs of Exposure to SH/RH Conditions at 1100ºF (Top Right); after 600 hrs of Exposure to SH/RH Conditions at 1300ºF (Bottom Left); after 600 hrs of Exposure to SH/RH Conditions at 1500ºF (Bottom Right) 19
FIGURE 5-13 Representative Backscatter SEM Images of Nanocoating A3 on 304 Substrate Material in the As-received Condition (Top Left); after 1000 hrs of Exposure to SH/RH Conditions at 1100ºF (Top Right); after 600 hrs of Exposure to SH/RH Conditions at 1300ºF (Bottom Left); after 600 hrs of Exposure to SH/RH Conditions at 1500ºF (Bottom Right) 20
FIGURE 5-14 Representative Backscatter SEM Images of Nanocoating A4 on 91 Substrate Material in the As-received Condition (Top Left); after 600 hrs of Exposure to SH/RH Conditions at 1100ºF (Top Right); after 600 hrs of Exposure to SH/RH Conditions at 1300ºF (Bottom Left); after 600 hrs of Exposure to SH/RH Conditions at 1500ºF (Bottom Right) 21
FIGURE 5-15 Representative Backscatter SEM Images of Nanocoating A5 on 304 Substrate Material in the As-received Condition (Top Left); after 600 hrs of Exposure to SH/RH Conditions at 1100ºF (Top Right); after 600 hrs of Exposure to SH/RH Conditions at 1300ºF (Bottom Left); after 600 hrs of Exposure to SH/RH Conditions at 1500ºF (Bottom Right) 22
FIGURE 5-16 Representative Backscatter SEM Images of Nanocoating B1 on 304 Substrate Material in the As-received Condition (Top Left); after 600 hrs of Exposure to SH/RH Conditions at 1100ºF (Top Right); after 600 hrs of Exposure to SH/RH Conditions at 1300ºF (Bottom Left); after 600 hrs of Exposure to SH/RH Conditions at 1500ºF (Bottom Right) 23
FIGURE 5-17 Representative Backscatter SEM Images of Nanocoating B2 on 304 Substrate Material in the As-received Condition (Top Left); after 600 hrs of Exposure to SH/RH Conditions at 1100ºF (Top Right); after 600 hrs of Exposure to SH/RH Conditions at 1300ºF (Bottom Left); after 600 hrs of Exposure to SH/RH Conditions at 1500ºF (Bottom Right) 24
FIGURE 5-18 Representative Backscatter SEM Images of Nanocoating B3 on 304 Substrate Material in the As-received Condition (Top Left); after 600 hrs of Exposure to SH/RH Conditions at 1100ºF (Top Right); after 600 hrs of Exposure to SH/RH Conditions at 1300ºF (Bottom Left); after 600 hrs of Exposure to SH/RH Conditions at 1500ºF (Bottom Right) 25
FIGURE 5-19 Representative Backscatter SEM Images of Nanocoating B4 on 304 Substrate Material in the As-received Condition (Top Left); after 600 hrs of Exposure to SH/RH Conditions at 1100ºF (Top Right); after 600 hrs of Exposure to SH/RH Conditions at 1300ºF (Bottom Left); after 600 hrs of Exposure to SH/RH Conditions at 1500ºF (Bottom Right) 26
FIGURE 5-20 Representative Backscatter SEM Images of Nanocoating B5 on 304 Substrate Material in the As-received Condition (Top Left); after 600 hrs of Exposure to SH/RH Conditions at 1100ºF (Top Right); after 600 hrs of Exposure to SH/RH Conditions at 1300ºF (Bottom Left); after 600 hrs of Exposure to SH/RH Conditions at 1500ºF (Bottom Right) 27
FIGURE 5-21 Representative Backscatter SEM Images of Nanocoating B6 on 304 Substrate Material in the As-received Condition (Top Left); after 600 hrs of Exposure to SH/RH Conditions

at 1100ºF (Top Right); after 600 hrs of Exposure to SH/RH Conditions at 1300ºF (Bottom Left); after 600 hrs of Exposure to SH/RH Conditions at 1500ºF (Bottom Right) 28
FIGURE 5-22 Representative Backscatter SEM Images of Nanocoating B7 on 304 Substrate Material in the As-received Condition (Top Left); after 600 hrs of Exposure to SH/RH Conditions at 1100ºF (Top Right); after 600 hrs of Exposure to SH/RH Conditions at 1300ºF (Bottom Left); after 600 hrs of Exposure to SH/RH Conditions at 1500ºF (Bottom Right) 29
FIGURE A-1 Nanocoating Samples Prior to Testing at 455ºC (850ºF) for Waterwall Conditions. The Coupons are Labeled with the Substrate Material Followed by the Coating Designation. 2
FIGURE A-2 Nanocoating Samples after Testing at 455ºC (850ºF) Under Waterwall Conditions. The Exposure Times are Indicated at the Top of Each Coupon. 3
FIGURE A-3 Nanocoating Samples Prior to Testing at 525ºC (975ºF) for Waterwall Conditions. The Coupons are Labeled with the Substrate Material Followed by the Coating Designation. 4
FIGURE A-4 Nanocoating Samples after Testing at 525ºC (975ºF) Under Waterwall Conditions. The Exposure Times are Indicated at the Top of Each Coupon 5
FIGURE A-5 Nanocoating Samples Prior to Testing at 595ºC (1100ºF) for Waterwall Conditions. The Coupons are Labeled with the Substrate Material Followed by the Coating Designation. 6
FIGURE A-6 Nanocoating Samples after Testing at 595ºC (1100ºF) Under Waterwall Conditions. The Exposure Times are Indicated at the Top of Each Coupon 7
FIGURE A-7 Nanocoating Samples Prior to Testing at 595ºC (1100ºF) for Superheater/Reheater Conditions (Board 1). The Coupons are Labeled with the Substrate Material Followed by the Coating Designation. 8
FIGURE A-8 Nanocoating Samples after Testing at 595ºC (1100ºF) for Superheater/Reheater Conditions (Board 1). The Exposure Times are Indicated at the Top of Each Coupon. 10
FIGURE A-9 Nanocoating Samples Prior to Testing at 595ºC (1100ºF) for Superheater/Reheater Conditions (Board 2). The Coupons are Labeled with the Substrate Material Followed by the Coating Designation 11
FIGURE A-10 Nanocoating Samples after Testing at 595ºC (1100ºF) for Superheater/Reheater Conditions (Board 2). The Exposure Times are Indicated at the Top of Each Coupon 12
FIGURE A-11 Nanocoating Samples Prior to Testing at 705ºC (1300ºF) for Superheater/Reheater Conditions (Board 1). The Coupons are Labeled with the Substrate Material Followed by the Coating Designation 13
FIGURE A-12 Nanocoating Samples after Testing at 705ºC (1300ºF) for Superheater/Reheater Conditions (Board 1). The Exposure Times are Indicated at the Top of Each Coupon 15
FI GURE A-13 Nanocoating Samples Prior to Testing at 705ºC (1300ºF) for Superheater/Reheater Conditions (Board 2). The Coupons are Labeled with the Substrate Material Followed by the Coating Designation 16
FIGURE A-14 Nanocoating Samples after Testing at 705ºC (1300ºF) for Superheater/Reheater Conditions (Board 2). The Exposure Times are Indicated at the Top of Each Coupon 18
FIGURE A-15 Nanocoating Samples Prior to Testing at 815ºC (1500ºF) for Superheater/Reheater Conditions (Board 1). The Coupons are Labeled with the Substrate Material Followed by the Coating Designation 19
FIGURE A-16 Nanocoating Samples after Testing at 815ºC (1500ºF) for Superheater/Reheater Conditions (Board 1). The Exposure Times are Indicated at the Top of Each Coupon 21
FIGURE A-17 Nanocoating Samples Prior to Testing at 815ºC (1500ºF) for Superheater/Reheater Conditions (Board 2). The Coupons are Labeled with the Substrate Material Followed by the Coating Designation 22
FIGURE A-18 Nanocoating Samples after Testing at 815ºC (1500ºF) for Superheater/Reheater Conditions (Board 2). The Exposure Times are Indicated at the Top of Each Coupon 24

LIST OF TABLES

TABLE 2-1 Nominal Composition and Semi-quantitative EDS Analysis of the As-received Nanocoating Materials 3
TABLE 3-1 Composition of the Synthetic Flue Gas Used in the Screening Tests 2
TABLE 3-2 Composition of the Synthetic Ash Deposits Used in the Screening Tests 2
TABLE 3-3 Synthetic Flue Gas Composition for the 1000 hr Corrosion Tests 3
TABLE 3-4 Composition of the Synthetic Ash Deposits Used in 1000 hour Corrosion Tests 4

1
INTRODUCTION

Coal-fired power plants are a significant part of the nation's power generating capacity, currently accounting for more than 55% of the country's total electricity production. Extending the reliable lifetimes of fossil fired boiler components and reducing the maintenance costs are essential for economic operation of power plants. Corrosion and erosion are leading causes of superheater and reheater boiler tube failures leading to unscheduled costly outages. Several types of coatings and weld overlays have been used to extend the service life of boiler tubes; however, the protection afforded by such materials was limited approximately one to eight years.

Power companies are more recently focused in achieving greater plant efficiency by increasing steam temperature and pressure into the advanced-ultrasupercritical (A-USC) condition with steam temperatures approaching 760°C (1400°F) and operating pressures in excess of 35MPa (5075 psig). Unfortunately, laboratory and field testing suggests that the resultant fireside environment when operating under A-USC conditions can potentially cause significant corrosion to conventional and advanced boiler materials[1-2]. In order to improve reliability and availability of fossil fired A-USC boilers, it is essential to develop advanced nanostructured coatings that provide excellent corrosion and erosion resistance without adversely affecting the other properties such as toughness and thermal fatigue strength of the component material.

Fireside Corrosion

Waterwalls

Fireside corrosion of boiler waterwalls continues to be the number one issue resulting in forced outages and boiler unavailability for conventional coal-fired fossil power plants, and the rate of corrosion has been a concern for many years. The introduction of nitrogen oxide emission controls (low NO_x) with the staged burners systems has increased reported waterwall wastage rates to as much as 3 mm (0.120") per year[3]. While the advent of low NO_x burners has also increased corrosion in subcritical boiler, the extent of wall loss is not nearly as severe as in supercritical units due to the lower wall temperatures[3]. Low NO_x burner systems create localized environments consisting of reducing (lower furnace), oxidizing/reducing (near over-fire airports) and oxidizing (above the airports) conditions, which, in combination with iron sulfide (FeS) and alkali-chloride deposits generated from incomplete coal combustion, have been identified as the primary cause of wastage.

Laboratory tests[4] indicate that most severe corrosion typically occurred under oxidizing conditions (free oxygen in the flue gas) due to the reactivity of FeS (deposits) with oxygen to form iron oxide (Fe_3O_4) and elemental sulfur (S) in the ash layer. This reaction produces an enhanced sulfur potential locally near the metal surface, thereby promoting sulfidation[5-6]. Since FeS deposits only form under reducing conditions and severe corrosion occurs under oxidizing conditions, accelerated wastage requires an alternating reducing and oxidizing environment

(such as locations where the substoichiometric flue gas in the lower furnace mixes with over-fired air from the airports). The requirement of oxidizing conditions for excessive corrosion to occur suggests that FeS deposits should be relatively inert under reducing conditions where excess concentrations (>7%) of carbon monoxide (CO) exist. However, even in the absence of free oxygen, high corrosion rates have been encountered in some areas of the furnace where CO concentrations of the flue gas are low (<3%) and the CO_2/CO ratio is high[5]. This seemingly contradictory behavior is believed to be due to CO_2 and H_2O in the flue gas acting as oxidants[6]. Subsequent studies have also shown that small amounts of alkali-chlorides in the deposits exacerbate corrosion caused by FeS. The increase in corrosion is attributed to the cyclic formation and decomposition $FeCl_2$ under FeS/Fe_3O_4 deposits[7]. Decomposition of $FeCl_2$ produces gaseous chloride species which further react with the iron in the tube material.

With regard to FeS deposition, the amount of FeS in the deposits will be dependent on the level of sulfur in the coal, the form of the sulfur, and the amount of iron oxide (as Fe_2O_3) in the ash[6]. In general, forms of sulfur in the coal include organic, sulfatic, and pyritic, which can be either included or excluded. Of the two, excluded pyrite is more problematic from a corrosivity standpoint as it is more likely to stick to tube surfaces and oxidize, thereby releasing sulfur into the ash deposits. An EPRI study[6] indicates that corrosion of low alloy steel significantly increases with FeS concentrations (for a fixed chloride level) in the deposits up to about 20%, under both oxidizing and mildly reducing conditions, with only modest increases expected for higher FeS concentrations. This study also substantiates the assertion that corrosivity under FeS deposits is greatly decreased under highly reducing conditions (>7% CO) compared to mildly reducing (2% CO) and oxidizing conditions. Insofar as the Fe_2O_3 in the ash, it has been theorized that the amount present is a strong indication of the pyrite concentration in the coal and the amount of FeS that can be expected to deposit under reducing conditions.

Current code-approved waterwall materials do not possess the requisite corrosion resistance for long-term, reliable service in unit experiencing corrosion problems. As a result, mitigation typically involves the use of protective highly-alloyed coatings, such as gas metal arc weld (GMAW) overlays, laser welded overlays, thermal spray coatings, and, to a much lesser extent, diffusion coatings[4]. However, laboratory and field testing of such materials suggest that reliable performance may be questionable under A-USC boiler conditions. Thus, new and advanced coatings and/or claddings are desperately required by the power generating industry to significantly reduce or eliminate waterwall damage.

Superheater/Reheaters

In coal-fired boilers, especially those burning high sulfur, high alkali coals, severe fireside wastage of superheater and reheater tube surfaces is generally attributed to coal ash corrosion resulting from the formation of molten alkali iron trisulfates[8-13]. Within the heat recovery areas, as alkali sulfate deposits build up on tube surfaces, the outermost material becomes sticky and captures fly ash particles. Breakdown and subsequent catalysis of sulfur compounds in the fly ash produces SO_3, which reacts with iron oxide and alkali sulfates in the deposits to form relatively low melting temperature alkali-iron trisulfates at the metal interface. Once formed, these molten alkali iron trisulfates flux the protective oxides from the metal surface, thereby leading to accelerated oxidation and sulfidation of the underlying metal. Corrosive losses resulting from coal ash corrosion generally increase very rapidly as temperatures exceed about 595ºC (1100ºF) then show a precipitous drop-off with increasing temperatures above about

735ºC (1350ºF). Thus, as operating steam temperatures and corresponding metal temperatures are continually increased, severe metal loss resulting from coal ash corrosion is expected to remain a critical concern that must be resolved before A-USC plants can be successfully deployed.

The installation of low-NOx burners has, in some cases, resulted in conditions within the superheater and reheater sections that have exacerbated the coal ash corrosion problem. Incomplete coal combustion (promoted by low NO_x burners) has generated carbon-containing ashes that deposit on tube surfaces[10]. The presence of these carbonaceous deposits promotes carburization of the outer tube surfaces such that the carbon reacts with the chromium in the alloy to form chromium carbides, which locally reduces the chromium concentration in the surrounding matrix, thus making the tube more susceptible to other operative corrosion mechanisms such as coal-ash corrosion and sulfidation. In a somewhat related matter, Powder River Basin (PRB) fuels that were previously thought to be non-corrosive have been found to cause very high wastage rates under certain less oxidizing operating conditions as well. There have been a number of literature reviews and recent updates discussing the variables affecting the corrosion mechanism. Approaches to solving the coal-ash corrosion problem have included changing fuel chemistry by blending various types of coal, providing protective baffling with sheaths of corrosion resistant material around tubing in susceptible areas, and utilizing higher-alloy, more corrosion-resistant materials, either in wrought form or coatings.

Objective

The goal of this investigation was to qualitatively evaluate the fireside corrosion resistance of various nanostructure material coatings exposed to synthetic waterwall and superheater/reheater conditions.

2
NANOSTRUCTURED COATINGS

Nanostructured materials are characterized by the fine size scale (<100 nm) of constituent grains, phases and/or precipitates that they are comprised of[14]. As a result, nanostructured materials may exhibit considerably different mechanical, thermal, electrical, magnetic, and chemical properties than conventional materials with the same general composition. Of particular importance for the boiler industry is the selective oxidation/corrosion properties that certain nanostructures may possess, which may enable the formation of highly protective scales with superior adhesion to the substrate materials for prolonged service life[14].

Nanocoatings Coupon Specimens

Science-based computational methods as well as lab and field corrosion test data were utilized for selecting the chemical compositions of nanostructured coatings that were tested in the simulated boiler environments for this corrosion test program. Once selected, the proposed coatings were applied to three distinctly different substrate materials that would be suitable for A-USC boiler conditions. The substrate materials included grade 91, a creep strength enhanced ferritic that may be used in the furnace area of an A-USC boiler, or within the heat recovery area of a subcritical boiler; 304H, a conventional austenitic that is commonly used in the heat recovery areas of subcritical and supercritical boilers; and Haynes 230, a high-strength nickel-based alloy that is currently proposed for potential A-USC boiler applications.

Southwest Research Institute (SwRI) procured wrought substrate 91, 304 and Haynes 230 materials. The rectangular coupon specimens were machined from the substrate rod or plates to the appropriate dimensions of approximately 25.4 mm x 19.1 mm x 3.2 mm (1" x ¾" x ⅛"). The samples were ground and polished using standard metallographic techniques at SwRI prior to application of the coatings. The coatings designated A1 through A3 were applied by two commercial vendors (a.k.a. 'commercial' nanocoatings). Coatings A4, A5, and B1 through B7 were applied by SwRI. After the coatings were applied, the test coupons were then sent to Foster Wheeler's R&D center in Livingston, NJ for testing and characterization.

Precharacterization of Nanocoating Materials

Figure 2-1 displays the representative condition of the nanocoating materials on a 304 substrate (except A4 which is on a 91 substrate) as they were received from the SwRI or the commercial vendors. Upon receiving the coated test coupon specimens, sacrificial samples were removed from each coating/substrate combination and prepared for microscopic analysis. The purpose of the evaluation was to pre-characterize the as-supplied coating compositions, thickness, and uniformity, and to identify potential flaws in the coatings that could lead to poor performance. Table 2-1 presents the nominal compositions (where available) and as-measured compositions by standardless semi-quantitative EDS analysis of the as applied coatings. For samples that were supplied on multiple substrate materials; the values presented in Table 2-1 represent the average composition for a given coating.

FIGURE 2-1
Representative Photograph of the Nanocoating Samples in the As-Supplied Condition on a 304 Substrate Coupon (A4 is on a 91 Substrate).

TABLE 2-1
Nominal Composition and Semi-quantitative EDS Analysis of the As-received Nanocoating Materials

Coating Designation	Nominal Composition	Layer	O	Mg	Al	Si	P	Ca	Ti	Cr	Mn	Fe	Co	Ni	Cu	Nb	Mo	W
A1	NA	Outer	42.0	3.8	1.9	0.7	13.0	0.3	18.2	13.9	-	0.3	-	-	5.9	-	-	-
		Inner	14.0	2.5	71.8	0.5	8.6	-	-	2.7	-	-	-	-	-	-	-	-
A2	NA	Bulk	13.1	2.1	75.2	-	7.0	-	-	2.0	-	0.5	-	-	-	-	-	-
A3	NA	Outer	44.7	-	43.7	-	10.1	0.2	-	0.3	-	0.7	-	-	-	-	-	-
		Inner	2.8	-	0.7	-	-	-	-	18.5	-	55.3	-	-	-	-	15.8	6.8
A4	Fe-18Cr-8Ni-10Al	Bulk	0.0	-	11.9	-	-	-	-	17.0	1.0	63.4	-	6.3	-	-	-	-
A5	Ni-20Cr-10Al	Bulk	-	-	8.9	0.2	-	-	-	19.3	-	0.4	-	71.3	-	-	-	-
B1	Fe-25Cr-20Ni-10Al	Bulk	-	-	12.8	0.7	-	-	-	23.9	0.7	47.6	-	14.4	-	-	-	-
B2	Fe-25Cr-37Ni-10Al	Bulk	-	-	11.2	0.5	-	-	-	23.6	0.3	32.9	-	31.0	-	0.6	-	-
B3	Fe-25Cr-37Ni	Bulk	-	-	0.2	0.6	-	-	-	26.4	0.2	37.0	-	34.9	-	0.8	-	-
B4	Ni-30Co-28Cr-3Si-10Al	Bulk	-	-	12.6	3.2	-	-	0.4	26.2	-	0.6	27.1	29.6	-	-	0.3	-
B5	Ni-30Co-28Cr-3Si	Bulk	-	-	0.3	3.3	-	-	0.5	29.4	0.2	0.8	30.4	34.9	-	-	0.4	-
B6	Co-23Ni-22-Cr-14W-10Al	Bulk	-	-	11.1	-	-	-	0.2	22.1	0.3	1.7	31.9	16.3	-	-	0.7	15.9
B7	C0-23Ni-22Cr-14W	Bulk	-	-	0.3	-	-	-	0.2	24.5	-	1.8	36.5	19.1	-	-	0.7	17.0

Figures 2-2 – 2-13 are representative SEM backscatter images showing each of the coating on a given substrate in the as-received condition. Preliminary evaluation was primarily performed in the SEM at relatively high magnifications due to the thinness of the coatings and correspondingly fine scale of the coating features. In general, most of the coatings (with the exception of A1, A2 and A3) were very dense (little to no observable porosity) and very uniform in thickness, but contained a high concentration of columnar grain boundaries and scattered through-thickness defects. Due to the thinness of the coatings, typically on the order of 25 μm (1.0 mil), the columnar grain boundaries and scattered through-thickness defects are potentially problematic as such defects could act as short-circuit diffusion paths for corrosive (oxide/sulfide/chloride) species. What follows is a brief description of the defining characteristics for each as-supplied coating.

A1 (Figure 2.2)

The nanocoating is comprised of two distinct layers that measure roughly 35 - 70 μm (1.4 - 2.8 mils) in total thickness. Each layer of the coating appears to be fairly uniform for a given sample, but the thicknesses of each (and subsequently the overall thickness) varied considerably from sample to sample. The outer (top) layer consists of high concentrations of oxygen, chromium, titanium and phosphorus with lesser concentrations of other alloying elements, including copper, magnesium and aluminum; while the inner layer has a mottled appearance consisting of globular aluminum-rich particles in a matrix of aluminum, oxygen, phosphorus, chromium and magnesium. Some scattered porosity and relatively tight cracks are present in the outer layer, but no such defects generally are apparent in the inner layer. Specifically, large pores were noted in the outer layer of the coating on the Haynes 230 substrate. Although this coating is considered a commercial nanocoating, a clear substructure on the micron level is observed in the optical micrographs suggesting the "nanocoating" is not fully nanostructured.

A2 (Figure 2.3)

Coating A2 is comprised of one layer that is very similar in appearance and composition to the inner layer of coating A1. The coating is fairly uniform and measures approximately 42 – 55 μm (1.7 – 2.2 mils) thick.

A3 (Figure 2.4)

Coating A3 consists of two distinct layers with a combined approximate thickness of 230 - 320 μm (9.1 – 12.6 mils). The outer layer is relatively thin, measuring approximately 10 – 30 μm (0.4 – 1.3 mils) and is comprised almost entirely of aluminum, oxygen and phosphorus. While the coating thickness varied considerably, the non-uniformity appears to be due to the undulating surface profile of the inner layer. Scattered porosity is also evident in some places. The inner layer measures between 215 – 290 μm (8.5 – 11.4 mils) thick and has the appearance of a thermal spray coating consisting of flattened splats of metal and oxide, with scattered pores noted throughout. A few cracks and fissures are also apparent in the inner layer, and generally emanate from the thermal spray surface. Similar to A1 and A2, the size of the coating substructure can be observed at the micron level in the backscattered SEM images suggesting the "nanocoating" is not fully nanostructured

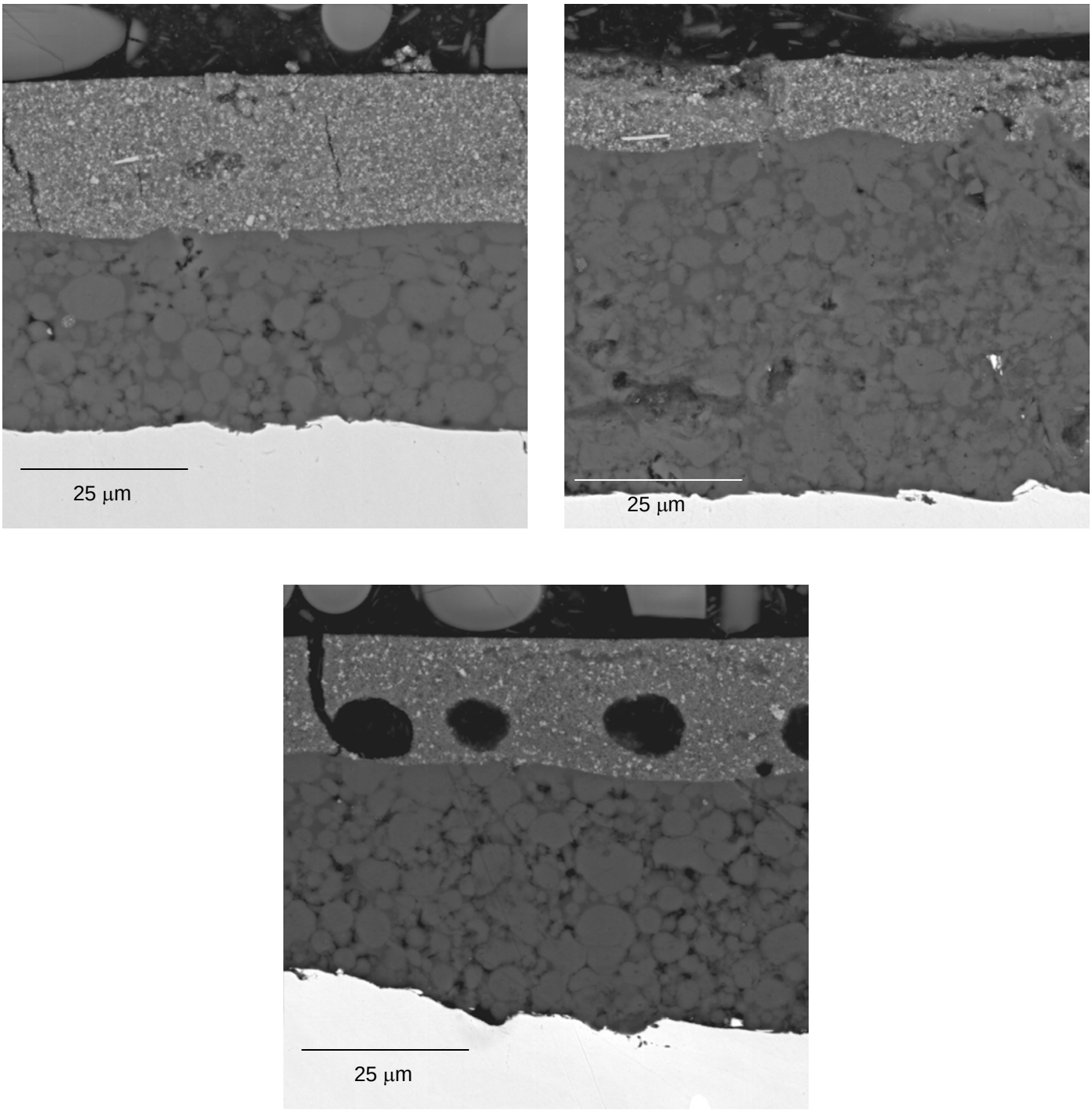

FIGURE 2-2
As-received Nanocoating A1 on 91 Substrate Material (Top Left), 304 Substrate Material (Top Right), and Haynes 230 Substrate Material (Bottom).

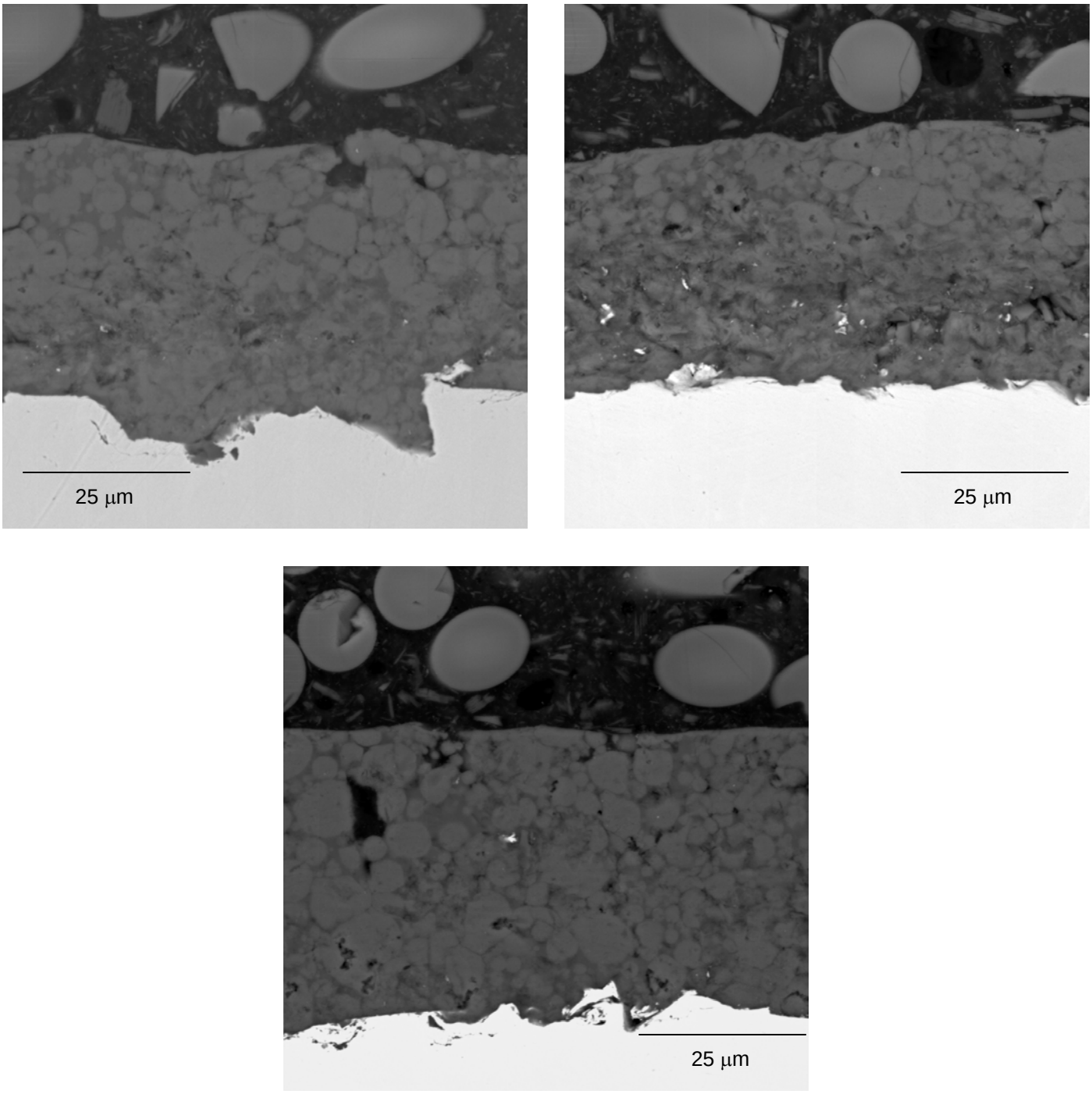

FIGURE 2-3
As-received Nanocoating A2 on 91 Substrate Material (Top Left), 304 Substrate Material (Top Right), and Haynes 230 Substrate Material (Bottom).

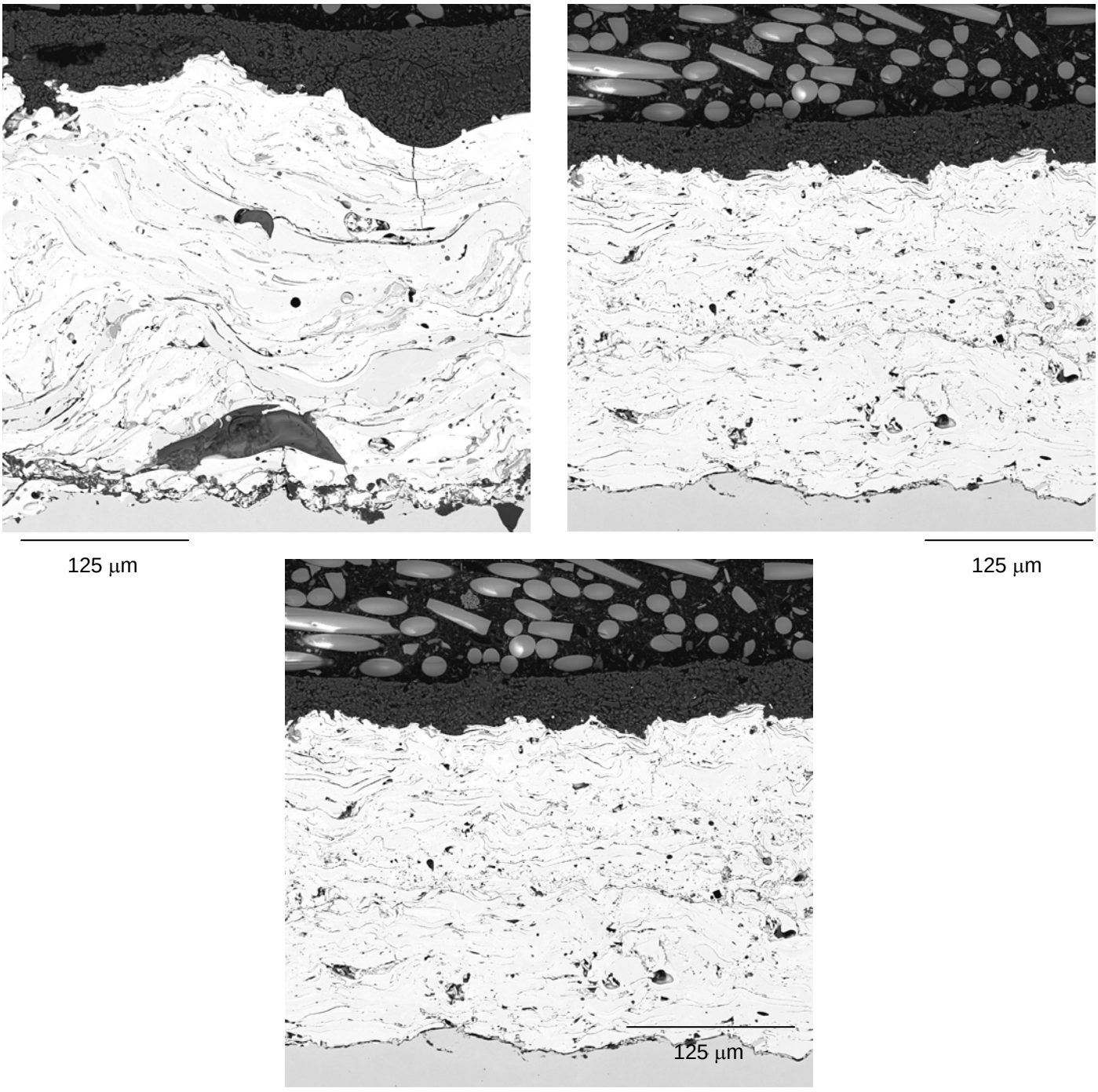

FIGURE 2-4
As-received Nanocoating A3 on 91 Substrate Material (Top Left), 304 Substrate Material (Top Right), and Haynes 230 Substrate Material (Bottom).

A4 (Figure 2.5)

Coatings A4 is very uniform in thickness and generally measures 25 - 33 μm (1.0 -1.3 mils) in thickness. Numerous columnar-like grain boundaries are apparent throughout the coating thickness; the boundaries produce a periodic scalloped morphology at the coating surface. Several globular, wedge-shaped defects (not shown in photomicrographs) are also apparent and generally span the entire coating thickness. There is also a very pronounced interface between the coating and substrate materials.

A5 (Figure 2.6)

Coating A5 has a very consistent thickness which generally varies from 31 - 33 μm (1.2 -1.3 mils) thick. As noted in A4, the interface between the coating and substrate materials is very pronounced. Numerous, straight, uniform columnar grain boundaries are evident through the coating thickness. The periodic nature of these grain boundaries also produced a scalloped surface morphology. Several cracks that follow along the grain boundaries and scattered globular defects (top-right photomicrograph) are also apparent throughout the coating.

B1 (Figure 2.7)

B1 is very similar in appearance to coating A4 and A5. The coating has a very uniform thickness measuring approximately 27 - 29 μm (1.1 mils) thick, but a comparatively more undulating surface morphology than the other coatings. The coating/substrate interface is very distinct with many columnar grains emanating from the interface; however, the arrangement of these grains is not consistent, thus producing a non-periodic surface morphology.

B2 (Figure 2.8)

Coating B2 is approximately 29 - 31 μm (1.1 -1.2 mils) thick. A periodic arrangement of columnar grain boundaries that traverse the entire coating thickness produces a microscopically undulating surface morphology. In several locations, wider, more pronounced cracks and/or fissures are also present and follow along these grain boundaries. The interface between the coating and substrate is very distinct.

B3 (Figure 2.9)

The B3 nanocoating has a very uniform thickness of about 20 μm (0.8 mils). The interface between the coating and substrate is not well defined by a clear demarcation like many of the other nanocoatings, but rather only subtly observable through Z-contrast (backscattered electron imaging mode). Many columnar grain boundaries were apparent through the coating thickness and terminated at the surface producing a scalloped surface morphology.

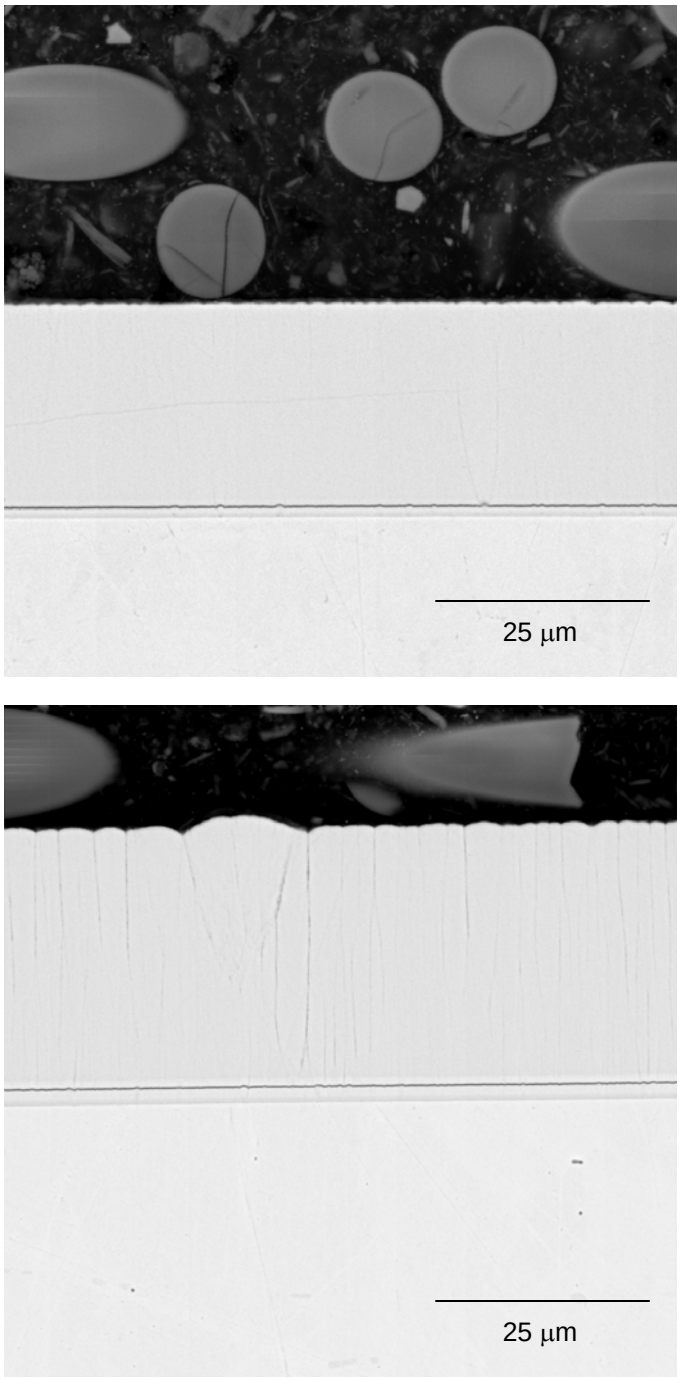

FIGURE 2-5
As-received Nanocoating A4 on 91 Substrate Material (Top) and 304 Substrate Material (Bottom).

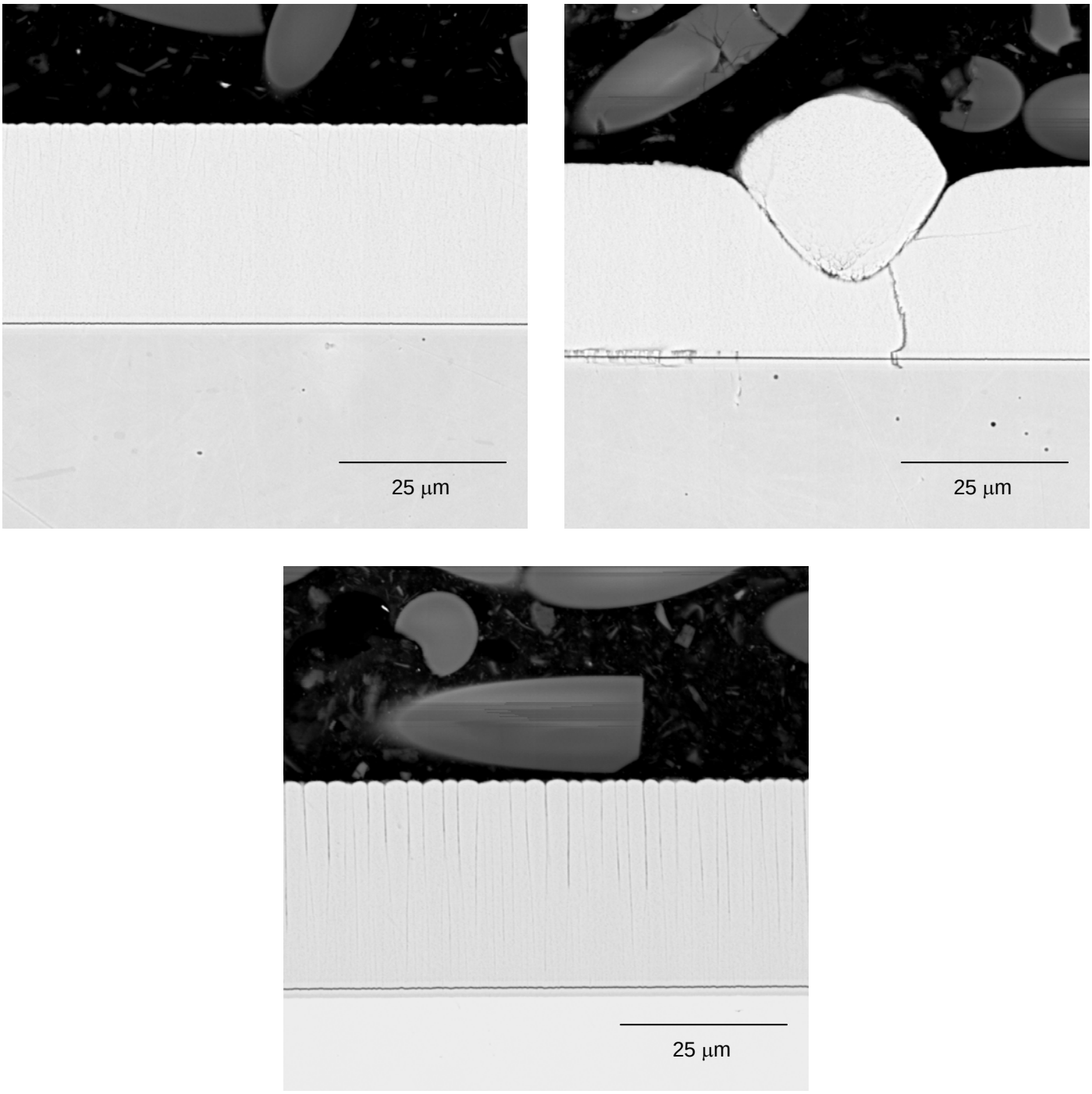

FIGURE 2-6
As-received Nanocoating A5 on 304 Substrate Material (Top) and Haynes 230 Substrate Material (Bottom).

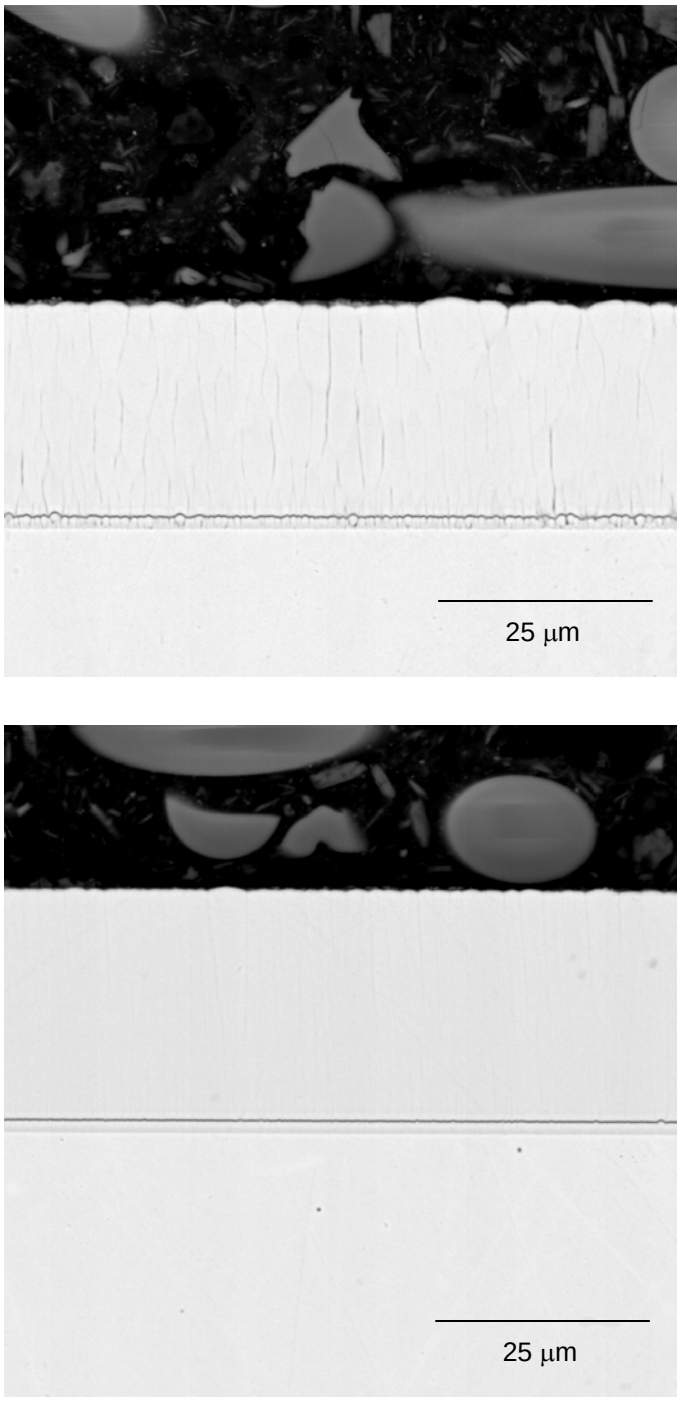

FIGURE 2-7
As-Received Nanocoating B1 on 91 Substrate Material (Top) and 304 Substrate Material (Bottom).

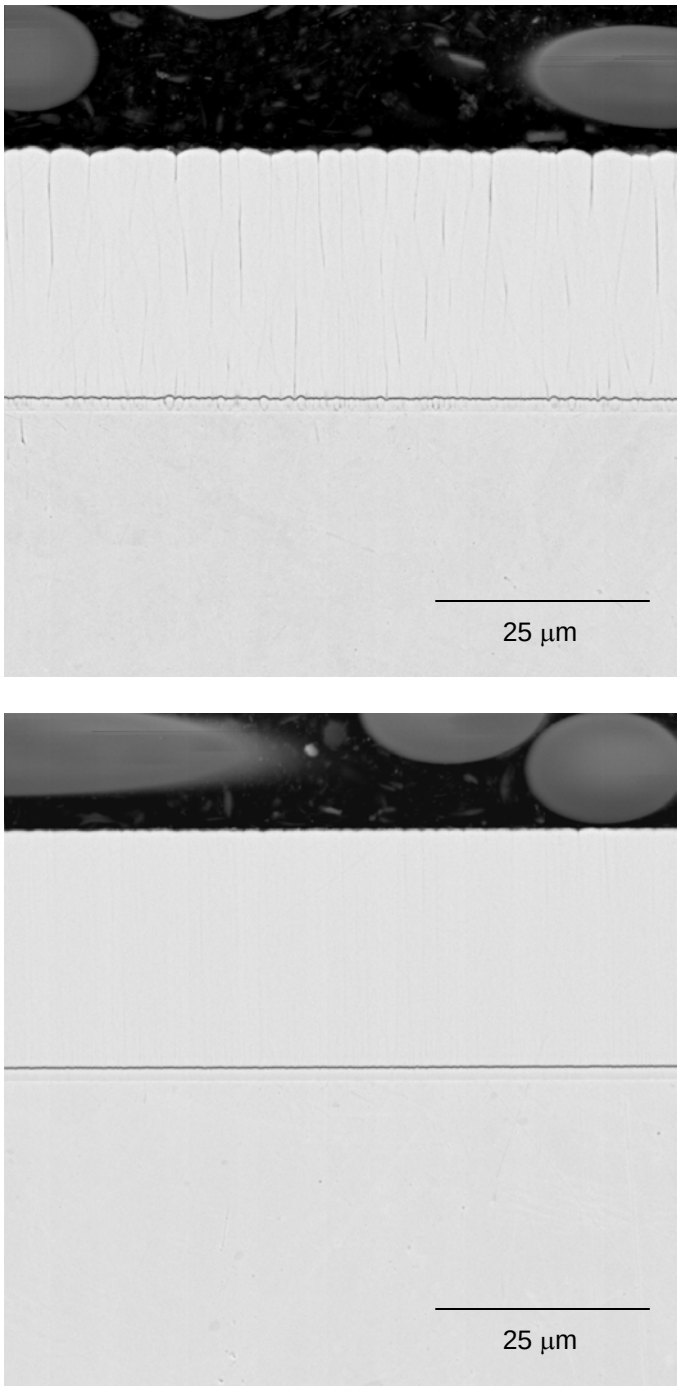

FIGURE 2-8
As-received Nanocoating B2 on 91 Substrate Material (Top) and 304 Substrate Material (Bottom).

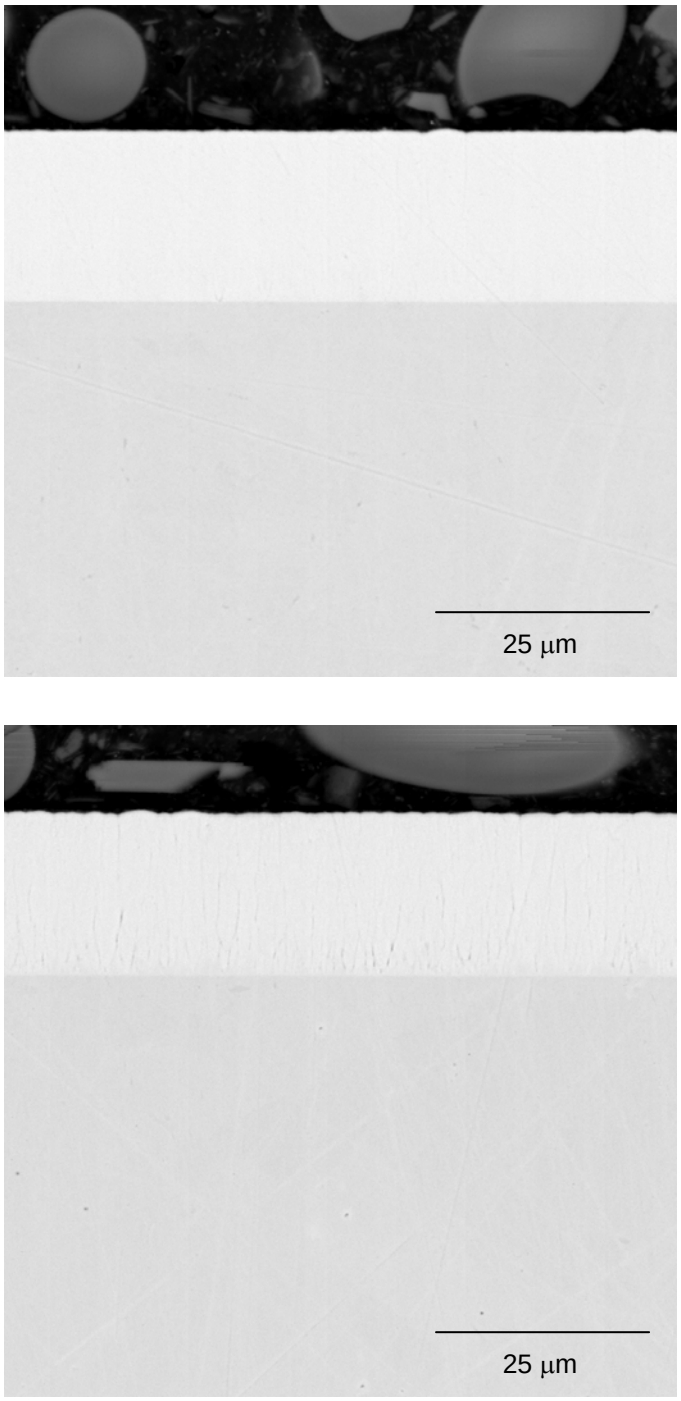

FIGURE 2-9
As-received Nanocoating B3 on 91 Substrate Material (Top) and 304 Substrate Material (Bottom).

B4 (Figure 2.10)

Nanocoating B4 is very uniform in thickness and generally measures approximately 30 - 32 μm (1.2 -1.3 mils) thick and the interface between coating and the substrate material is very well defined. Numerous columnar grain boundaries are evident throughout the coating thickness and produce a microscopically undulating surface profile. No cracks, fissures, or globular defects were noted on the sections examined.

B5 (Figure 2.11)

Nanocoating B5 has a very uniform thickness, but only measures about 18 μm (0.7 mils) thick. Like nanocoating B3, no clearly defined interface is apparent between the coating and substrate material; however the interface is observable through Z-contrast. Several globular defects and/or flaws appear to be embedded in the coating at scattered intervals. Many columnar grain boundaries are present in all locations.

B6 (Figure 2.12)

Nanocoating B6 has a very uniform thickness that generally ranges from 30 – 35 μm (1.2 -1.4 mils), but does not vary in thickness by more than 1 μm (<0.04 mil) for a given sample. While the interface between the coating and substrate is very prominent, no evidence of columnar grains initiating at the interface is observed. Instead, discoloration which is presumably due to a large number of discrete phases and/or boundaries, is present in the coating, but generally confined to the upper half, nearest the surface. Even though the columnar grain boundaries were not observed, the coating exhibited a microscopically scalloped surface morphology.

B7 (Figure 2.13)

Sample B7 has a very uniform coating thickness that ranges from 18 – 23 μm (0.7 -0.9 mils), depending upon the sample. The interface between the coating and substrate is not pronounced, but is observable by through backscatter electron imaging. While columnar grain boundaries are apparent through the thickness, the grain boundaries are somewhat muted and relatively ill-defined. The surface morphology of the coating appears to be microscopically irregular as extraneous coating material is present along the surface in multiple locations.

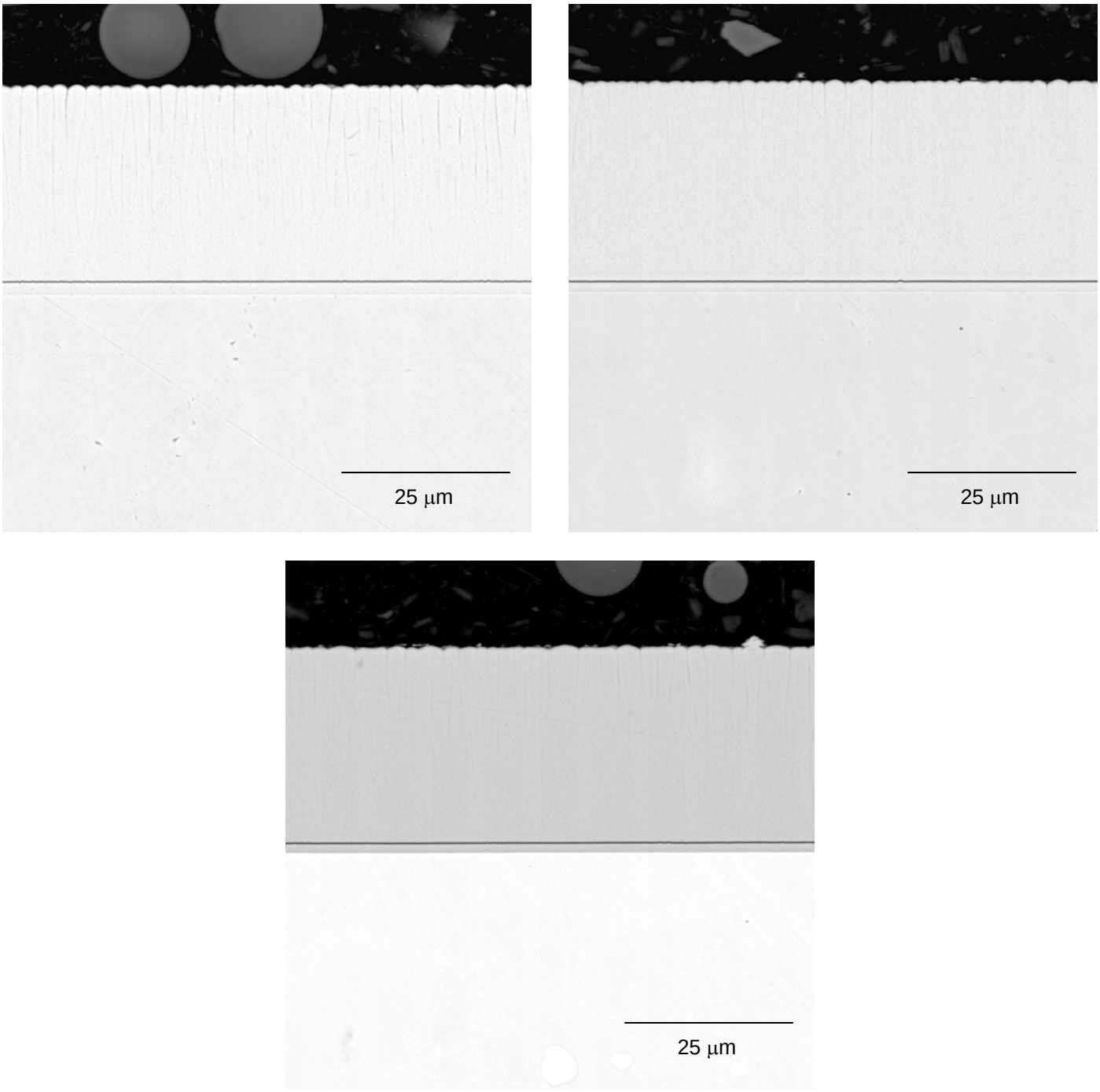

FIGURE 2-10
As-received Nanocoating B4 on 91 Substrate Material (Top Left), 304 Substrate Material (Top Right), and Haynes 230 Substrate Material (Bottom).

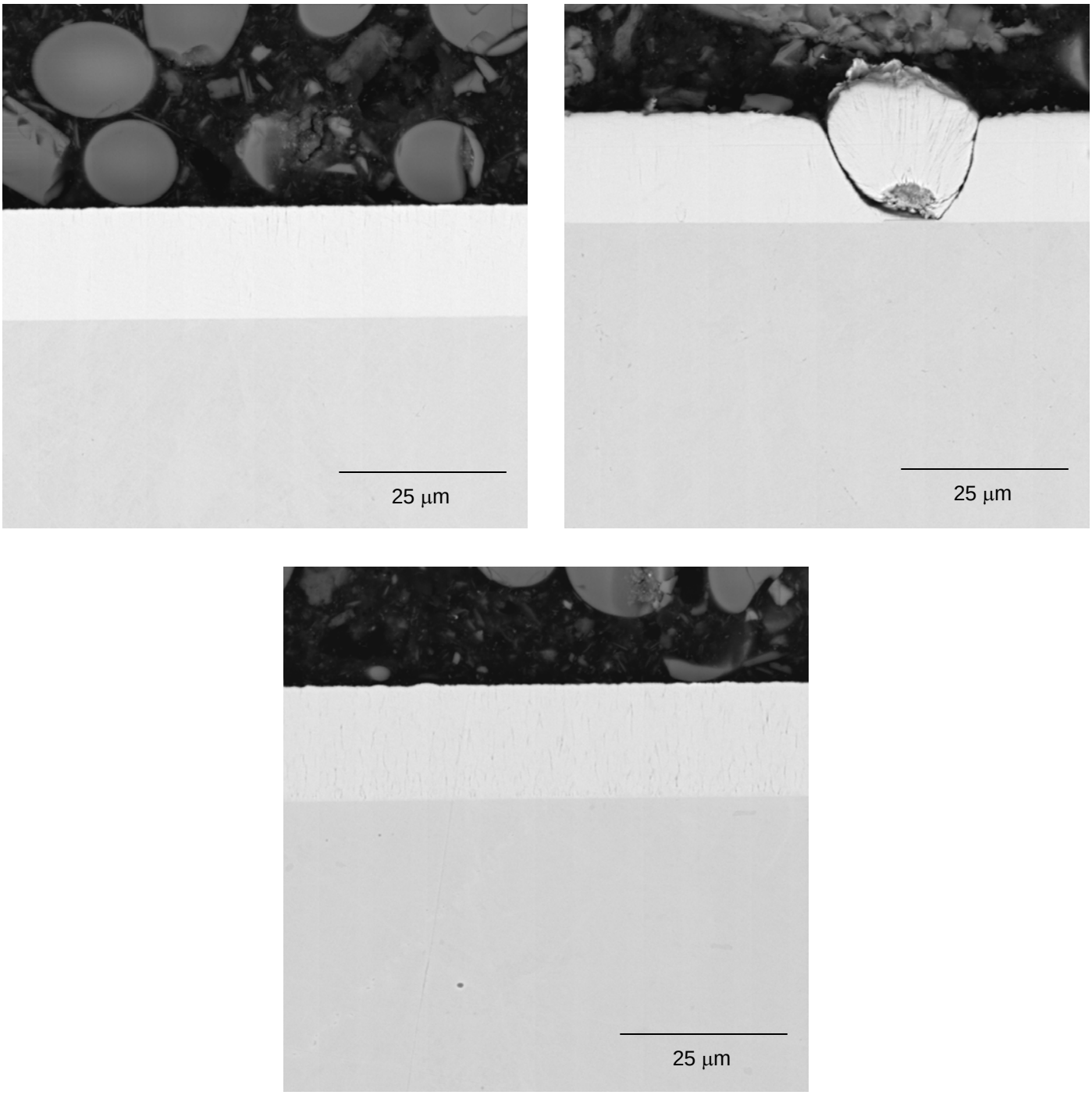

FIGURE 2-11
As-received Nanocoating B5 on 91 Substrate Material (Top) and 304 Substrate Material (Bottom).

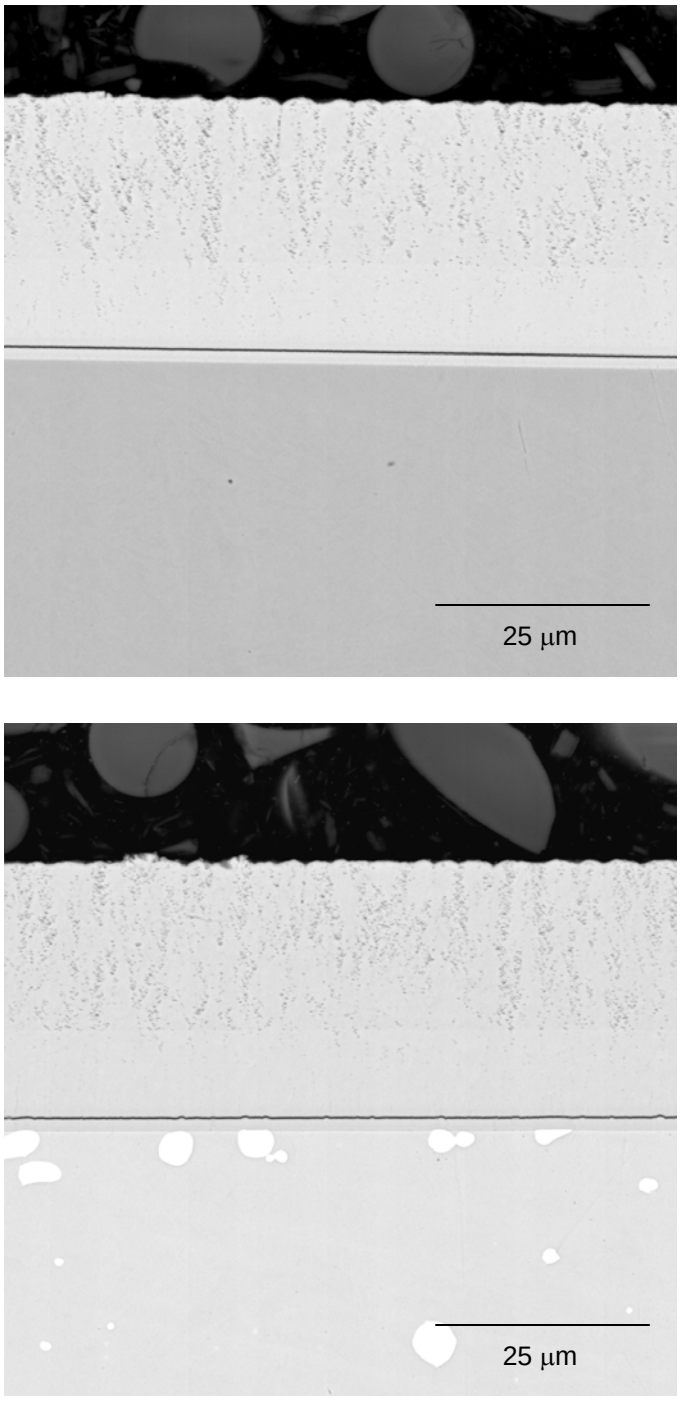

FIGURE 2-12
As-received Nanocoating B6 on 304 Substrate Material (Top) and Haynes 230 Substrate Material (Bottom).

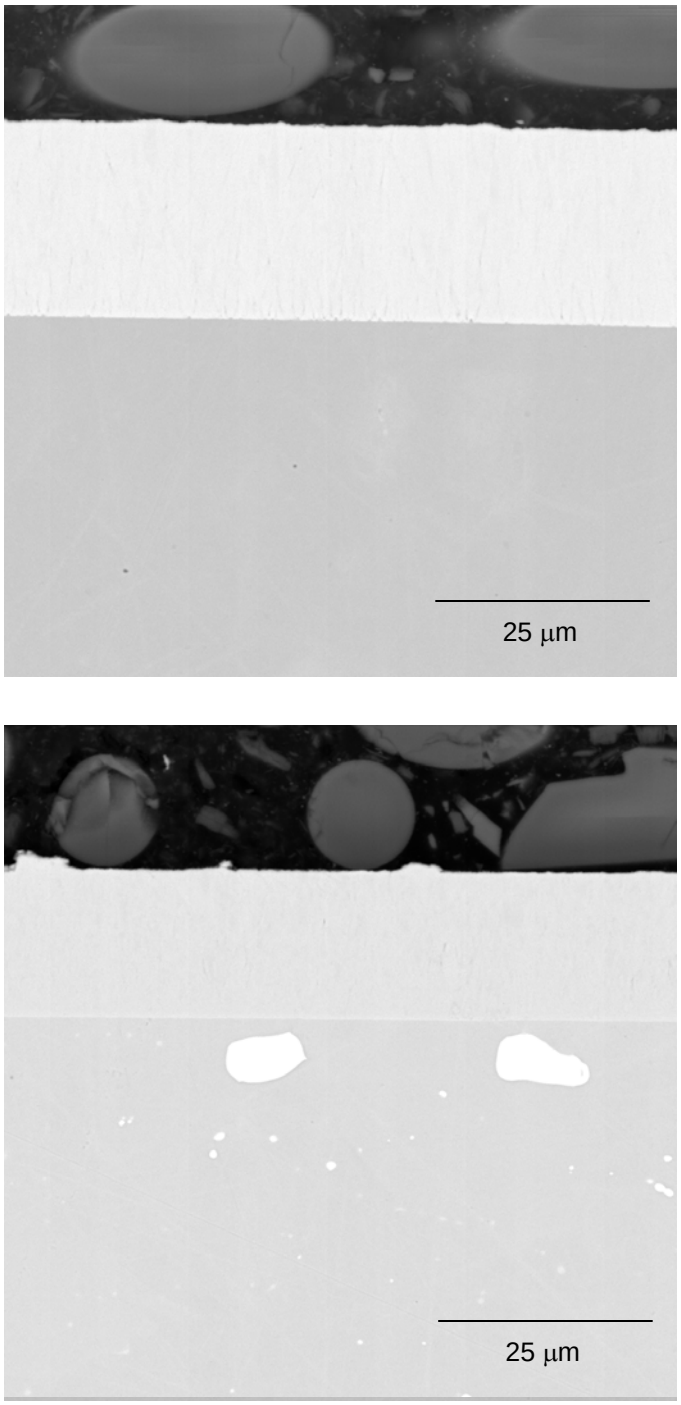

FIGURE 2-13
As-received Nanocoating B7 on 304 Substrate Material (Top) and Haynes 230 Substrate Material (Bottom).

3
EXPERIMENTAL AND APPROACH

The fireside corrosion resistance of the nanostructured coatings was evaluated through laboratory testing whereby the test coupons were coated with synthetic ash deposits, placed inside an insulated, tubular electric furnace, and exposed to a steady stream of synthetic flue gas. The blends of synthetic ash deposits and flue gas mixtures were designed to be moderately aggressive and contain fairly high concentrations of the corrosive constituents typically found in North American bituminous coals. Test parameters were configured to simulate the corrosive conditions that may prevail in the furnace and heat recovery areas of supercritical and/or A-USC boilers burning bituminous coal. For waterwall conditions, the flue gas was mildly reducing and the ash contained FeS as the primary corrosive constituent, while under superheater/reheater conditions, the flue gas was oxidizing and the primary corrodent in the synthetic ash was alkali sulfates (equal parts sodium and potassium sulfate). Small amounts of carbon where added to the deposits for both test conditions, whereas chlorine was added as solid chloride compounds in the deposits of the waterwall tests and as HCl to the flue gas in the superheater/reheater tests.

100 Hour Preliminary Screen Tests

Prior to full-scale testing, several nanaocoating materials (i.e., B1, B3, B4, B5, B6 and B7) were subjected to 100 hour screening tests under very aggressive waterwall and superheater/reheater conditions. The purpose of this screening test was to generate a basic understanding of the high temperature corrosion behavior of the nanocoating materials, and then use the data obtained to optimize the test parameters (deposit, gas and temperature conditions) for the full-scale 1000 hour tests. The temperature of the 100-hour test was 649ºC (1200ºF) for superheater/reheater conditions and 524ºC (975ºF) for waterwall condition; the flue gas and deposit compositions for each test are presented in Tables 3-1 and 3-2, respectively. Initially, duplicate samples of the specific nanocoating materials as well as bare coupons were covered with ash and placed into the furnace for testing. After 50 hours of exposure, half of the samples (one of each) were removed from the furnace and prepared for post-exposure evaluation, while the other samples were re-coated with fresh ash and returned to the furnace for an additional 50 hours of testing. When the 100 hour exposure period was completed, the remaining samples were removed from the furnace and prepared for post-exposure evaluation.

TABLE 3-1
Composition of the Synthetic Flue Gas Used in the Screening Tests

Gas Species	Waterwall	Superheater
N_2	74.63	70.88
CO_2	17.00	15.00
H_2O	6.00	10.00
CO	2.00	0.00
SO_2	0.37	0.50
O_2	0.00	3.60
HCl	0.00	0.02
Total	100.00	100.00

TABLE 3-2
Composition of the Synthetic Ash Deposits Used in the Screening Tests

Compound	Waterwall (wt. %)	Superheater (wt. %)
Fe_3O_4	10.00	0.00
FeS	75.00	0.00
Fe_2O_3	0.00	50.00
C	5.00	2.50
SiO_2	4.50	8.80
Al_2O_3	4.50	8.70
NaCl	0.50	0.00
KCl	0.50	0.00
Na_2SO_4	0.00	15.00
K_2SO_4	0.00	15.00
Total	100.00	100.00

1000 Hour Corrosion Tests

Synthetic Flue Gas

Following the evaluation of the 100 hour screen test specimens (see Section 4), the flue gas mixtures that would be used for both superheater/reheater and waterwall conditions for the 1000 hour test were determined; the compositions are given in Table 3-3, respectively. With the exception of the water vapor, the gases were continuously blended from cylinder gases that were controlled and measured by precision-calibrated flowmeters. The required levels of CO_2, CO,

N_2, and O_2 were initially blended together, then passed through a temperature controlled humidifying column in order to entrain the gas mixtures with the required amount of water vapor (by volume). Once leaving the humidifying column, the gas mixture was carried to the furnace test area in heat traced lines to ensure that the gas was maintained at a temperature of 120° C (250° F) to prevent condensation. Just before entering the superheater/reheater test furnaces, the humidified gas was blended with the prescribed concentrations of SO_2 and/or HCl, and subsequently passed through catalyst reaction chambers, which catalyzed the SO_2 to SO_3. The total gas flow rates were maintained at 1888 cm^3/m (4 ft^3/h) for each furnace.

TABLE 3-3
Synthetic Flue Gas Composition for the 1000 hr Corrosion Tests

Gas Species	Waterwall	Superheater
N_2	74.88	71.14
CO_2	17.00	15.00
H_2O	6.00	10.00
CO	2.00	0.00
SO_2	0.12	0.25
O_2	0.00	3.60
HCl	0.00	0.01
Total	100.00	100.00

Synthetic Fuel Ash

The compositions of synthetic ash deposits used in the 1000 hour tests were also formulated after evaluation of the 100 hour screen test specimens. The compositions represent moderately aggressive ash deposits that would be found in the waterwall and superheater/reheaters areas of a boiler burning North American bituminous coal. The ash was prepared by blending dried powders of various compounds together in weighted proportions and ball milling to ensure homogeneity of the mixture. Just prior to coating, a small amount of camphor binder in an ethanol solution was added to the ash so that proper adhesion was maintained with the test coupon. The ash was applied to both sides of the specimens in a controlled manner to ensure consistency from one specimen to another. The synthetic fuel ash compositions for the superheater/reheater and waterwall conditions are presented in Table 3.4.

TABLE 3-4
Composition of the Synthetic Ash Deposits Used in 1000 hour Corrosion Tests

Compound	Waterwall (wt. %)	Superheater (wt. %)
Fe_3O_4	45.00	0.00
FeS	40.00	0.00
Fe_2O_3	0.00	30.60
C	5.00	2.50
SiO_2	4.90	31.30
Al_2O_3	4.90	30.60
NaCl	0.10	0.00
KCl	0.10	0.00
Na_2SO_4	0.00	2.50
K_2SO_4	0.00	2.50
Total	**100.00**	**100.00**

Corrosion Testing

After coating, the specimens were suspended from alumina rods atop corrosion test racks and placed inside a furnace. The ends of the furnace retort were then sealed and purged with nitrogen to prevent premature oxidation while the units were heated to the target temperatures of 455º C (850º F), 524º C (975º F), and 595º C (1100º F) for waterwall conditions and 593º C (1100º F), 705º C (1300º F), and 815º C (1500º F) for superheater/reheater conditions. Once the target temperature was reached, the flue gas mixtures were introduced and steady flow was maintained throughout the test cycle. To ensure that fresh corrodent species were continuously in contact with the metal surfaces, the appropriate synthetic ash mixtures were replenished at 100 hour intervals. After each 100 hour test cycle, the retorts were cooled under a nitrogen purge until ambient temperature was reached; the specimens were then removed, cleaned of the spent coal-ash, re-coated with fresh ash, and returned to the retort. Upon completion of the 1000-hour tests, the test specimens were stored in drying ovens until post-test evaluation commenced.

Post Exposure Evaluation

Representative photomacrographs of several nanocoating and uncoated samples after 1000 hours of testing are shown in Appendix A (Figures A-1 – A-18). The coated specimens were evaluated both macroscopically and microscopically for evidence of gross deterioration (such as cracking or spallation) and penetration of corrosive species into the base metal. The macroscopic evaluation was performed using a low-powered stereomicroscope to identify areas of distress on the coatings. Since the ash was not completely removed from the test samples during each 100 hour exposure interval, the macroscopic evaluation was primarily focused on the upper portion of the sample where the deposits were not applied. Following the macroscopic analysis,

specimens measuring approximately 6.4 mm x 19.1 mm x 3.2 cm (¼" x ¾" x ⅛") were cut from the lower portion of each coupon, mounted in a phenolic-based thermosetting mounting media, roughly ground on SiC abrasive paper and finely polished to a 0.05 micron finish. Due to the thinness of the nanocoatings (typically between <35μm [1.4 mils]), conventional optical microscopy was inadequate to fully assess the corrosion behavior of the nanocoating materials. Instead, each sample was evaluated using a scanning electron microscope (SEM) that was equipped with an energy dispersive x-ray (EDX) spectrometer. This allowed for the samples to be evaluated for evidence of distress such as cracks/fissures, corrosion, subsurface penetration, spallation, and/or coating defects, while also having the ability to analyze the composition of the constituents residing at and near the distressed sites. The fact that the samples were in the form of polished metallographic cross-sections necessitated the use of a backscattered electron detector for imaging, which relies on atomic number or Z-contrast to produce an image, instead of a secondary electron detector which utilizes surface roughness for imaging.

4
RESULTS – 100 HOUR SCREENING TEST

As mentioned in Section 3, preliminary screening test of 100 hour duration was carried out on a six different nanocoating materials (B1, B3, B4, B5, B6 and B7) for both waterwall and superheater/reheater conditions. The waterwall test was carried out at 975°F (524°C) using a deposit containing 75% FeS and 1% alkali chlorides, while the superheater/reheater test was performed at 1200°F (649°C) using a deposit containing 30% alkali sulfates. Although these deposit formulations are more aggressive for their respective environments than FW traditionally uses, with little to no experience with these materials, the intent of the screening test was to acquire a basic understanding of the corrosion performance of nanocoating materials when exposed to boiler environments. The nanaocoatings that were tested under waterwall conditions included B1, B3, B4 and B5 on 91 substrate material; for superheater/reheater conditions the screening test samples included nanocoatings B1, B3, B4, and B5 on a 91 substrate material and B1, B3, B4, B5, B6, and B7 on a 304SS substrate material. Figures 4-1 and 4-2 illustrate the conditions of the nanocoating materials (and uncoated control samples) prior to exposure to waterwall and superheater/reheater screen test conditions, respectively.

Macroscopic Evaluation

Waterwall Conditions

Following exposure to waterwall conditions, the coated surfaces of the coupon specimens were mostly covered with relatively thick, somewhat friable, reddish-orange deposits, as illustrated in Figure 4-3. Within the areas not covered with the deposits, the surfaces appeared slightly oxidized and had an orange-brown hue. Close examination with a low-powered stereomicroscope did not indicate any evidence of coating spallation or complete coating consumption; however, cracking and fissuring was noted within the deposit-free region and along the edges of specimens B1, B4, and B6. Specimens B3, B5 and B7 appeared to be intact and showed no macroscopic evidence of degradation within these areas. Figures 4-4 and 4-5 are representative photomacrographs showing the region not covered with deposits during the exposure period for several nanocoating specimens. In general, nanocoating materials not containing significant aluminum additions (~10%) did not exhibit cracking, while those containing aluminum were prone to cracking.

Superheater/Reheater Conditions

The post-exposed surfaces of the superheater/reheater samples are displayed in Figure 4-6. The coupon specimens were generally covered with fairly friable, red synthetic ash deposits, except at and near the machined hole at the upper portion of the coupon, which was deliberately left free of deposits. Within this area, most of the coupons appeared to be slightly oxidized, as evidenced by the discoloration (relative to the as-supplied coating). Subsequent examination of test coupons with a low-powered stereomicroscope revealed cracking and fissuring of several coating materials, very similar to what was observed for the waterwall test samples. As with the

waterwall samples, macroscopic cracking/crazing was generally noted in coating samples which contained aluminum, such as B1, B4 and B6; while materials that did not contain aluminum generally showed little to no evidence of cracking/crazing. Figures 4-7 – 4-9 are representative stereomicrographs illustrating the post condition of the deposit-free region on several coating materials following exposure to synthetic superheater/reheater conditions.

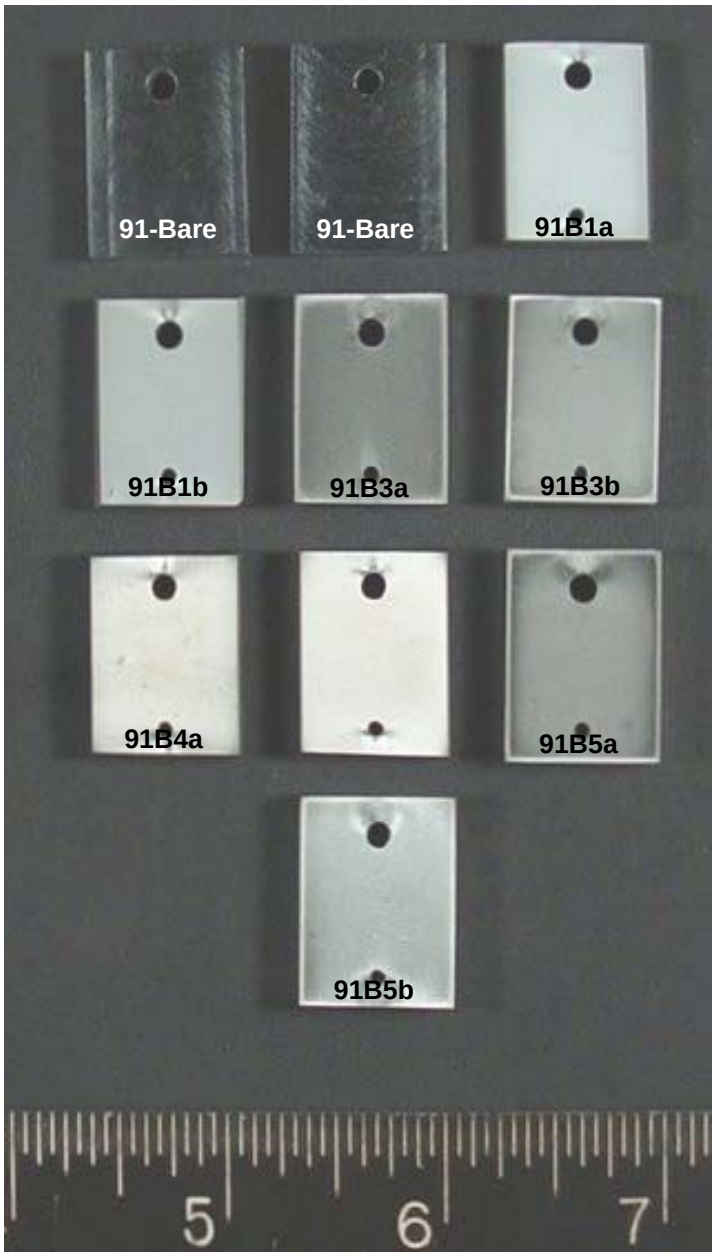

FIGURE 4-1
Representative Photograph Showing the Nanocoating and Uncoated Control Samples in the As-supplied Condition, Prior to Performing the Screening Test Under Synthetic Waterwall Conditions. Duplicate Samples Were Removed after 50 Hours.

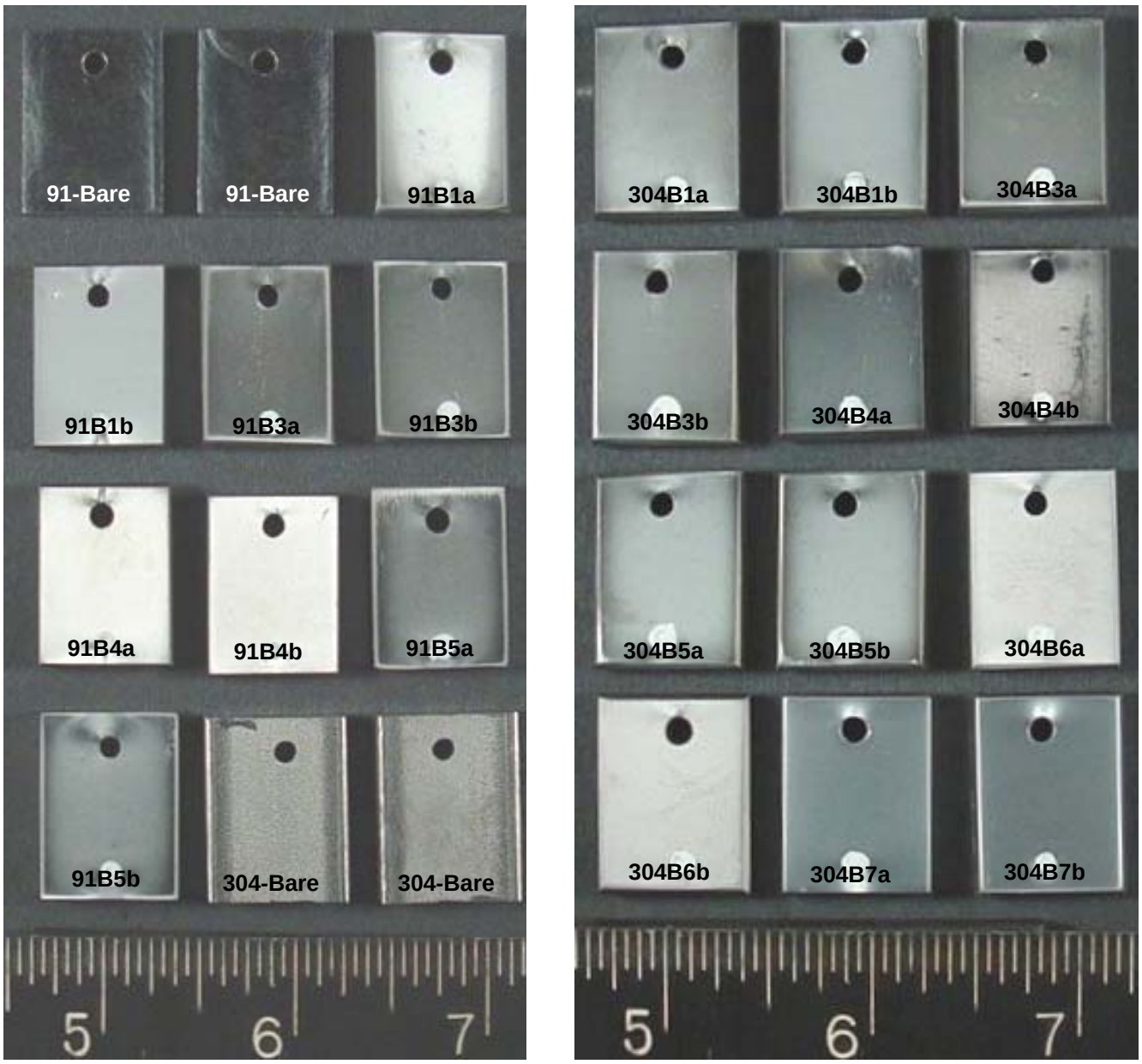

FIGURE 4-2
Representative Photograph Showing the Nanocoating and Uncoated Control Samples in the As-supplied Condition, Prior to Performing the Screening Test under Synthetic Superheater/Reheater Conditions.

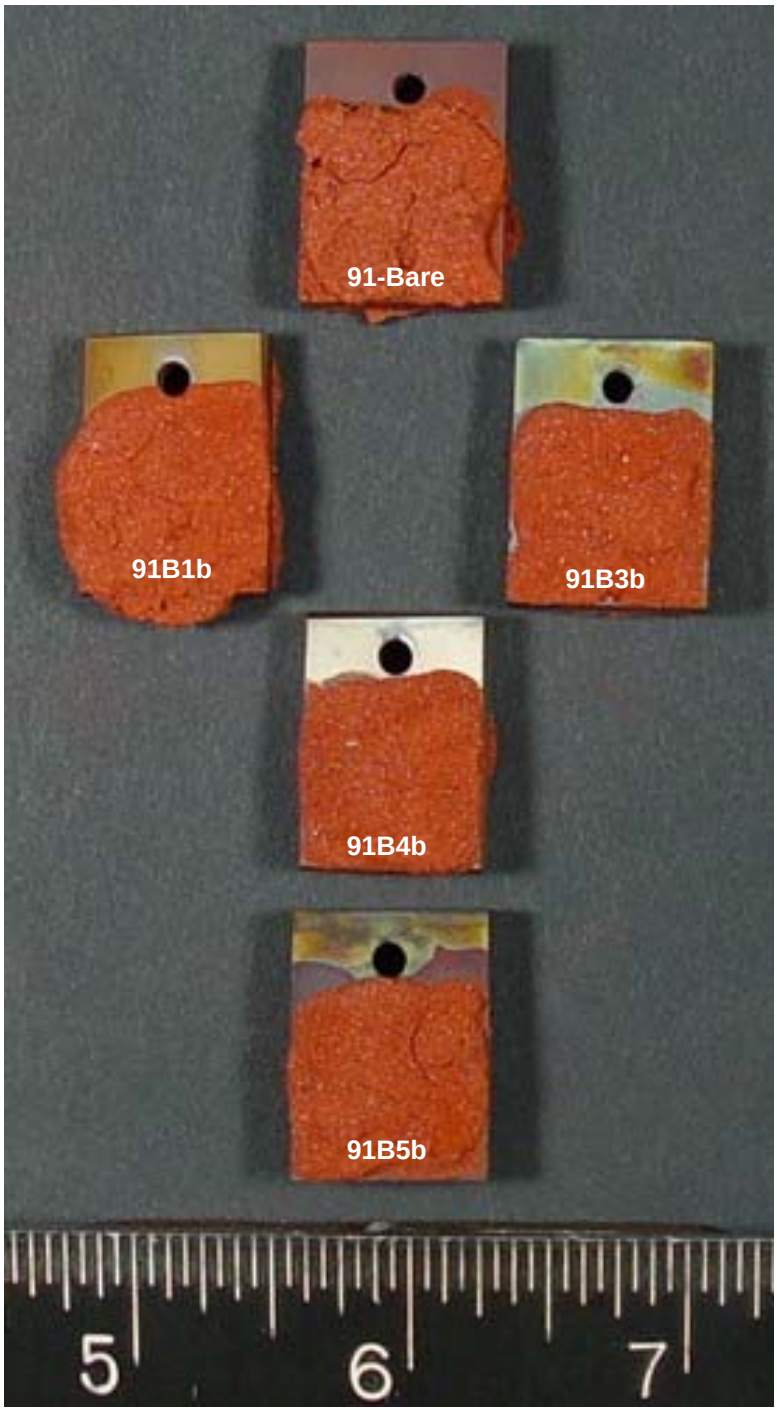

FIGURE 4-3
Screening Test Samples Following 100 Hours of Exposure to Aggressive Waterwall Conditions. Note that the Uppermost Portion of the Samples Were Not Coated with Deposits.

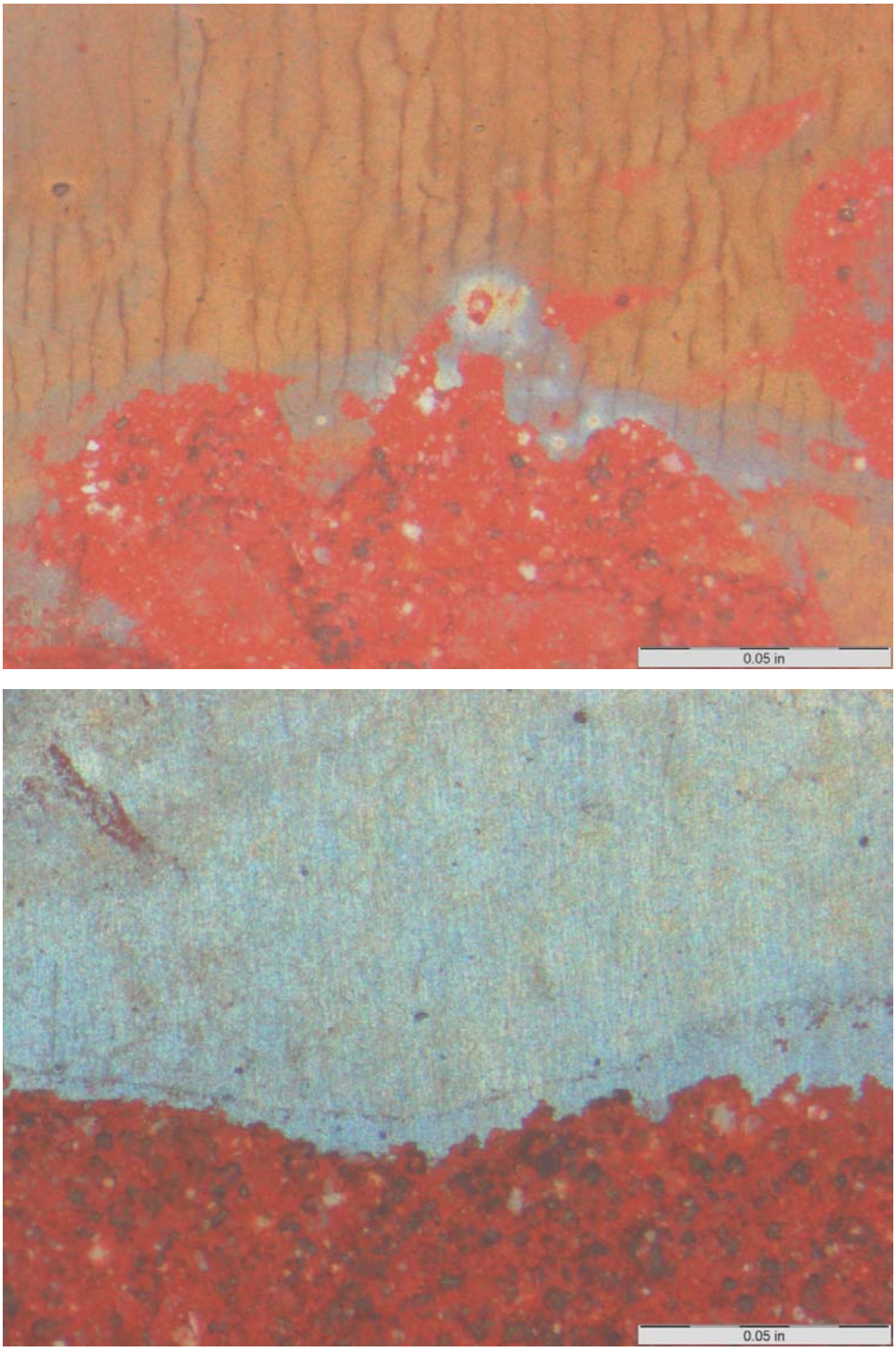

FIGURE 4-4
Stereomicrographs of Nanocoating Samples B1 (Top) and B3 (Bottom) in the Region Not Covered with Deposit after 100 Hours of Exposure to Aggressive Waterwall Conditions. Note the High Number Density of Crack and Fissures on Sample B1.

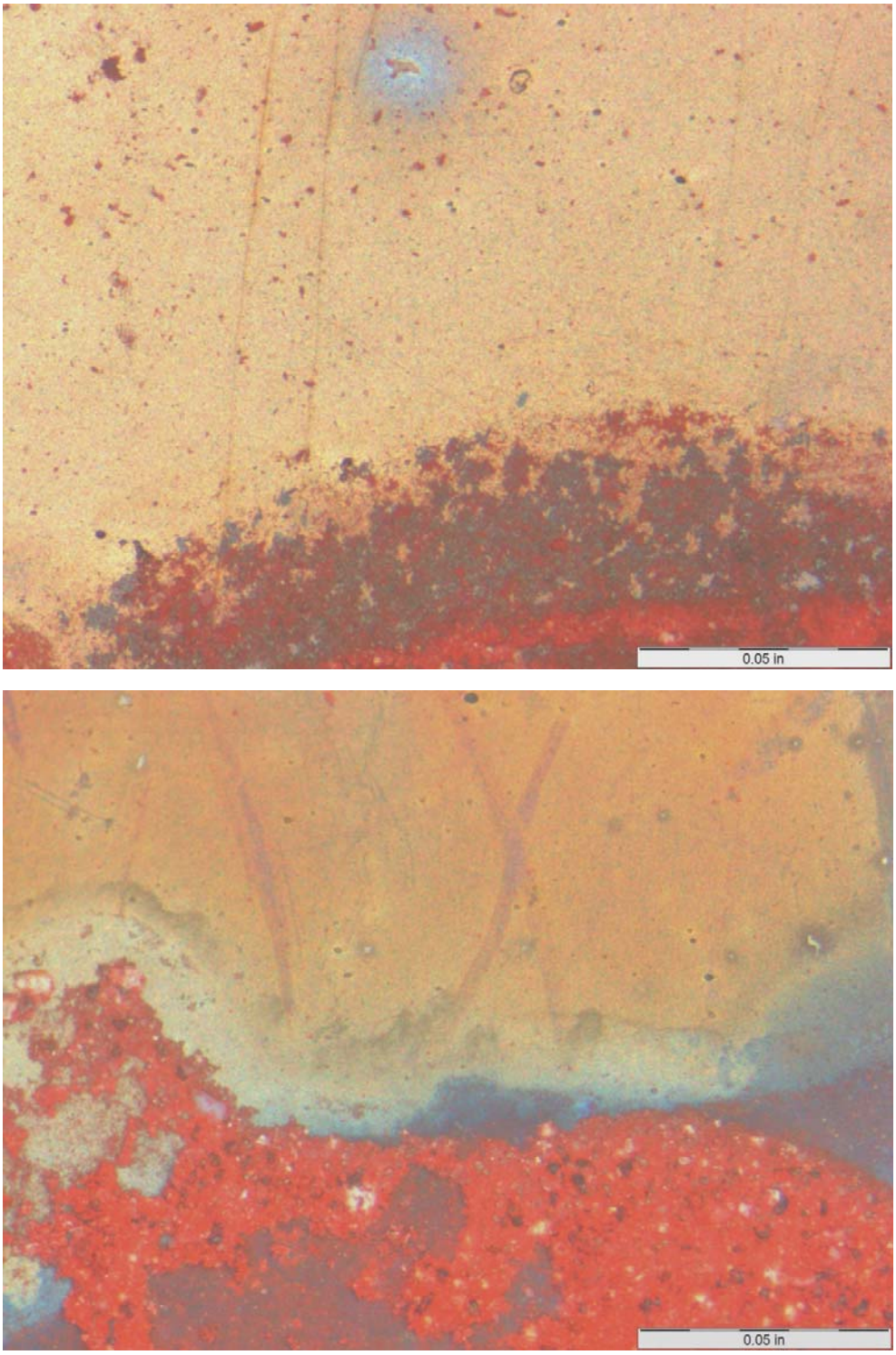

FIGURE 4-5
Stereomicrographs of Nanocoating Samples B4 (Top) and B5 (Bottom) in the Region Not Covered with Deposit after 100 Hours of Exposure to Aggressive Waterwall Conditions. Several Cracks and Fissures are Present in Coating Sample B4.

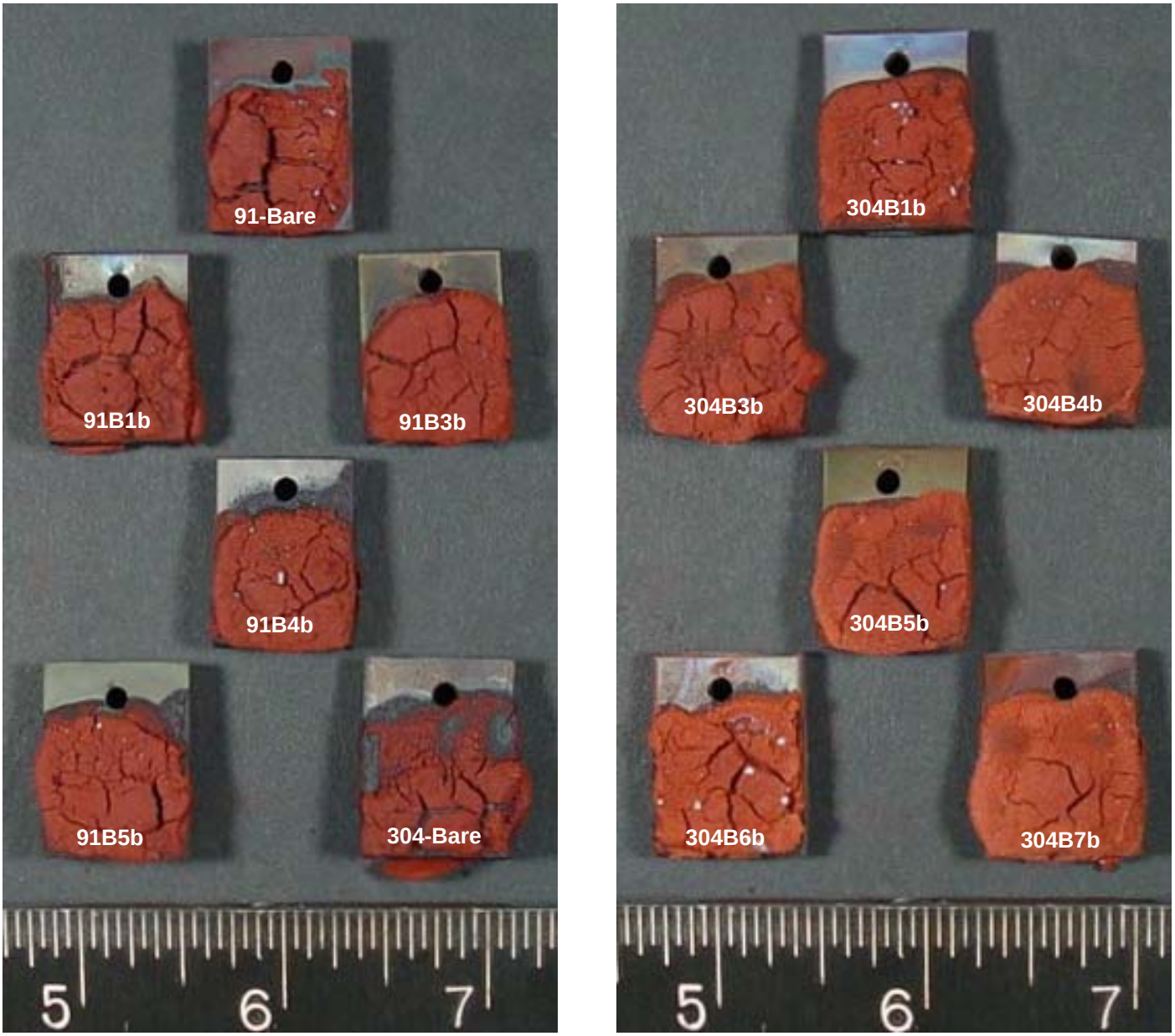

FIGURE 4-6
Screening Test Samples Following 100 Hours of Exposure to Aggressive Superheater/Reheater Conditions. As with the Waterwall Materials, the Uppermost Portion of the Samples were Not Coated with Deposits.

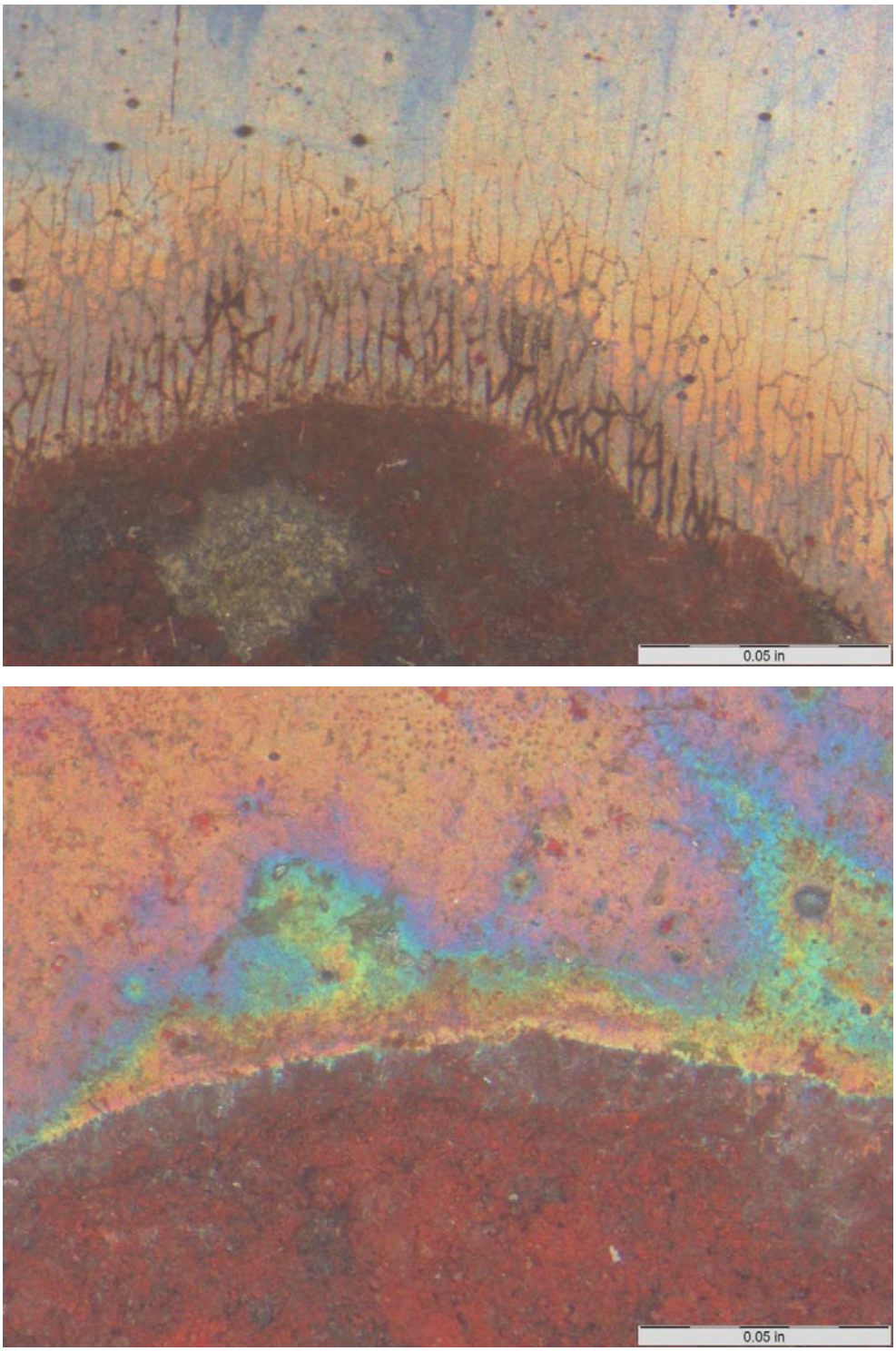

FIGURE 4-7
Stereomicrographs of Nanocoating Samples B1 (Top) and B3 (Bottom) after 100 hrs of Exposure to Aggressive SH/RH Conditions. Numerous Cracks and Fissures Created a Crazed Appearance in the Area Not Covered with Deposits on B1.

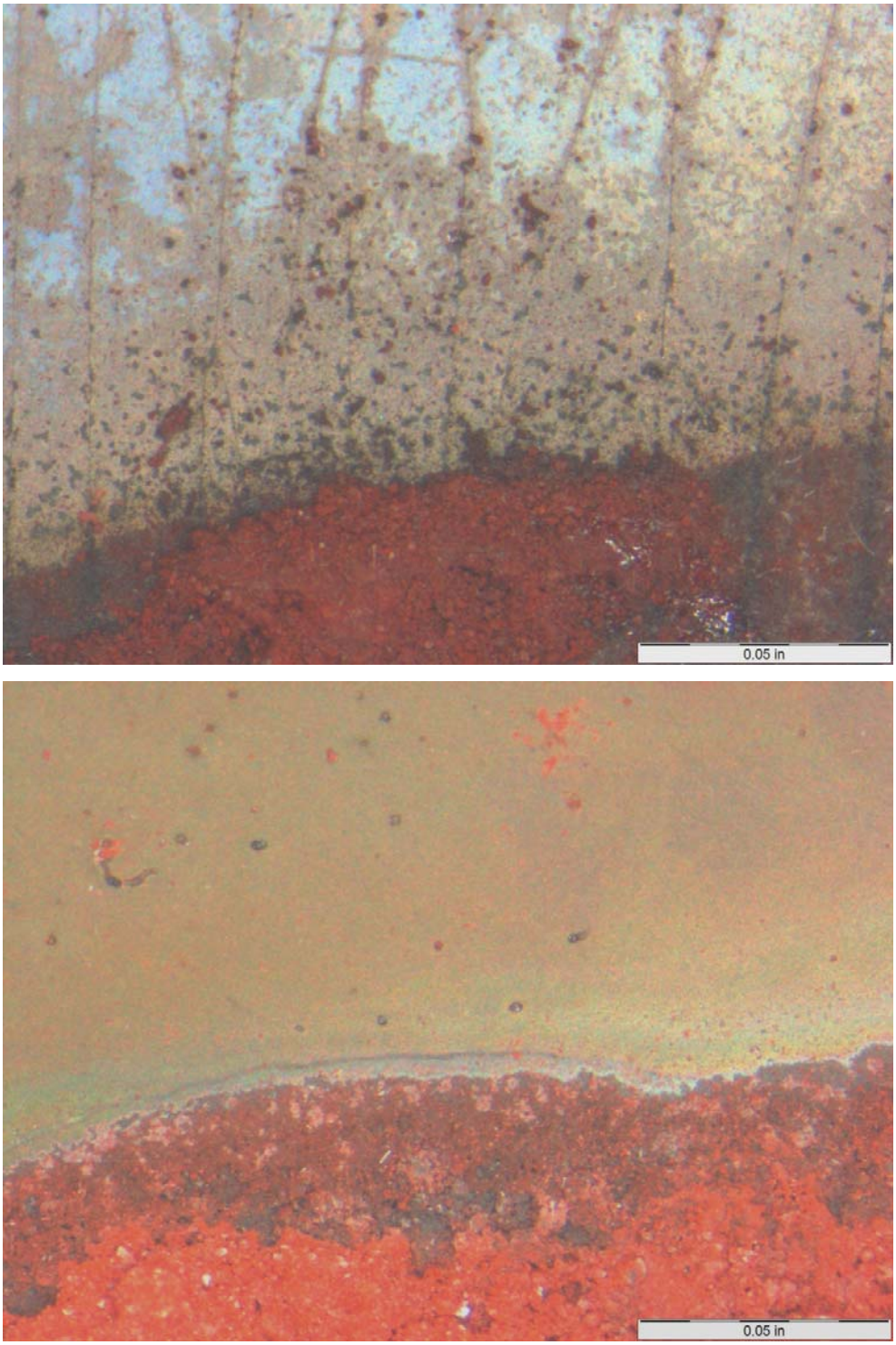

FIGURE 4-8
Stereomicrographs of Nanocoating Samples B4 (Top) and B5 (Bottom) after 100 hrs of Exposure to Aggressive SH/RH Conditions. B4 Contains Several, Relatively Straight Cracks and Fissures in the Region Not Covered with Deposits.

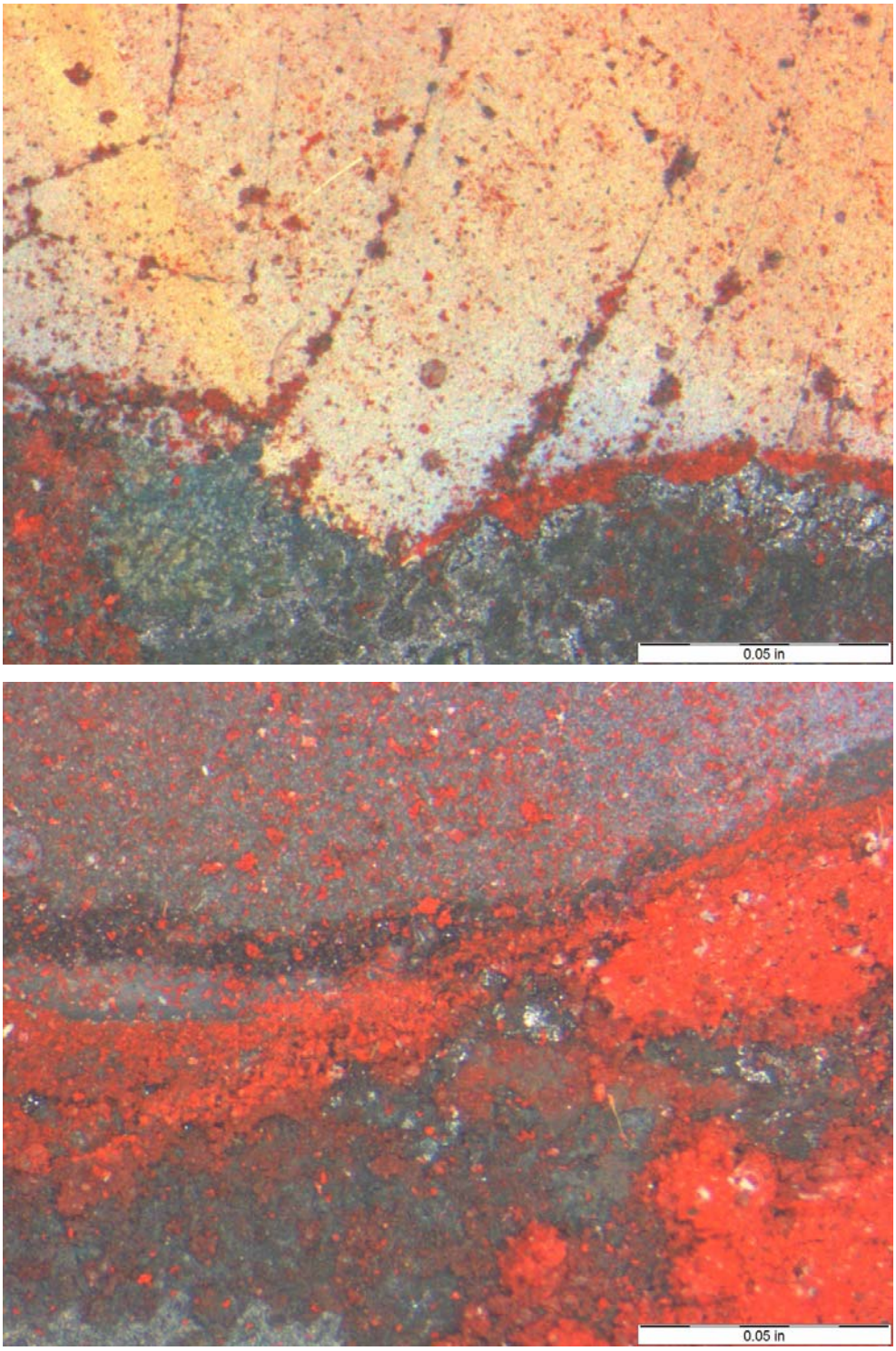

FIGURE 4-9
Stereomicrographs of Nanocoating Samples B6 (Top) and B7 (Bottom) after 100 hrs of Exposure to Aggressive SH/RH Conditions. Scattered Cracks are Apparent in the Region Not Covered with Deposits on Coating B6

Microscopic Evaluation

As mentioned previously, the corrosion resistance of each nanocoating material to the synthetic boiler environment was primarily assessed through microscopic examination of the area beneath the deposits. High magnification backscattered electron imaging was used to identify any breaches, cracks, fissures, areas of spallation, gross evidence of corrosion, or other forms of degradation that may have existed in the coating material, as the existence of such defects is perceived to be unacceptable due to the inevitable penetration of aggressive species through the coating and into the underlying substrate material. Thus, the evaluation was purely qualitative as no direct measure of the penetration depth was made.

Figures 4-10 – 4-15 are representative backscatter SEM images illustrating the as received and post exposure state of the various nanocoatings subjected to aggressive waterwall conditions at 975°F (524°C) and superheater/reheater conditions at 1200°F (649°C).

As clearly evidenced in the SEM images, some degree of distress was noted on every coating material; however, the nanocoatings subjected to waterwall conditions generally fared much better than those tested under superheater/reheater conditions. Degradation due to synthetic waterwall conditions was mainly in the form of cracks and fissures that tended to follow along preexisting morphological features such as the columnar grain boundaries and/or globular imperfections that were noted in the as-received coatings. Nanocoating materials tested under superheater/reheater conditions, on the other hand, exhibited severe bulk corrosion resulting in partial or complete consumption of the coating materials in multiple locations and subsequent attack of the substrate material. Furthermore, wastage of the superheater/reheater coating materials did not appear to be confined to imperfection sites, but rather were distributed across the entire sample surface.

Conclusions

Based on the less than desirable performance of the nanocoatings subjected to the 100 hours screening tests, the compositions of the flue gas mixtures and synthetic ash deposits for both waterwall and superheater/reheater conditions were changed from very aggressive to moderately aggressive as indicated in Tables 3-3 and 3-4, respectively.

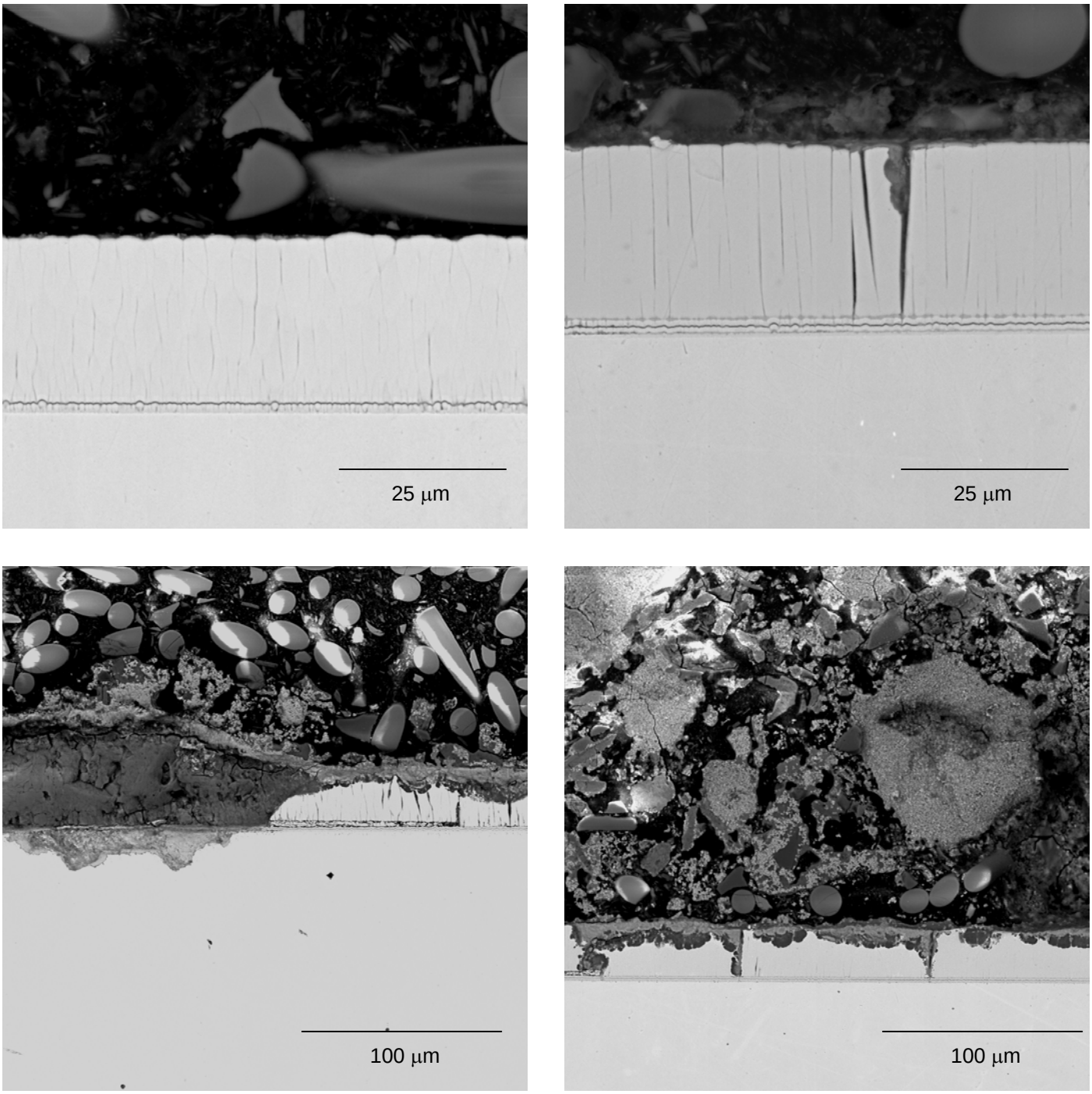

FIGURE 4-10
Representative Backscatter SEM Images of Nanocoating B1 in the As-received Condition (Top Left); Exposed for 100hr to Aggressive Waterwall Conditions on 91 Substrate (Top Right); Exposed for 100 hrs to Aggressive Superheater Conditions on 91 Substrate (Bottom Left) and 304 Substrate (Bottom Right)

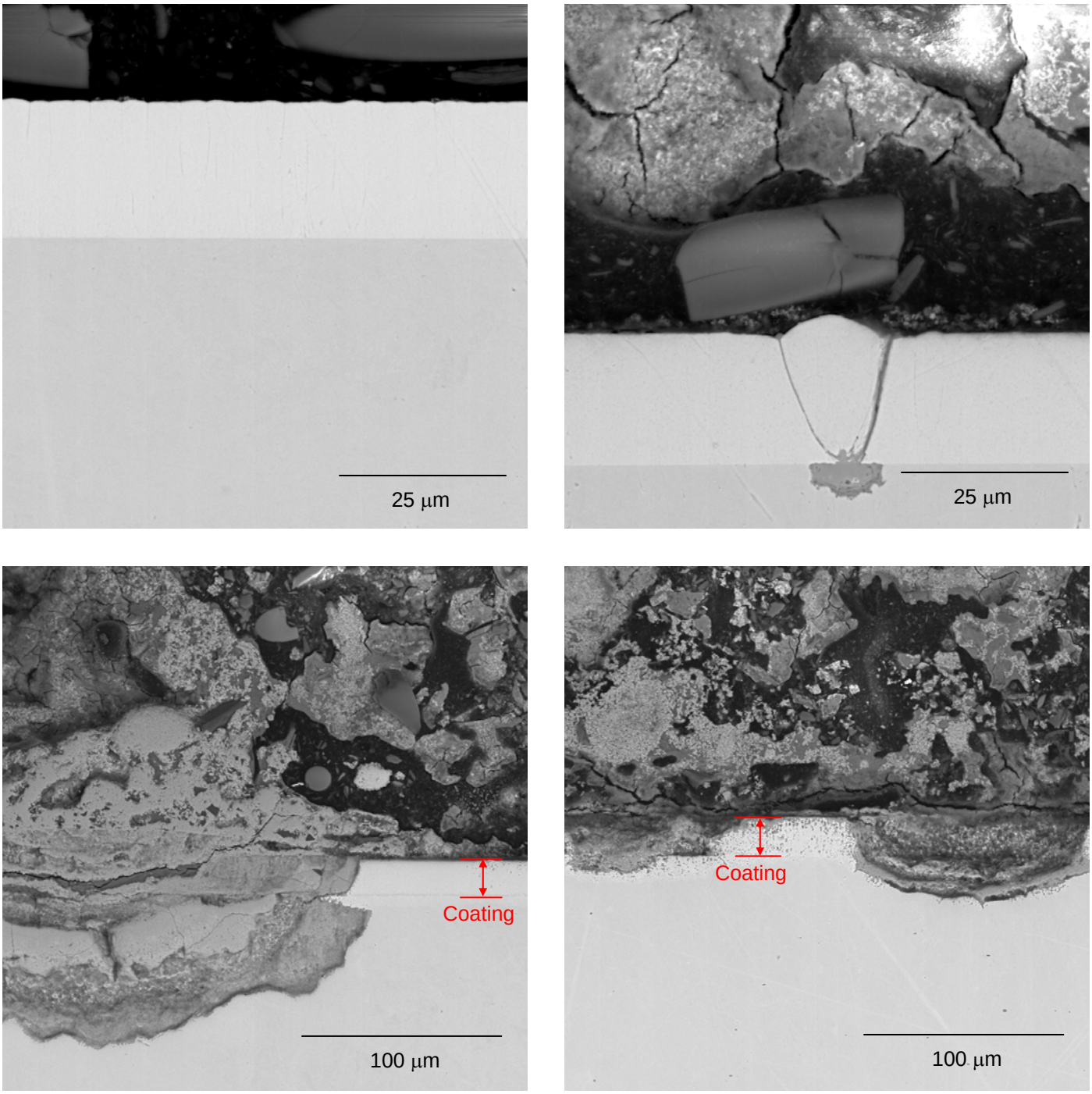

FIGURE 4-11
Representative Backscatter SEM Images of Nanocoating B3 in the As-received Condition (Top Left); Exposed for 100hr to Aggressive Waterwall Conditions on 91 Substrate (Top Right); Exposed for 100 hrs to Aggressive Superheater Conditions on 91 Substrate (Bottom Left) and 304 Substrate (Bottom Right)

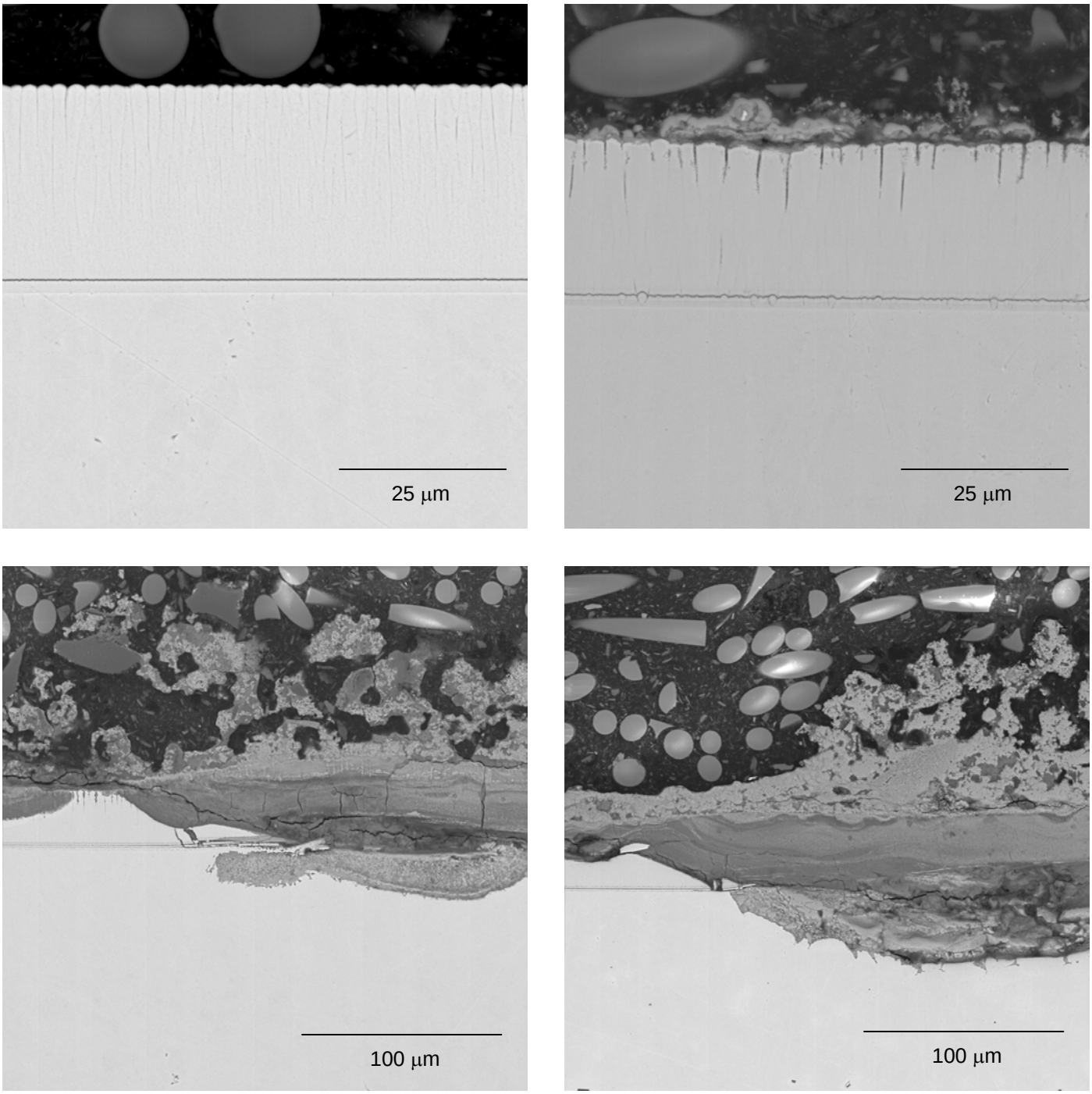

FIGURE 4-12
Representative Backscatter SEM Images of Nanocoating B4 in the As-received Condition (Top Left); Exposed for 100hr to Aggressive Waterwall Conditions on 91 Substrate (Top Right); Exposed for 100 hrs to Aggressive Superheater Conditions on 91 Substrate (Bottom Left) and 304 Substrate (Bottom Right)

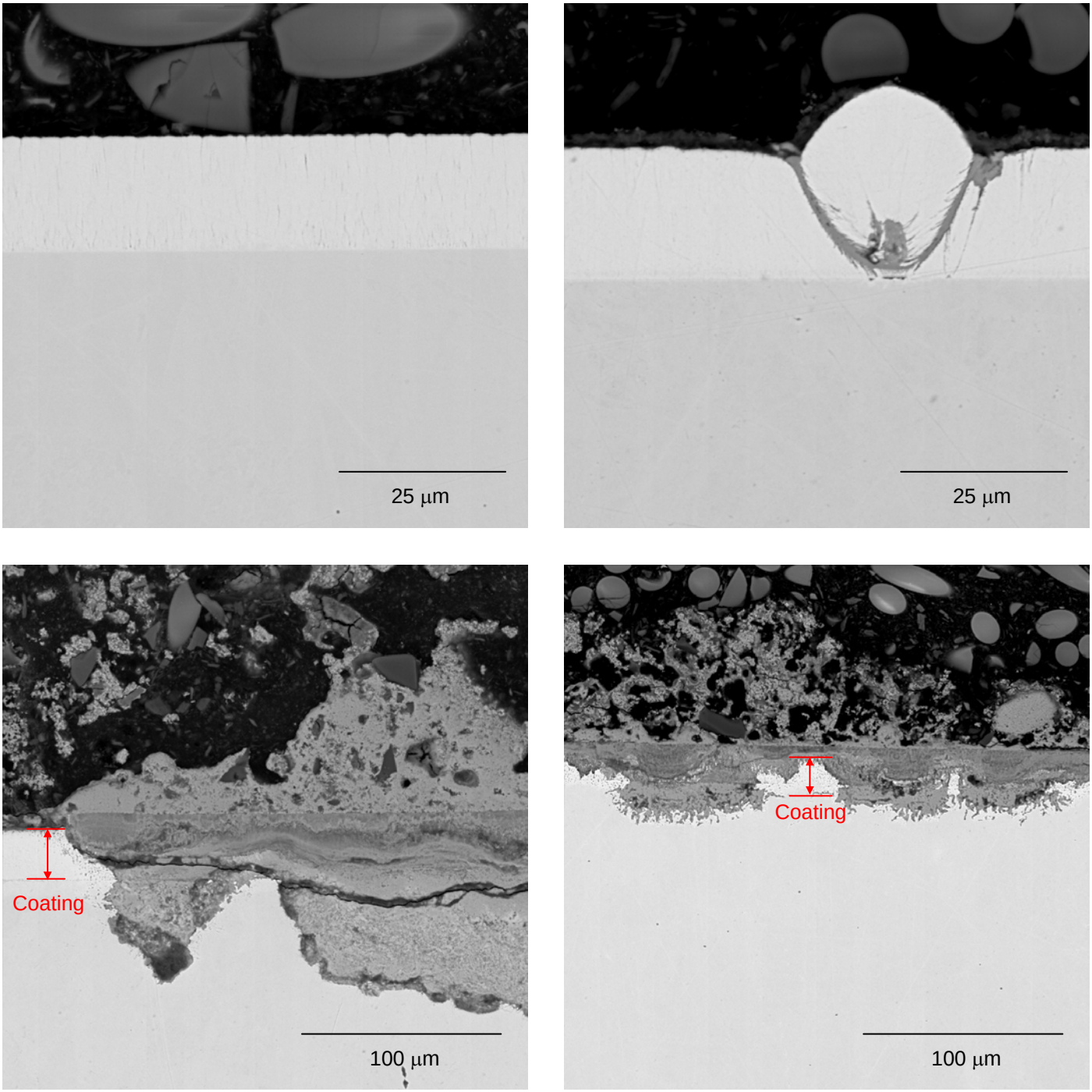

FIGURE 4-13
Representative Backscatter SEM Images of Nanocoating B5 in the As-received Condition (Top Left); Exposed for 100hr to Aggressive Waterwall Conditions on 91 Substrate (Top Right); Exposed for 100 hrs to Aggressive Superheater Conditions on 91 Substrate (Bottom Left) and 304 Substrate (Bottom Right)

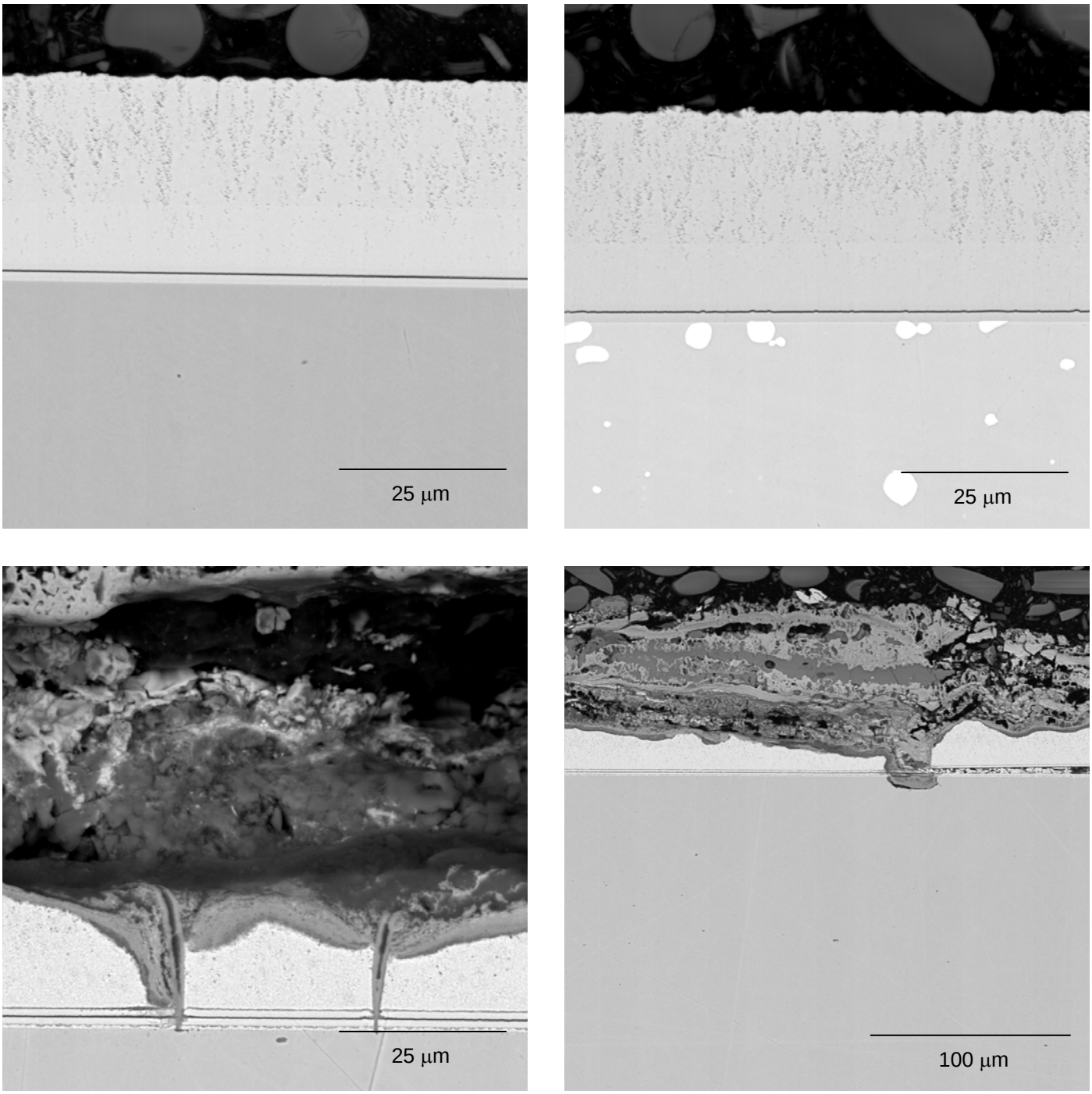

FIGURE 4-14
Representative Backscatter SEM Images of Nanocoating B6 in the As-received Condition on 304 Substrate (Top Left) and Haynes 230 Substrate ((Top Right); Exposed for 100 hrs to Aggressive Superheater Conditions on 304 Substrate (Bottom)

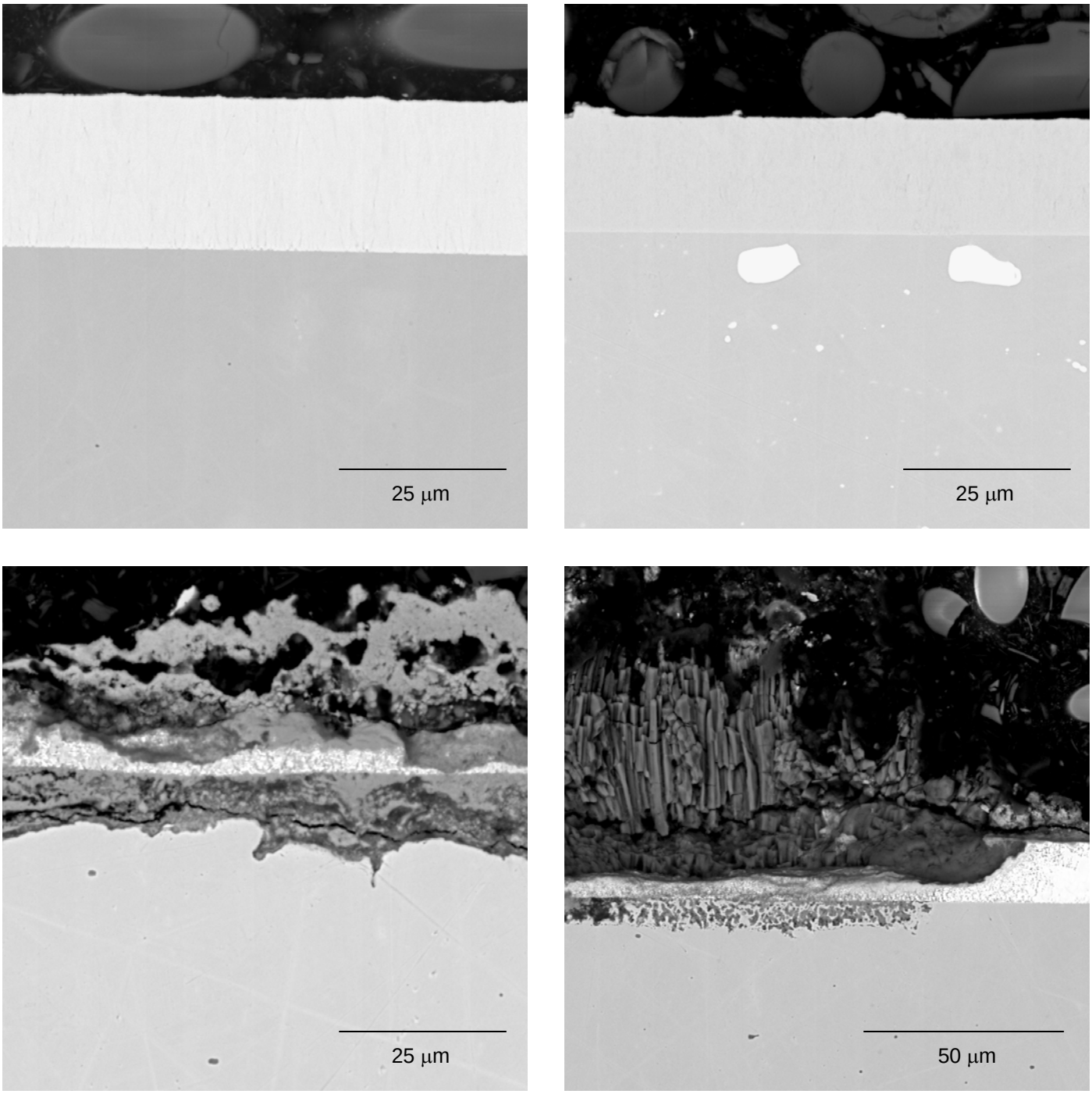

FIGURE 4-15
Representative Backscatter SEM Images of Nanocoating B7 in the As-received Condition on 304 Substrate (Top Left) and Haynes 230 Substrate ((Top Right); Exposed for 100 hrs to Aggressive Superheater Conditions on 304 Substrate (Bottom

5
RESULTS – 1000 HOUR CORROSION TESTS

The results of the 100-hour screening test indicated that many (if not all) of the nanocoating materials may be susceptible to severe and rapid degradation when exposed to aggressive superheater/reheater conditions. Screen testing also suggested that aggressive waterwall conditions may be problematic for nanocoating materials containing high concentrations of aluminum due to the propensity for cracking. Since the intention of the test program was to evaluate the long-term (1000 hour) corrosion behavior of such materials subjected to supercritical and/or A-USC boiler conditions, the aggressiveness of the deposit and flue gas compositions was scaled-back to be more representative of conditions that may prevail in boilers burning moderately aggressive coals. Thus, the blends of synthetic ash deposits and flue gas mixtures for the 1000 hour test were identical to the "Eastern coal conditions" in the DOE-USC laboratory corrosion test program. Photomacrographs illustrating the pre and post-exposure condition of the test coupons are presented in Appendix A.

Due to the large number of materials that were tested, the relatively poor results of the screen tests, and the fact that most of the coatings were applied to different substrate materials, the initial evaluations were carried out on coatings applied atop 91 substrate material for waterwall conditions and 304 substrate material for SH/RH conditions. Unfavorable results stemming from the evaluations of these materials did not warrant further testing of other coating/substrate combinations.

It should be mentioned that once the coatings were applied to the individual substrate materials, no identifying marks could be punched, stamped, or scribed into each of the test specimens. Nothwithstanding that great care was taken to minimize the possibility of a mix-up, some 91substrate materials that were intended for exposure to waterwall test conditions were inadvertently evaluated under superheater/reheater conditions. The samples included nanocoating material A2 tested at 815º C (1500º F) and nanocoating material A4 tested at all three superheater/reheater temperatures. Consequently, nanocoating material A4 coated on the 304 substrate and intended for exposeure to superheater/reaheater test conditions were inadvertently exposed to the waterwall conditions. Coatings applied to Haynes 230 substrate materials were also unintentionally used in lieu of those applied to 91substrate material for nanocoatings B2 and B4 exposed waterwall conditions at 595º C (1100º F), and for nanocoating B6 exposed to all three waterwall exposure temperatures.

Macroscopic Evaluation.

In light of the results from the screening tests, each long-term (1000 hour) test coupon was visually inspected for evidence of gross degradation following every 100 hour exposure period. Upon completion of 500 hours, and every subsequent 100 hour test period, a more detailed stereoscopic evaluation was also performed on every coupon to assess the coating integrity. After 600 hours of testing, coupons with coatings displaying significant evidence of distress,

either in the form of cracking, fissuring, spallation and/or obvious wastage were removed from the test rig and placed in drying ovens to await further, in-depth evaluation.

Waterwall Conditions

Following exposure to the prescribed waterwall conditions, the coupon surfaces were generally covered with friable and/or flaky reddish-brown deposits. In places where the deposit exfoliated from the surface or was not applied, thin oxide and/or corrosion product layers were apparent. After 600 hours of exposure, several of the coating materials, namely A4, B1, B4 and B5, displayed macroscopic evidence of distress similar to that shown in Figures 4-4 and 4-5, and thus were exempt from further testing.

Superheater/Reheater Conditions

The surfaces of the superheater/reheater nanocoating test coupons were generally covered with relatively hard, flaky, red deposits that overlaid hard, tenacious black and brown oxide and/or corrosion product layers. In some places where the deposits had spalled/flaked from the surface, little to no evidence of coating material remained. After 600 hours of exposure, corrosion testing of SH/RH materials at 705ºC (1300ºF), and 815ºC (1500ºF) was discontinued due considerable visual (macroscopic) evidence of degradation on every test sample. Degradation was typically in the form of cracks/fissures in the upper portion of the coupon where the deposits were not applied or pitting/chipping (spallation) of the coating in the region where the coating was applied, as typified in the photomacrographs presented in Figures 4-7 – 4-9. Regarding the 595ºC (1100ºF) test samples, samples displaying visual evidence of distress and/or gross degradation were removed after 600 hours, while those that appeared to be intact were tested for the entire 1000 hour duration. In total, only a select few samples were exposed for the prescribed 1000 hour test period.

Microscopic Evaluation

Waterwall Conditions

Figures 5-1 – 5-10 are representative backscatter SEM images showing, where applicable, the deposits, oxides and/or corrosion products covering the surfaces of several waterwall nanocoating materials and the degree to which the coatings were compromised due to exposure to the prescribed temperature/time condition. Nanocoatings that appeared mottled (i.e., not as a dense monolithic layer) and contained high concentrations of oxygen (like A1 and A2) provided seemingly little to no protection even at the lowest test temperatures. The dense, more uniform coatings (A4, B1 – B6) on the other hand, especially those containing more than 20% Cr, tended to resist widespread corrosive attack, but exhibited penetration of oxide and sulfide species, especially along the columnar grain boundaries and gross defects. Where corrosion was noted, the depth or extent of attack tended to increase with increasing temperature, and was often manifested along the grain boundaries and defects.

Superheater/Reheater Conditions

Representative backscatter SEM images showing the as-received and post exposure condition of the various nanocoating materials tested under synthetic superheater/reheater conditions are

presented in Figures 5-11 – 5-22. As clearly evidenced in the SEM images, regardless of temperature, every nanocoating material tested under such conditions sustained some degree of general corrosive attack. If fact, with the exception of nanocoating B5, all of the nanocoating materials were completely compromised in at least one location after 600 hours of exposure at 705ºC (1300º F), and 815ºC (1500ºF), and all of the samples (including B5) exhibited penetration of corrosive species into the substrate materials at the aforementioned test temperatures. Furthermore, unlike the samples tested under waterwall conditions, in which the coating materials displayed little evidence of gross attack, most, if not all of coatings and underlying substrate material tested under superheater/reheater conditions sustained widespread corrosion; the corrosion of the coatings was not generally associated with, (or more severe at)defects and/or columnar grain boundaries.

Post Exposure Characterization

A1 (Figures 5-1 and 5-11)

Under waterwall conditions, nanocoating A1 offered little to no protection to the underlying substrate as oxide and sulfides species were noted at the coating/substrate interface for all three exposure temperatures. Penetration of aggressive species through the coating was particularly severe at 525ºC (975ºF) and 595ºC (1100ºF), resulting in a continuous layer of mixed oxides and sulfides at the surface of the substrate. In addition to several obvious cracks and fissures that were noted in the outer layer, which likely served as points of oxygen and sulfur ingress, many small, discrete oxide and sulfide particles were also distributed throughout the inner layer of the coating.

The nanocoating displayed very poor resistance to the prescribed superheater/reheater conditions. For all test temperatures, no significant evidence of either the inner or outer coating layer was present anywhere on the coupon surfaces, suggesting that the coating was completely consumed by corrosion. In most places on the 595º C (1100ºF) test specimen however, a relatively thin, almost continuous aluminum-rich interdiffusion layer was apparent on the substrate surface, but was interrupted by scattered, shallow (<0.001”) depressions. Specimens tested at 705ºC (1300ºF) and 815ºC (1500ºF) exhibited severe bulk wastage of the substrate material, and subsequent subsurface penetration of oxides and sulfide species.

A2 (Figures 5-2 and 5-12)

Aside from the lack of a thin outer layer, nanocoating A2 was very similar in appearance and composition to coating A1 (inner layer). As such, the corrosion resistance of coating A2 was also comparable to A1. For all waterwall testing temperatures oxide and sulfide species were apparent at the substrate surface in all locations examined. While general, widespread attack of the substrate material was noted in all three test samples, the morphology of the attack was somewhat different depending on the testing temperature. Exposure to the lowest waterwall test temperature produced more uniform attack, which resulted in a nearly continuous layer of corrosion products, while exposure to the higher waterwall test temperatures produced more isolated attack, resulting in extensive pitting.

Following exposure to superheater/reheater conditions, no evidence of the nanocoating material was evident on any of the specimens; however, as was found with coating A1, the substrate

surface of 595ºC (1100ºF) test specimen was covered with a relatively thin aluminum-rich interdiffusion layer. While some attack was apparent within the interdiffusion layer, corrosion did not appear to extend into the substrate beneath this layer. Regarding the 705ºC (1300ºF) and 815ºC (1500ºF) test specimens, the substrate materials both sustained gross wastage in addition to subsurface penetration of oxide and sulfide species. It should be mentioned that while 91 substrate material was unintentionally used for exposure at 815ºC (1500ºF), the resulting wastage on the coating and depth of subsurface penetration into the substrate material was very similar to what was observed on sample A1, suggesting that the substrate metallurgy had little influence over the outcome for the coating material.

A3 (Figures 5-3 and 5-13)

Following exposure to waterwall conditions, nanocoating A3 appeared to remain relatively intact as no evidence of widespread corrosive attack or complete spallation was noted. However close examination of the test specimens revealed that the outer coating layer was peppered with small, discrete oxide and sulfide particles, while the moderately thick inner (thermal spray) layer was marked with several oxide/sulfide lined cracks and fissures. Although most of the cracks and fissures did not penetrate completely through the thickness of the inner coating (except in the specimen exposed to the lowest test temperature), sulfur-containing species were identified at the coating/substrate interface in multiple locations for all test temperatures, suggesting that interconnected networks of crack fissures existed to provided pathways for corrodent species to reach the substrate surface.

No evidence of nanocoating A3 was apparent on any of the specimens tested under superheater/reheater conditions. While complete spallation was observed during the metallographic preparation of the sample tested at 705ºC (1300ºF) or 815ºC (1500ºF), the fact that oxide and/or corrosion products covered the underlying substrate surface in all locations on every sample indicates that the coating did not afford adequate protection.

A4 (Figures 5-4 and 5-14)

Exposure to waterwall conditions (on 304 substrates) caused significant cracking in the nanocoating, with the vast majority of cracks propagating completely through the coating and terminating at the coating/substrate interface. While little bulk corrosion of the coating was evident on the specimens exposed at 455ºC (850ºF) and 525ºC (975ºF), severe wastage and exfoliation of the coating was apparent on the specimen tested at the highest exposure temperature - 593ºC (1100ºF).

Nanocoating A4 (on 91 substrates) displayed poor resistance to corrosion under the prescribed superheater/reheater conditions. While the coating was generally apparent in most locations along the surface of the specimen exposed to 595ºC (1100ºF), both significant wastage and severe cracking was prevalent. Exposure to the higher test temperatures caused complete consumption of the coating material in all locations and varying degrees of subsequent attack to the underlying substrate. The undulating surface profiles observed along the substrate surfaces indicated severe attack had occurred, suggesting that the coating provided little to no protection during the limited 600 hour exposure period.

A5 (Figure 5-15)

No testing was performed under waterwall conditions.

Little to no corrosion protection was afforded by nanocoating A5 upon exposure to synthetic superheater/reheater conditions as the coating was either entirely consumed or completely debonded from the substrate at all locations for all test temperatures. Wastage to the underlying substrate was relatively minor at 595ºC (1100ºF); however scattered pitting and moderately deep subsurface penetration of oxide and sulfide species was prevalent at the higher test temperatures.

B1 (Figures 5-5 and 5-16)

Nanocoating B1 sustained relatively shallow bulk corrosive attack due to exposure to waterwall conditions; however, for all test temperatures, numerous cracks and fissures (and a few scattered defects) were noted in the coating. The cracks generally penetrated completely through the thickness, ultimately terminating at the substrate/coating interface. In some places, shallow penetration of oxide and sulfide species was noted in the substrate material beneath the cracks and fissures.

As with most of the other coatings, nanocoating B1 experienced considerable degradation following exposure to superheater/reheater conditions. In addition to bulk wastage, which typically penetrated half-way through the coating thicknesss, the specimen tested at 595ºC (1100ºF) contained numerous through-wall cracks and fissures. Exposure to the higher testing temperatures generally resulted in complete consumption of the coating materials and subsequent attack to the underlying substrate, both in the form of bulk wastage (corrosion) and subsurface penetration of oxide and sulfide species.

B2 (Figures 5-6 and 5-17)

Nanocoating B2 remained relatively intact following exposure to waterwall conditions, as very little evidence of widespread corrosion and no evidence of complete spallation of the coating was noted. In several locations, however, pre-existing columnar grain boundaries and globular imperfections (much like those observed in the pre-characterization study) were lined with oxide and sulfur-containing corrosion products, some of which penetrated completely through the coating thickness. While the occurrence of shallow corrosion on the outermost surface of the coating tended to increase with increasing test temperature, the number of oxide/sulfide-lined fissures penetrating through the coating thickness was fairly consistent.

Nanocoating B2 exhibited very poor resistance to corrosion under the prescribed superheater/reheater conditions. Exposure to lowest test temperature caused severe through-wall cracking and complete coating wastage in numerous locations along the specimen surface. Testing at 705ºC (1300ºF) and 815ºC (1500ºF) resulted in complete consumption in most places and subsequent gross wall loss and severe subsurface penetration of oxides and sulfides.

B3 (Figures 5-7 and 5-18)

Exposure to waterwall conditions produced relatively minor gross corrosive attack in the form of shallow pits and depressions on nanocoating B3; however, several, corrosion-product lined, through-wall cracks were noted on all test specimens examined. Cracking was generally most prevalent at and near the corners of the specimens tested at 455ºC (850ºF) and 525ºC (975ºF),

and tended to decrease in number density with increasing distance from coupon edges. Although the number density and extent of cracking was typically less severe on the specimen tested at 595ºC (1100ºF), this specimen was peppered with profuse round, discrete oxide and sulfide particles that appeared be preferentially located along the faint outlines of columnar grain boundaries. No evidence of penetration into the substrate material was noted.

The B3 nanocoating specimens exposed to superheater/reheater conditions at 595ºC (1100ºF) and 705ºC (1300ºF) sustained considerable gross wastage in most locations. Wastage generally resulted in complete consumption of the coating material and subsequent wall loss to the underlying substrate. Subsurface penetration of oxygen and sulfur-rich species into the substrate was noted in most areas surrounding the wastage and in scattered location beneath the intact coating. The specimen tested at 815ºC (1500ºF) sustained relatively minor corrosion in most locations as evidenced by a continuous coating layer along the entire surface; however, some discrete oxide and sulfur-rich particles were evident in the substrate material beneath the coating suggesting penetration through the coating had occurred.

B4 (Figures 5-8 and 5-19)

For all test temperatures, exposure to waterwall conditions caused degradation of nanocoating B4 in the form of sulfide and oxide corrosion product-lined, through-wall cracks. While the cracks typically terminated at the coating/substrate interface, corrosion product-filled depressions formed in the substrate at the crack tip at several locations. The specimens tested at 455ºC (850ºF) and 525ºC (975ºF) also sustained relatively minor general wastage along the coating surface, which tended to highlight and, in some cases, follow along the columnar grain boundaries noted in the pre-characterization.

Exposure to synthetic superheater/reheater conditions resulted in severe corrosion of nanocoating B4 for all testing temperatures. Although the specimen tested at 595ºC (1100ºF) did not sustain complete wastage due to corrosion, several through-wall cracks and some shallow penetration of oxygen and sulfur-rich species into the substrate material were noted. Testing at higher temperatures generally resulted in complete coating loss and subsequent corrosive attack to the underlying substrate material. Even in areas even in areas where remnants of the nanocoating remained, severe penetration of oxygen and sulfur-rich species was noted in the substrate material.

B5 (Figures 5-9 and 5-20)

Nanocoating B5 sustained relatively shallow corrosive loss for all waterwall test conditions. Wastage generally propagated along the columnar grain boundaries and imperfections in the coating, and penetrated to varying depths. No evidence of corrosion and/or subsurface penetration into the substrate material was noted, however. While specimens exposed to 525ºC (975ºF) and 595ºC (1100ºF) contained some corrosion product lined cracks, the vast majority of these cracks were located at or near the edges (corners) of the coupon specimens with very few being noted along the faces.

Gross wastage of nanocoating B5 was noted for all test temperatures after exposure to superheater/reheater conditions. Although the extent of gross wastage on the coating material tended to decrease with increasing test temperature, degradation to the underlying substrate (due

to oxidation/sulfidation) was particularly severe on the specimen exposed to the highest temperature. Furthermore, while comparatively little wastage was noted on the specimen tested at 815ºC (1500ºF), EDS analysis indicated significant changes in the chemical composition of the coating and substrate material immediately beneath the coating. The nominal composition of the coating material was altered from 35Ni-30Cr-30Co-3Si-1Fe to 33Fe-25Ni-19Co-18Cr-2.5O-1.8Si, indicating considerable bulk diffusion occurred between the nanocoating and substrate material, which further suggests that the coating material may not have been stable at the test temperature. It should be mentioned that some diffusion of the substrate material into the coating was also noted in the sample(s) tested at 705ºC (1300ºF), but the extent of diffusion (and dilution) was not as severe as that observed in the 815ºC (1500ºF) specimen. Since coating B5 was not applied to a Haynes 230 substrate, the effect of a higher alloyed substrate material (with a low iron content) on the noted post-test compositional changes in the coating could not be evaluated.

B6 (Figures 5-10 and 5-21)

The surfaces of the nanocoating B6 specimens exposed to waterwall conditions were generally covered with oxide and/or corrosion products. Very little gross attack and subsurface penetration was noted in all places on the specimens tested at 455ºC (850ºF) and 595ºC (1100ºF), but the specimen exposed to 525ºC (975ºF) exhibited severe wastage in one location, ultimately resulting in complete consumption of the coating. Several, oxide and corrosion product-lined cracks and a few tight fissures were observed on all test specimens and generally penetrated completely through the coatings, terminating at the substrate coating interface. No significant attack to the underlying substrate material was observed.

Exposure to superheater/reheater conditions resulted in complete consumption of nanocoating B6 at all test temperature. Corrosion was particularly severe for specimens exposed to 705ºC (1300ºF) and 815ºC (1500ºF), such that no evidence of the coating remained and significant wastage of the underlying substrate material was observed following 600 hours of exposure. In addition to the gross wall loss, the substrate material also sustained considerable subsurface penetration of oxides and sulfides in most locations.

B7 (Figure 5-22)

No testing was performed under waterwall conditions.

Nanocoating B7 sustained considerable degradation upon exposure to the prescribed superheater/reheater conditions for all test temperatures. Complete coating loss due to gross corrosive attack was noted in numerous locations and generally resulted in severe bulk wall loss and subsurface penetration to the underlying substrate material. Furthermore even areas where the coating remained relatively intact exhibited significant ingress of oxide and sulfide species, which subsequently penetrated into the substrate material.

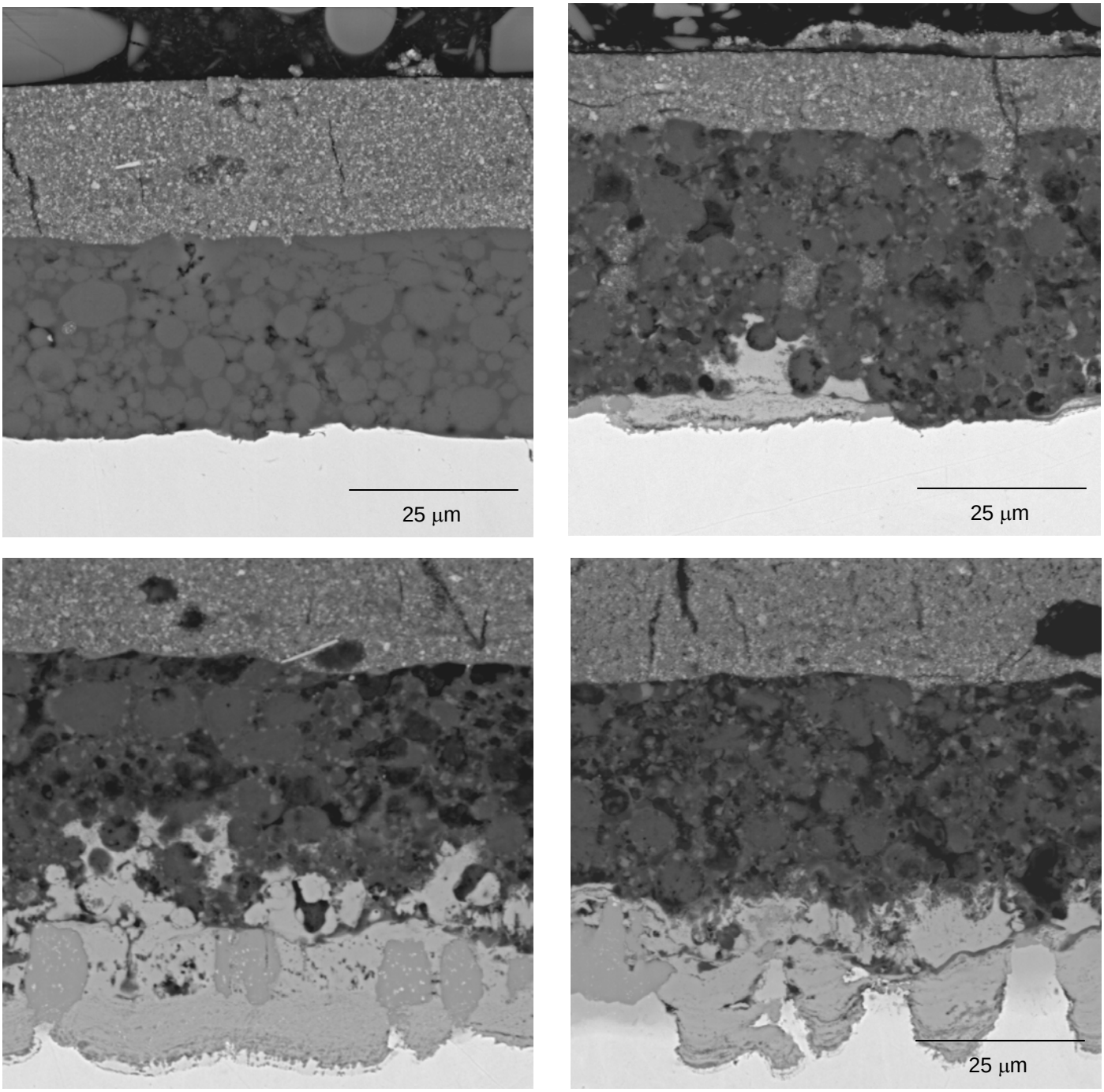

FIGURE 5-1
Representative Backscatter SEM Images of Nanocoating A1 on 91 Substrate Material in the As-received Condition (Top Left); after 1000 hrs at 850ºF (Top Right); after 1000 hrs at 975ºF (Bottom Left); after 1000 hrs at 1100ºF (Bottom Right)

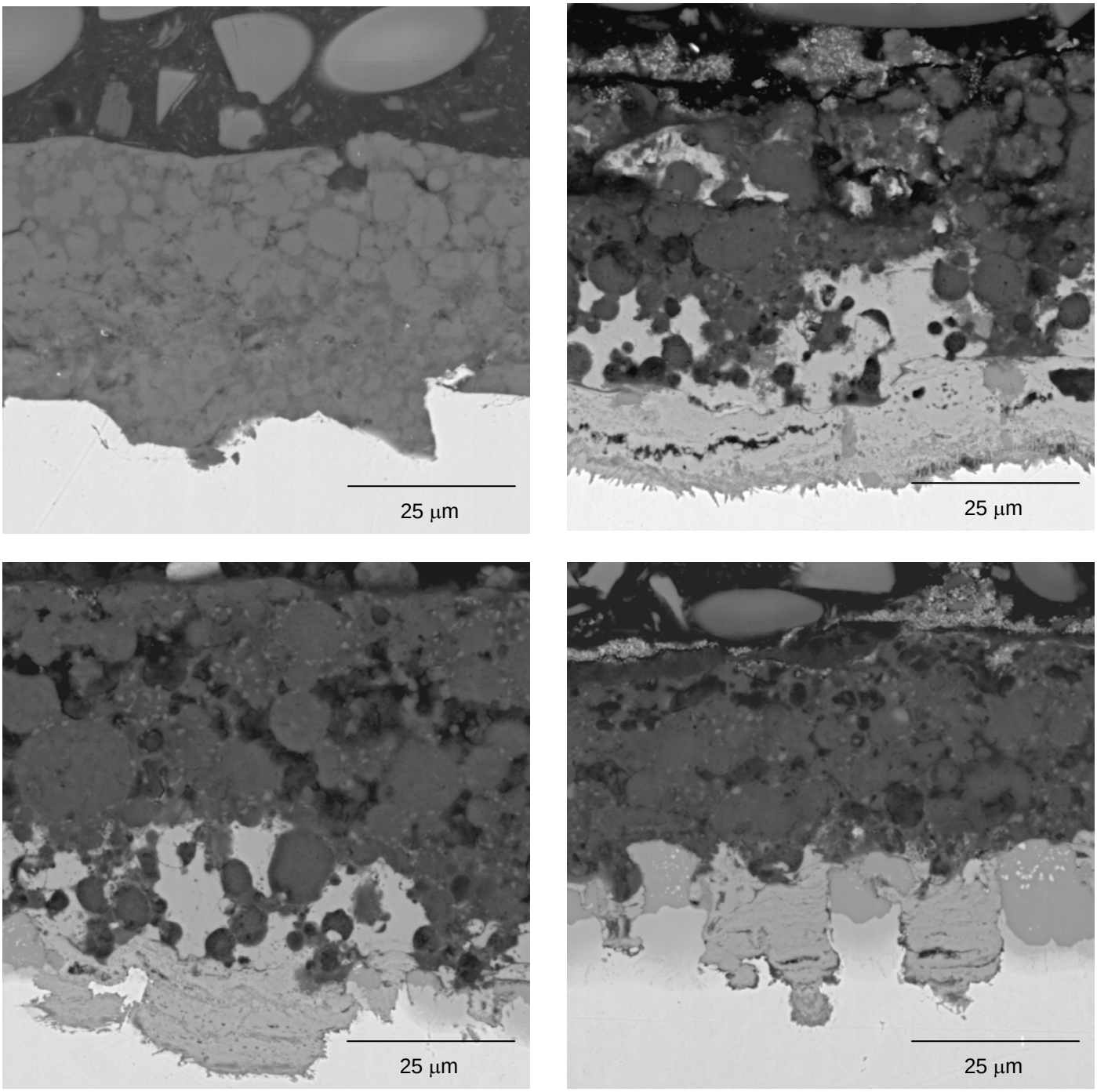

FIGURE 5-2
Representative Backscatter SEM Images of Nanocoating A1 on 91 Substrate Material in the As-received Condition (Top Left); after 1000 hrs at 850ºF (Top Right); after 1000 hrs at 975ºF (Bottom Left); after 1000 hrs at 1100ºF (Bottom Right)

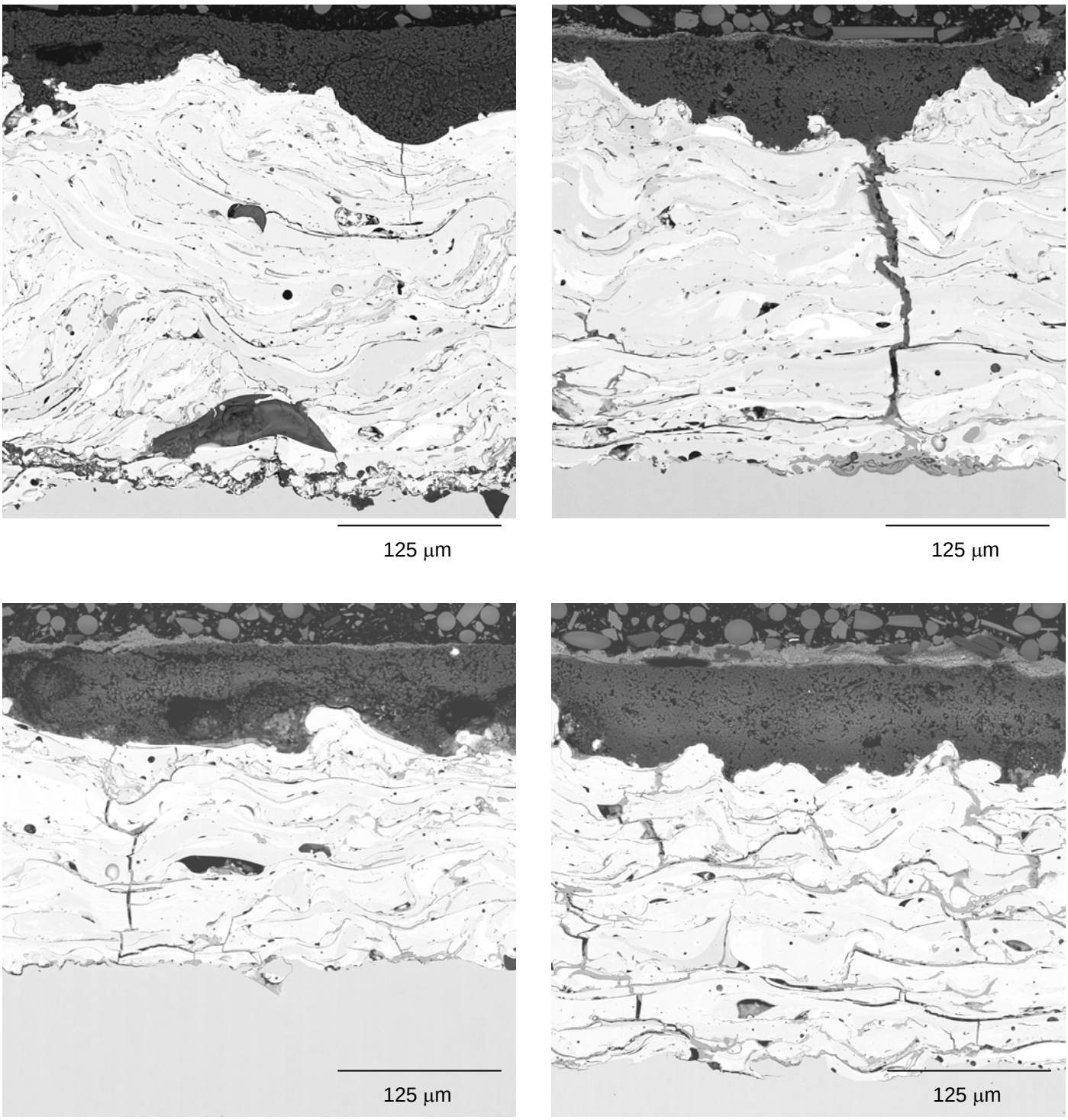

FIGURE 5-3
Representative Backscatter SEM Images of Nanocoating A3 on 91 Substrate Material in the As-received Condition (Top Left); after 1000 hrs at 850ºF (Top Right); after 1000 hrs at 975ºF(Bottom Left); after 1000 hrs at 1100ºF (Bottom Right)

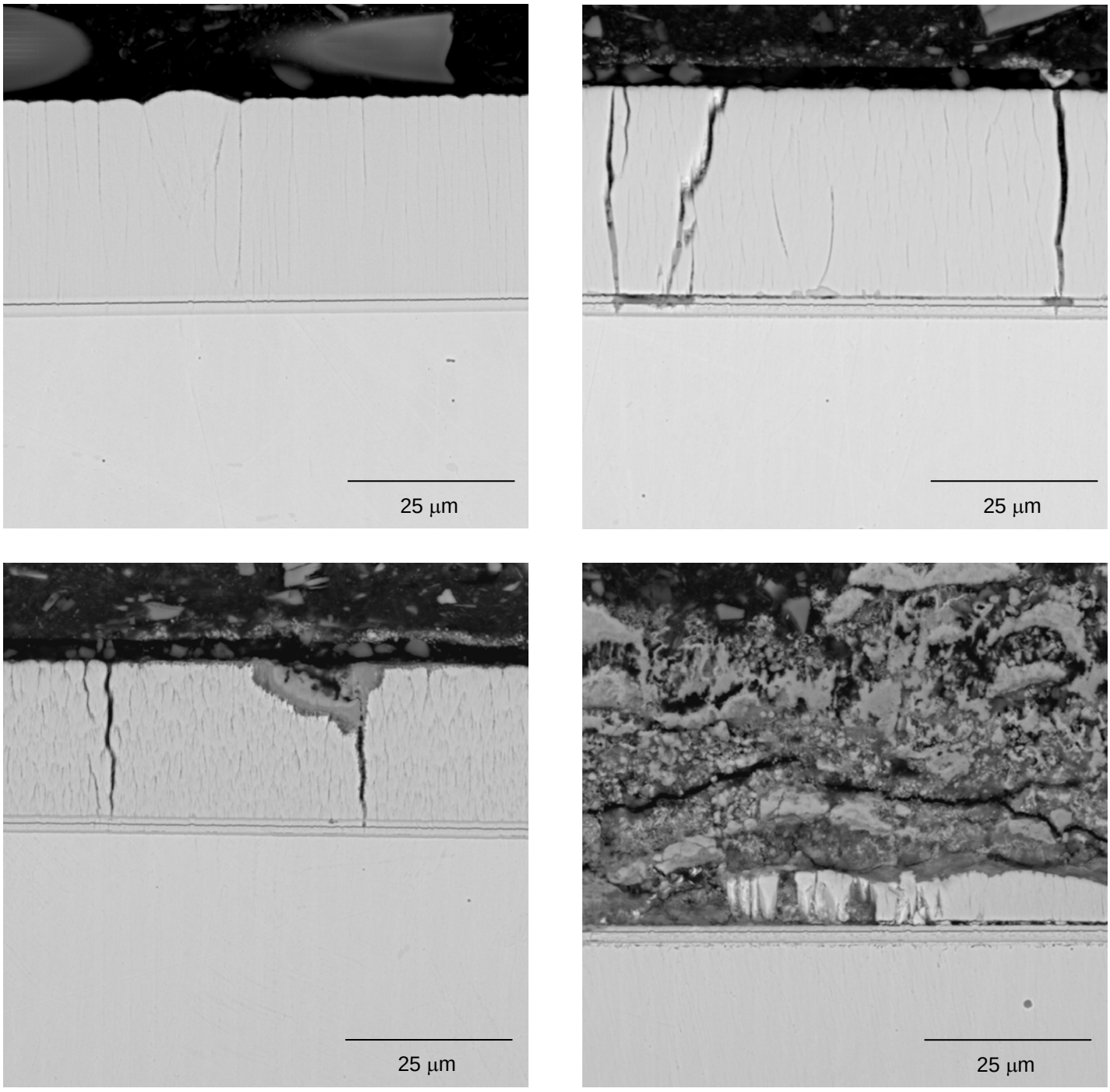

FIGURE 5-4
Representative Backscatter SEM Images of Nanocoating A4 on 304 Substrate Material in the As-received Condition (Top Left); after 600 hrs at 850ºF (Top Right); after 600 hrs at 975ºF (Bottom Left); after 600 hrs at 1100ºF (Bottom Right)

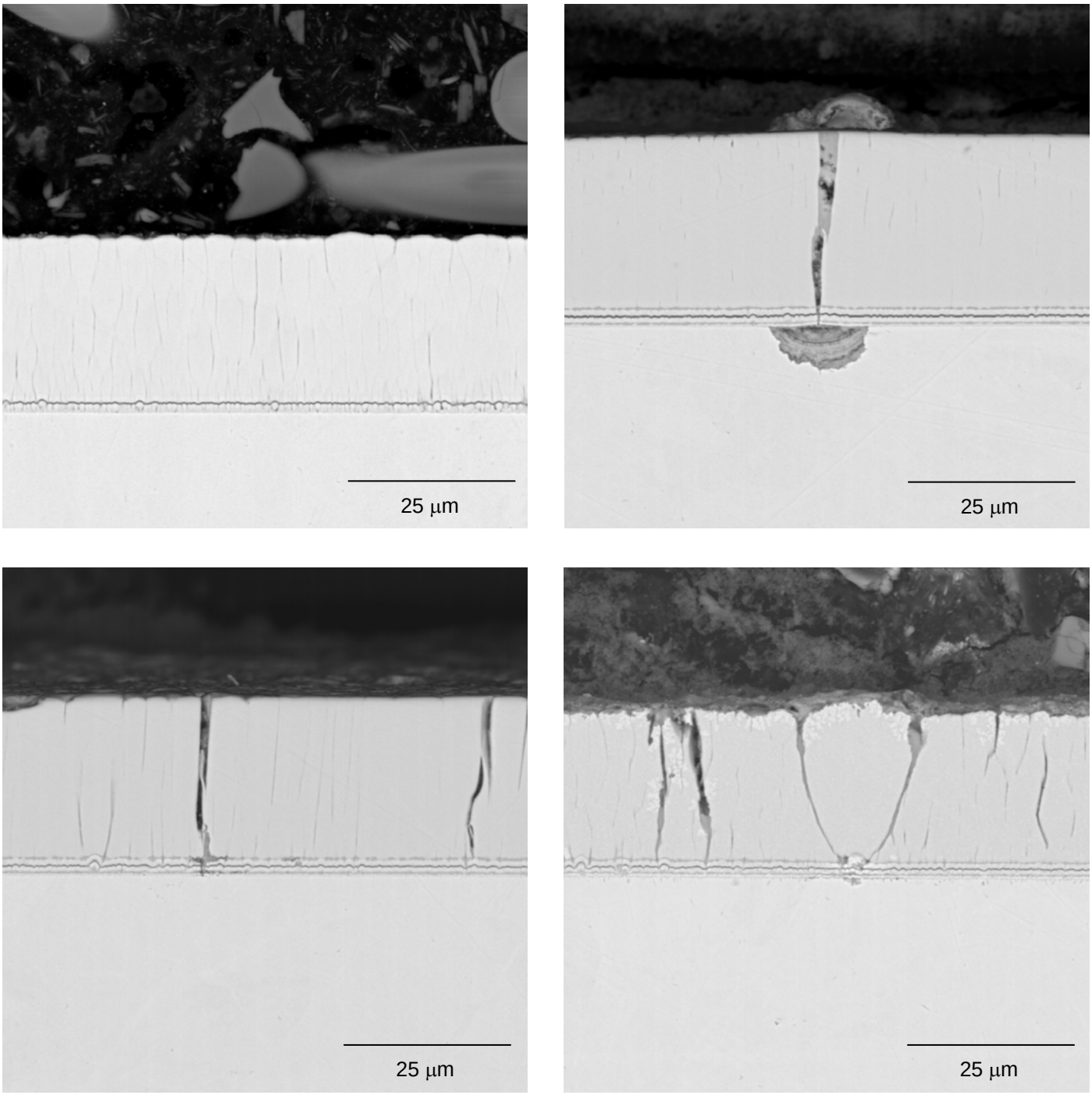

FIGURE 5-5
Representative Backscatter SEM Images of Nanocoating B1 on 91 Substrate Material in the As-received Condition (Top Left); after 600 hrs at 850ºF (Top Right); after 600 hrs at 975ºF (Bottom Left); after 1000 hrs at 1100ºF (Bottom Right)

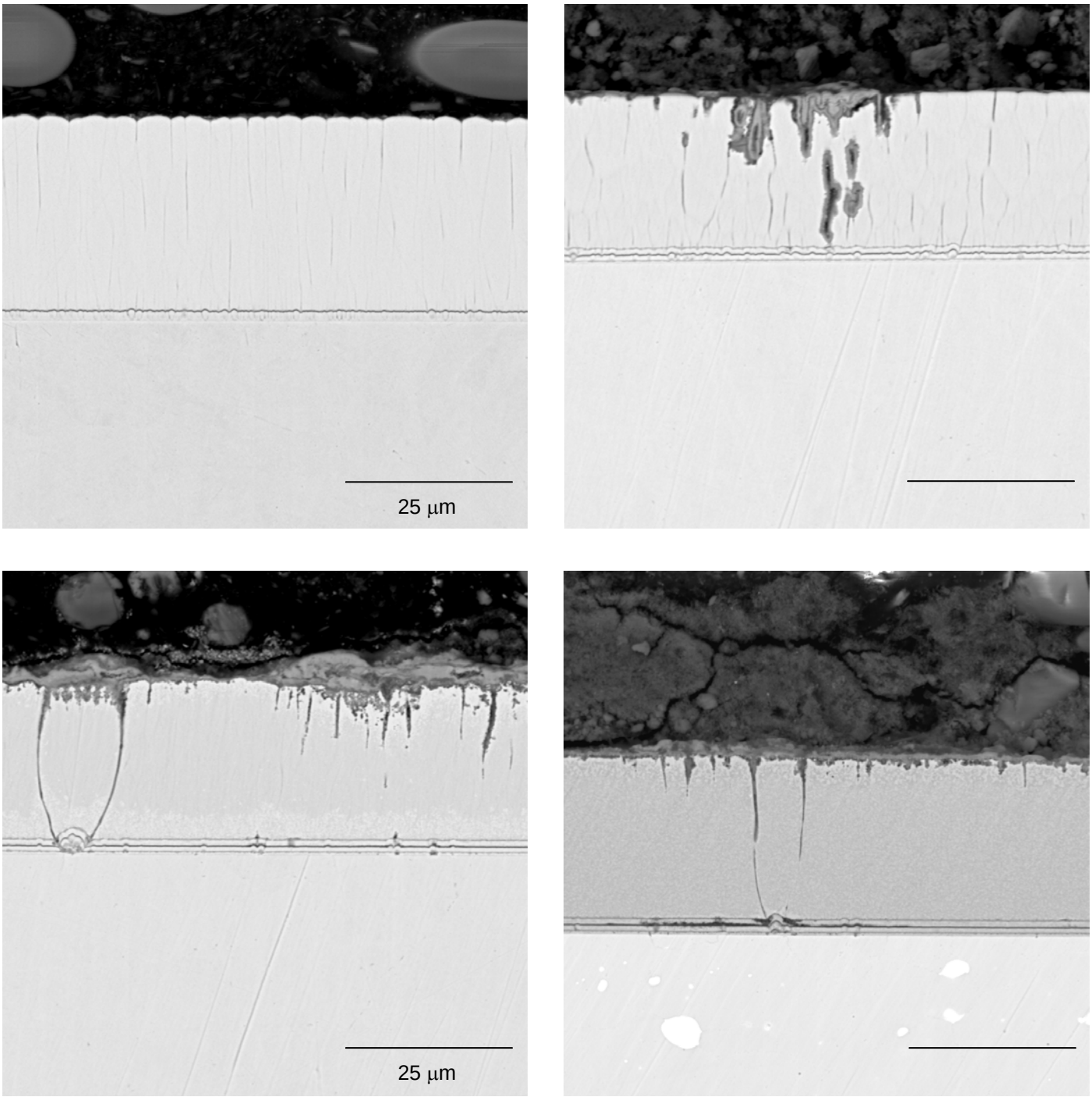

FIGURE 5-6
Representative Backscatter SEM Images of Nanocoating B2 on 91 Substrate Material in the As-received Condition (Top Left); after 1000 hrs at 850ºF (Top Right); after 1000 hrs at 975ºF (Bottom Left); after 1000 hrs at 1100ºF (Bottom Right)

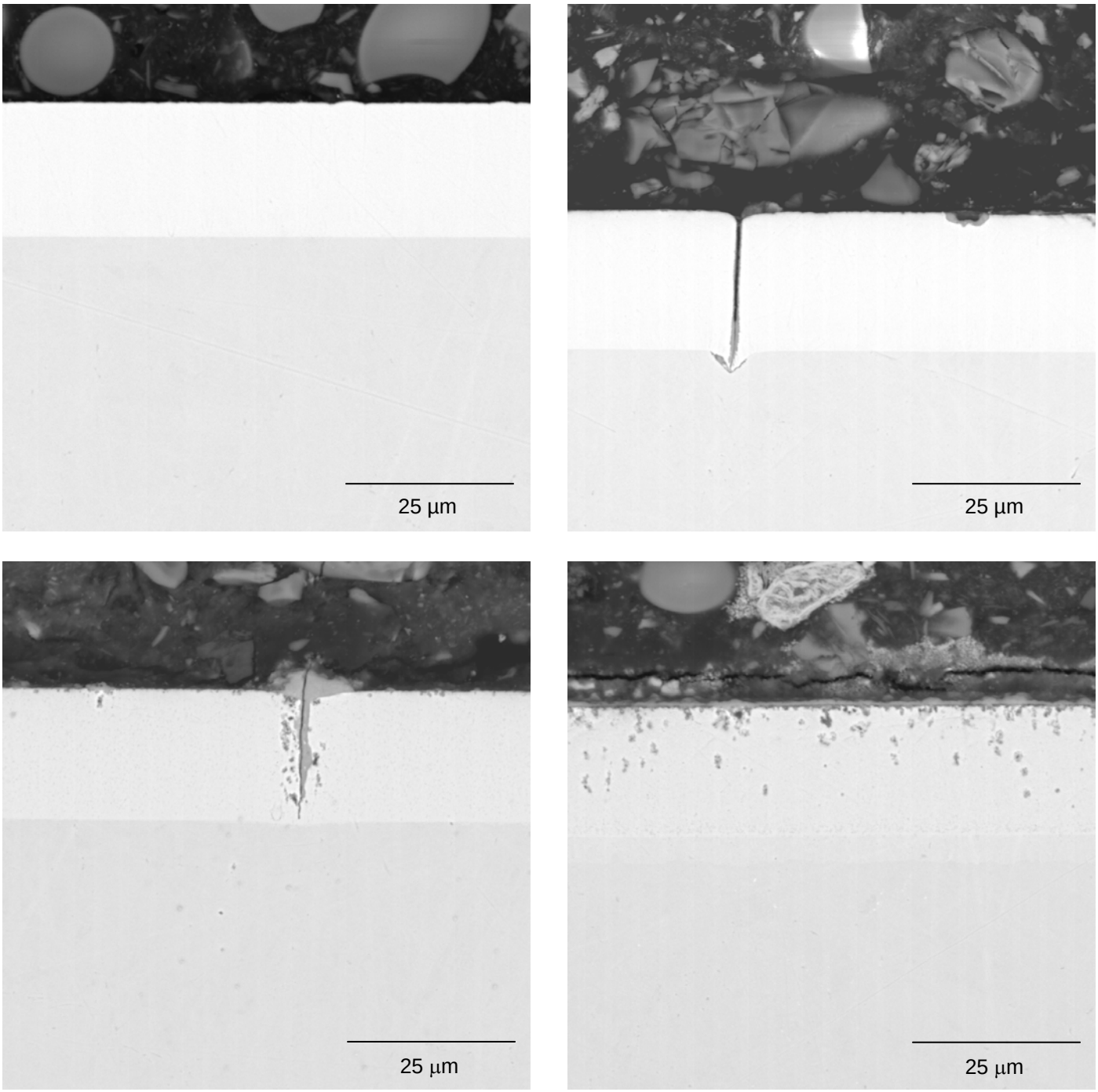

FIGURE 5-7
Representative Backscatter SEM Images of Nanocoating B3 on 91 Substrate Material in the As-received Condition (Top Left); after 1000 hrs at 850ºF (Top Right); after 1000 hrs at 975ºF (Bottom Left); after 1000 hrs at 1100ºF (Bottom Right)

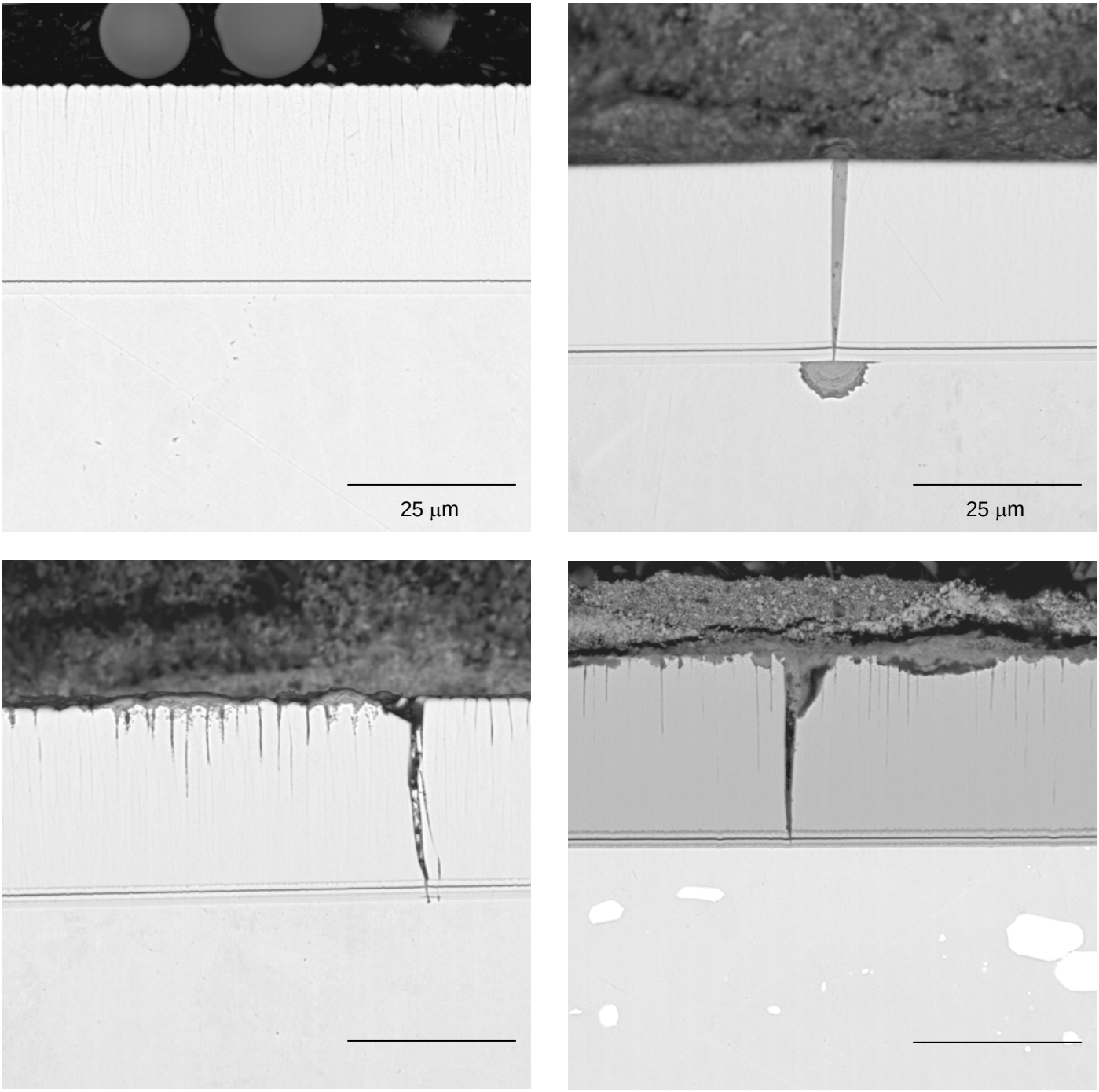

FIGURE 5-8
Representative Backscatter SEM Images of Nanocoating B4 on 91 Substrate Material in the As-received Condition (Top Left); after 600 hrs at 850ºF (Top Right); after 600 hrs at 975ºF (Bottom Left); after 1000 hrs at 1100ºF (Bottom Right)

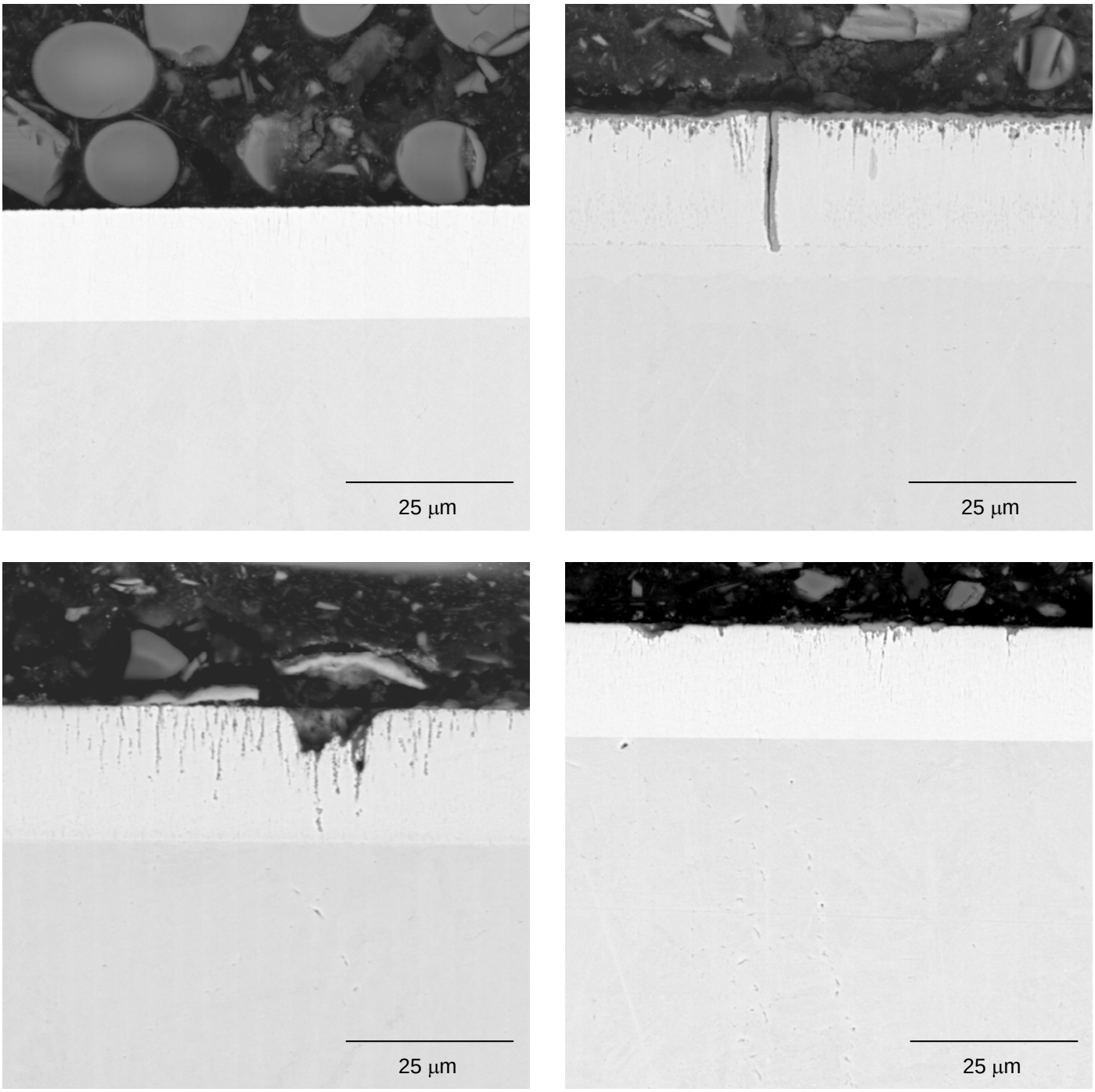

FIGURE 5-9
Representative Backscatter SEM Images of Nanocoating B5 on 91 Substrate Material in the As-received Condition (Top Left); after 600 hrs at 850ºF (Top Right); after 1000 hrs at 975ºF (Bottom Left); after 1000 hrs at 1100ºF (Bottom Right)

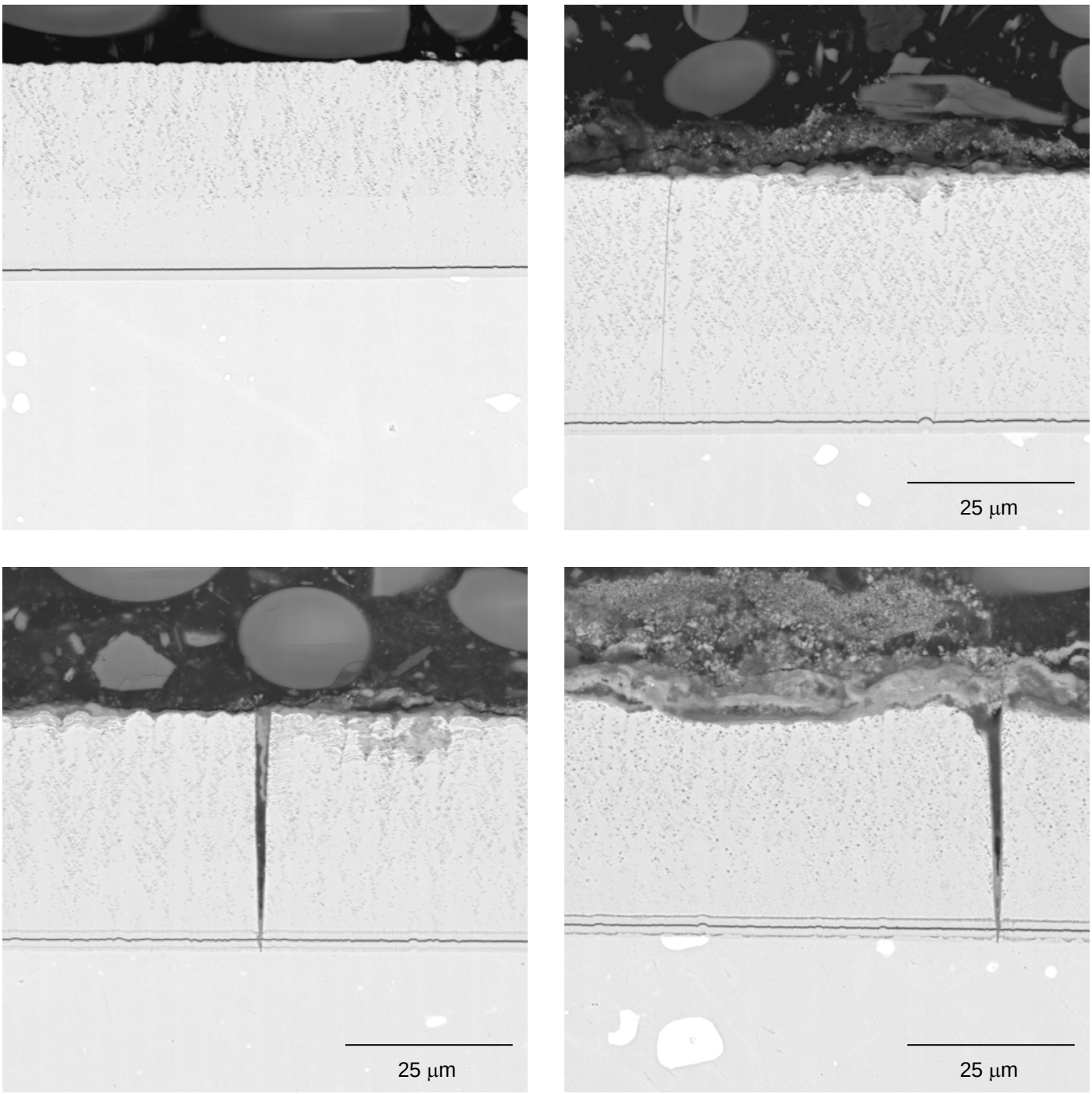

FIGURE 5-10
Representative Backscatter SEM Images of Nanocoating B6 on Haynes 230 Substrate Material in the As-received Condition (Top Left); after 600 hrs at 850ºF (Top Right); after 1000 hrs at 975ºF (Bottom Left); after 1000 hrs at 1100ºF (Bottom Right)

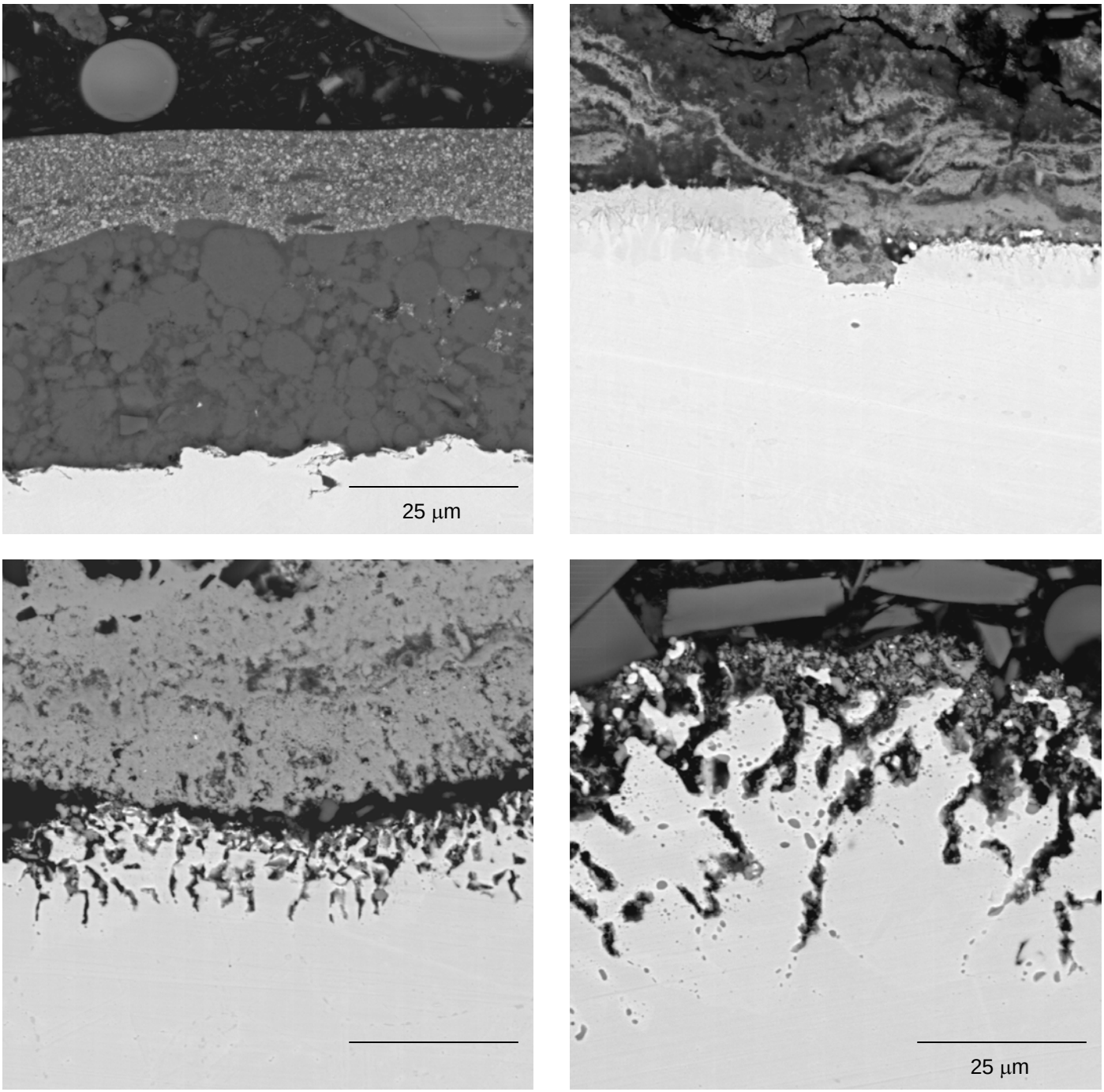

FIGURE 5-11
Representative Backscatter SEM Images of Nanocoating A1 on 304 Substrate Material in the As-received Condition (Top Left); after 600 hrs of Exposure to SH/RH Conditions at 1100ºF (Top Right); after 600 hrs of Exposure to SH/RH Conditions at 1300ºF (Bottom Left); after 600 hrs of Exposure to SH/RH Conditions at 1500ºF (Bottom Right)

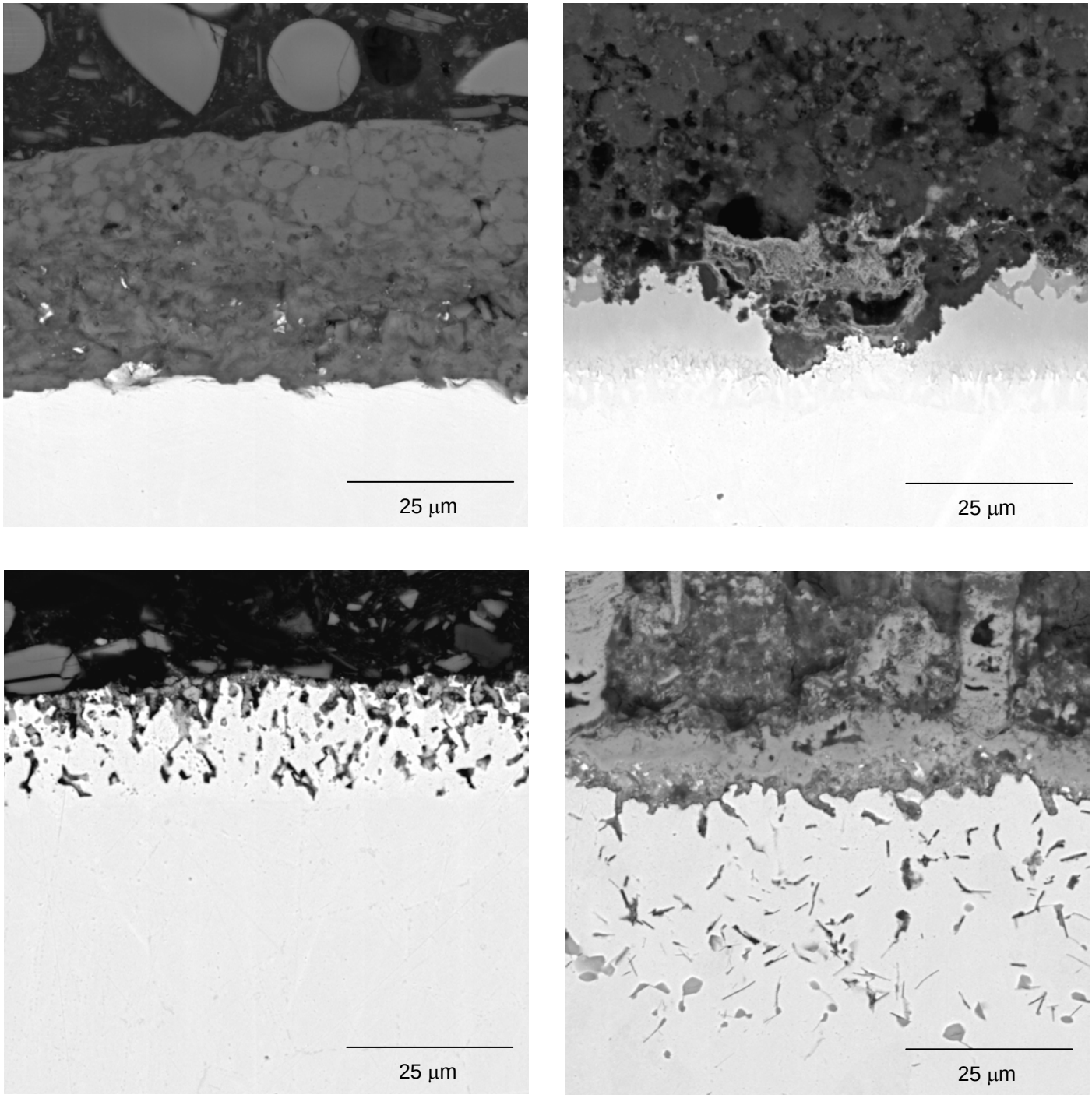

FIGURE 5-12
Representative Backscatter SEM Images of Nanocoating A2 on 304 Substrate Material in the As-received Condition (Top Left); after 600 hrs of Exposure to SH/RH Conditions at 1100ºF (Top Right); after 600 hrs of Exposure to SH/RH Conditions at 1300ºF (Bottom Left); after 600 hrs of Exposure to SH/RH Conditions at 1500ºF (Bottom Right)

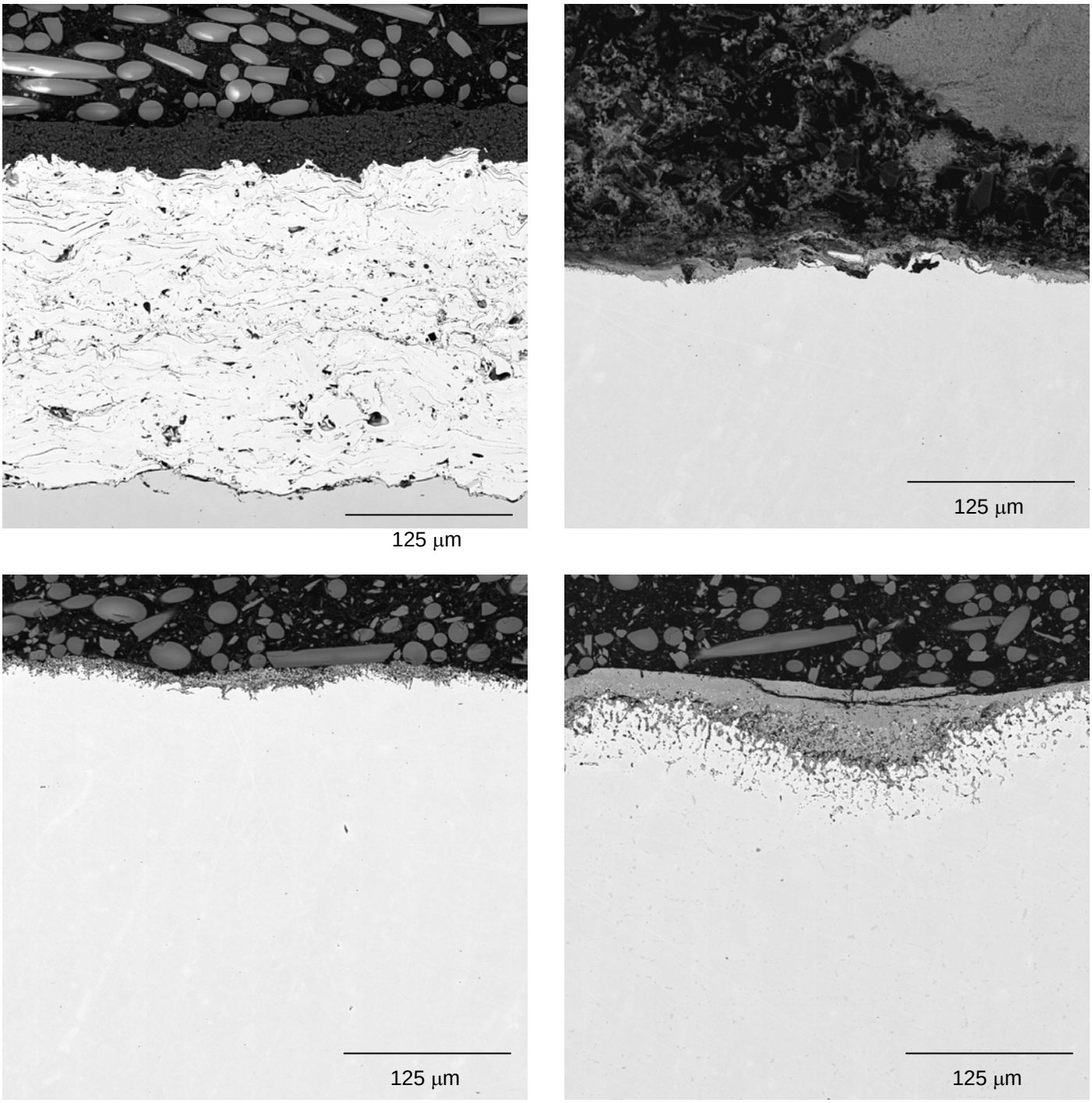

FIGURE 5-13
Representative Backscatter SEM Images of Nanocoating A3 on 304 Substrate Material in the As-received Condition (Top Left); after 1000 hrs of Exposure to SH/RH Conditions at 1100ºF (Top Right); after 600 hrs of Exposure to SH/RH Conditions at 1300ºF (Bottom Left); after 600 hrs of Exposure to SH/RH Conditions at 1500ºF (Bottom Right)

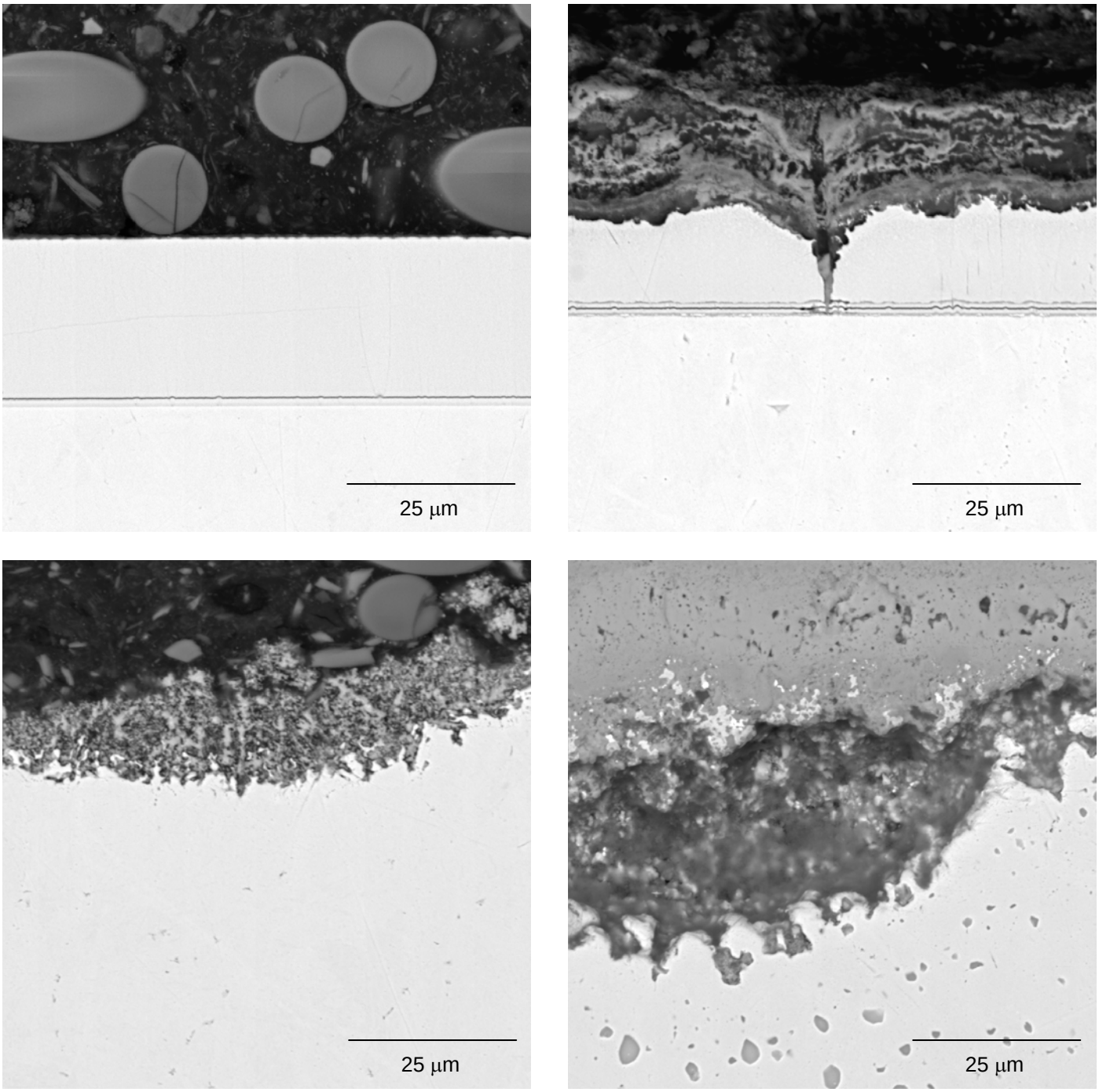

FIGURE 5-14
Representative Backscatter SEM Images of Nanocoating A4 on 91 Substrate Material in the As-received Condition (Top Left); after 600 hrs of Exposure to SH/RH Conditions at 1100ºF (Top Right); after 600 hrs of Exposure to SH/RH Conditions at 1300ºF (Bottom Left); after 600 hrs of Exposure to SH/RH Conditions at 1500ºF (Bottom Right)

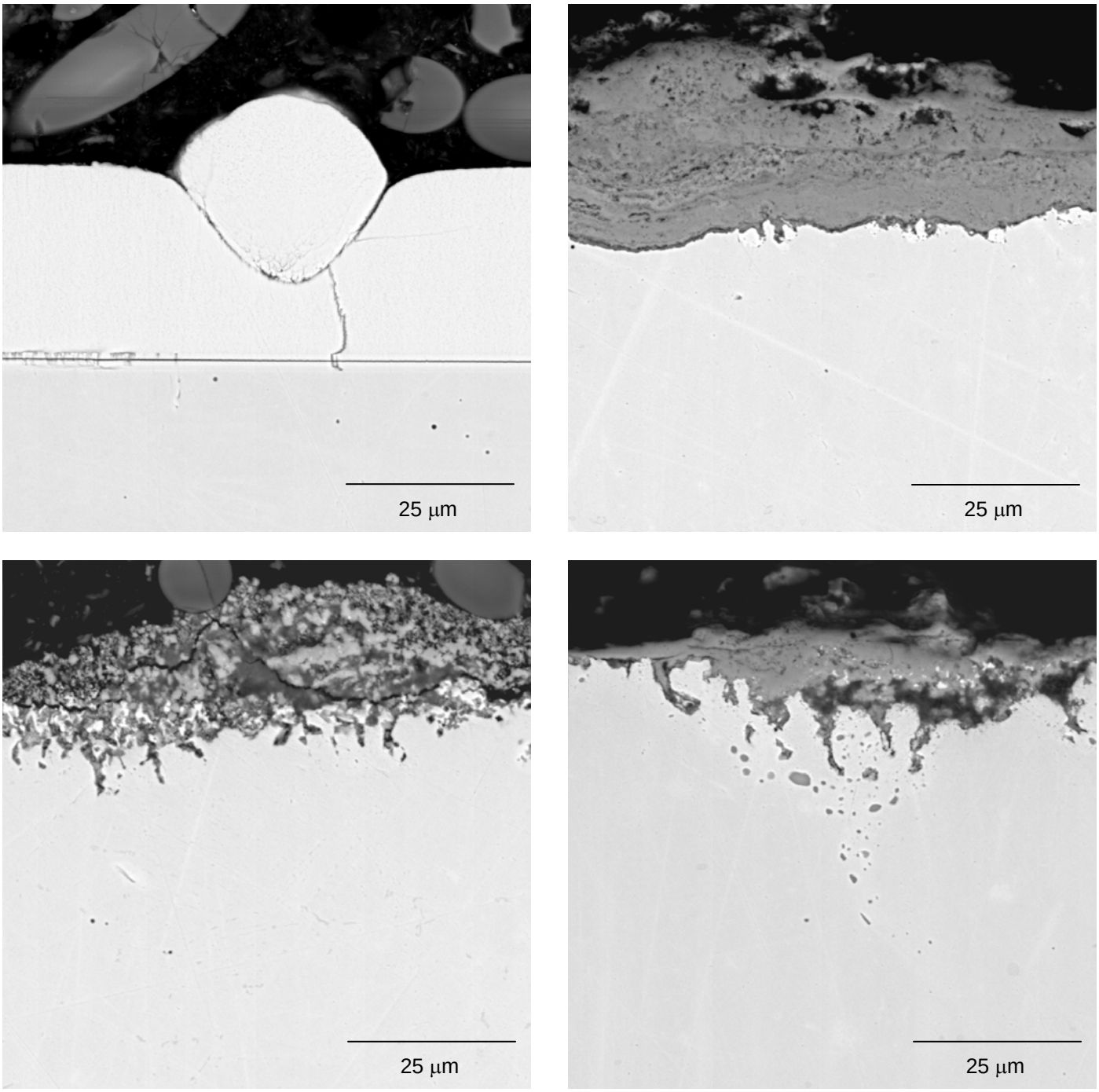

FIGURE 5-15
Representative Backscatter SEM Images of Nanocoating A5 on 304 Substrate Material in the As-received Condition (Top Left); after 600 hrs of Exposure to SH/RH Conditions at 1100ºF (Top Right); after 600 hrs of Exposure to SH/RH Conditions at 1300ºF (Bottom Left); after 600 hrs of Exposure to SH/RH Conditions at 1500ºF (Bottom Right)

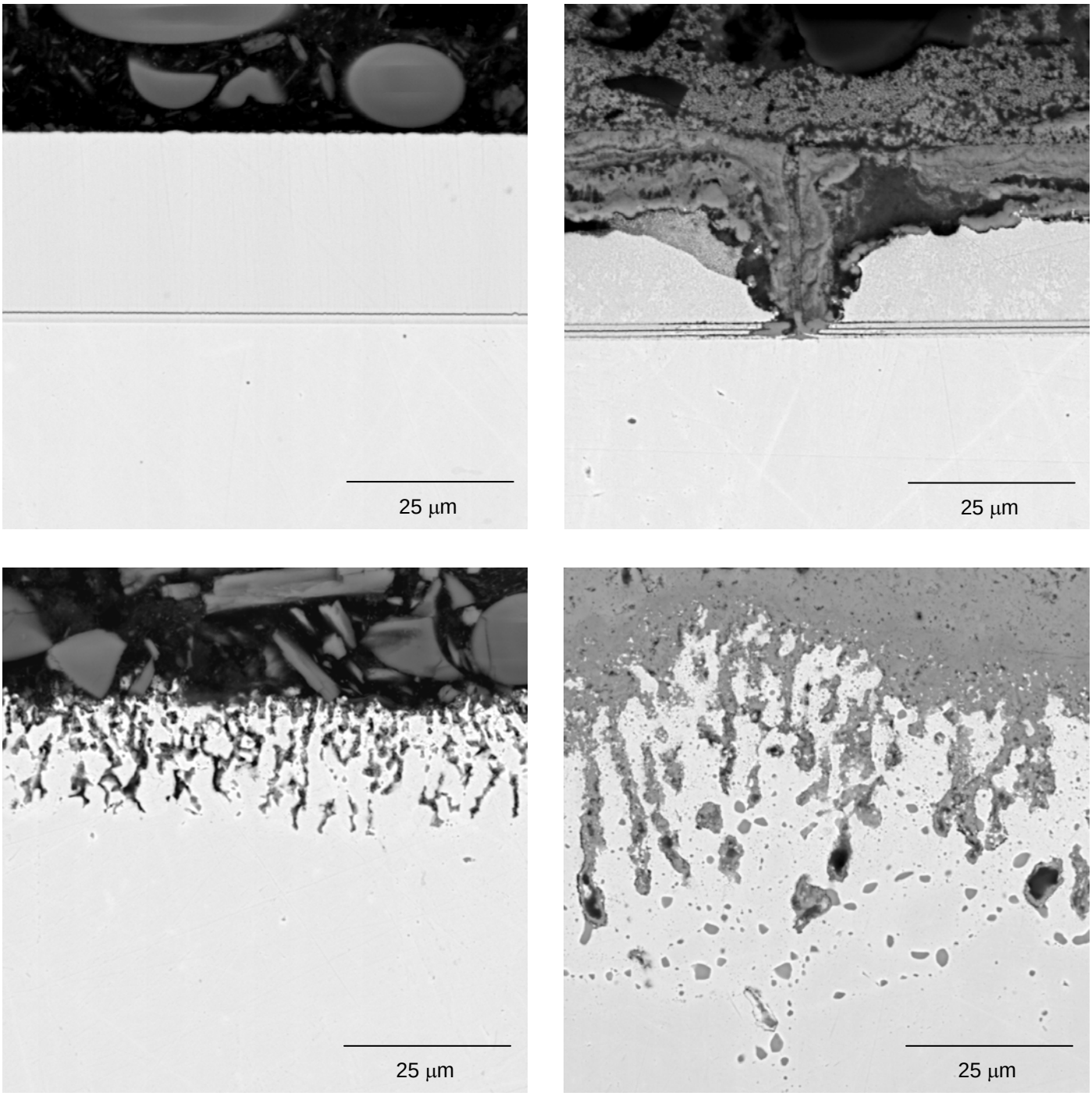

FIGURE 5-16
Representative Backscatter SEM Images of Nanocoating B1 on 304 Substrate Material in the As-received Condition (Top Left); after 600 hrs of Exposure to SH/RH Conditions at 1100ºF (Top Right); after 600 hrs of Exposure to SH/RH Conditions at 1300ºF (Bottom Left); after 600 hrs of Exposure to SH/RH Conditions at 1500ºF (Bottom Right)

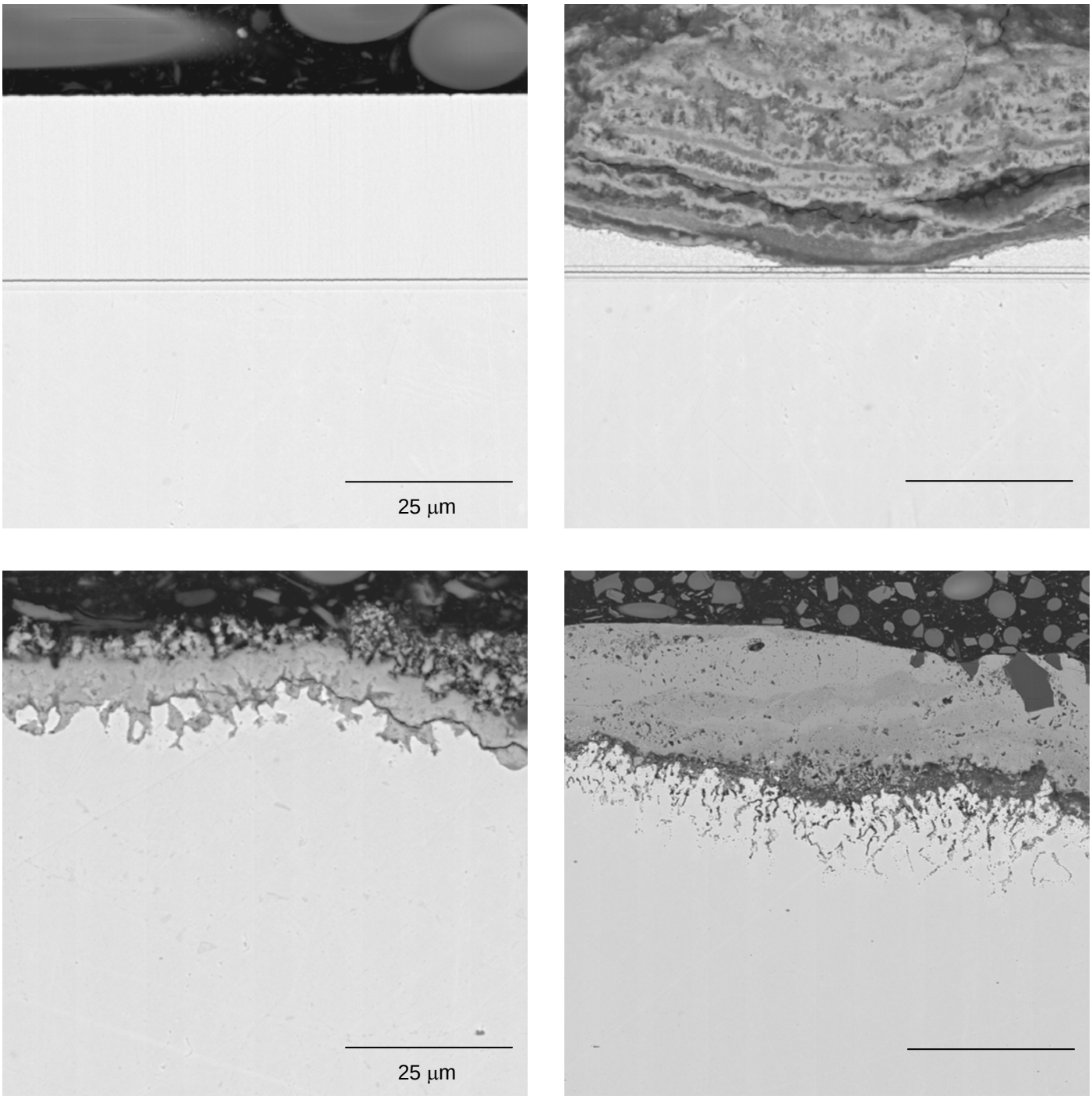

FIGURE 5-17
Representative Backscatter SEM Images of Nanocoating B2 on 304 Substrate Material in the As-received Condition (Top Left); after 600 hrs of Exposure to SH/RH Conditions at 1100ºF (Top Right); after 600 hrs of Exposure to SH/RH Conditions at 1300ºF (Bottom Left); after 600 hrs of Exposure to SH/RH Conditions at 1500ºF (Bottom Right)

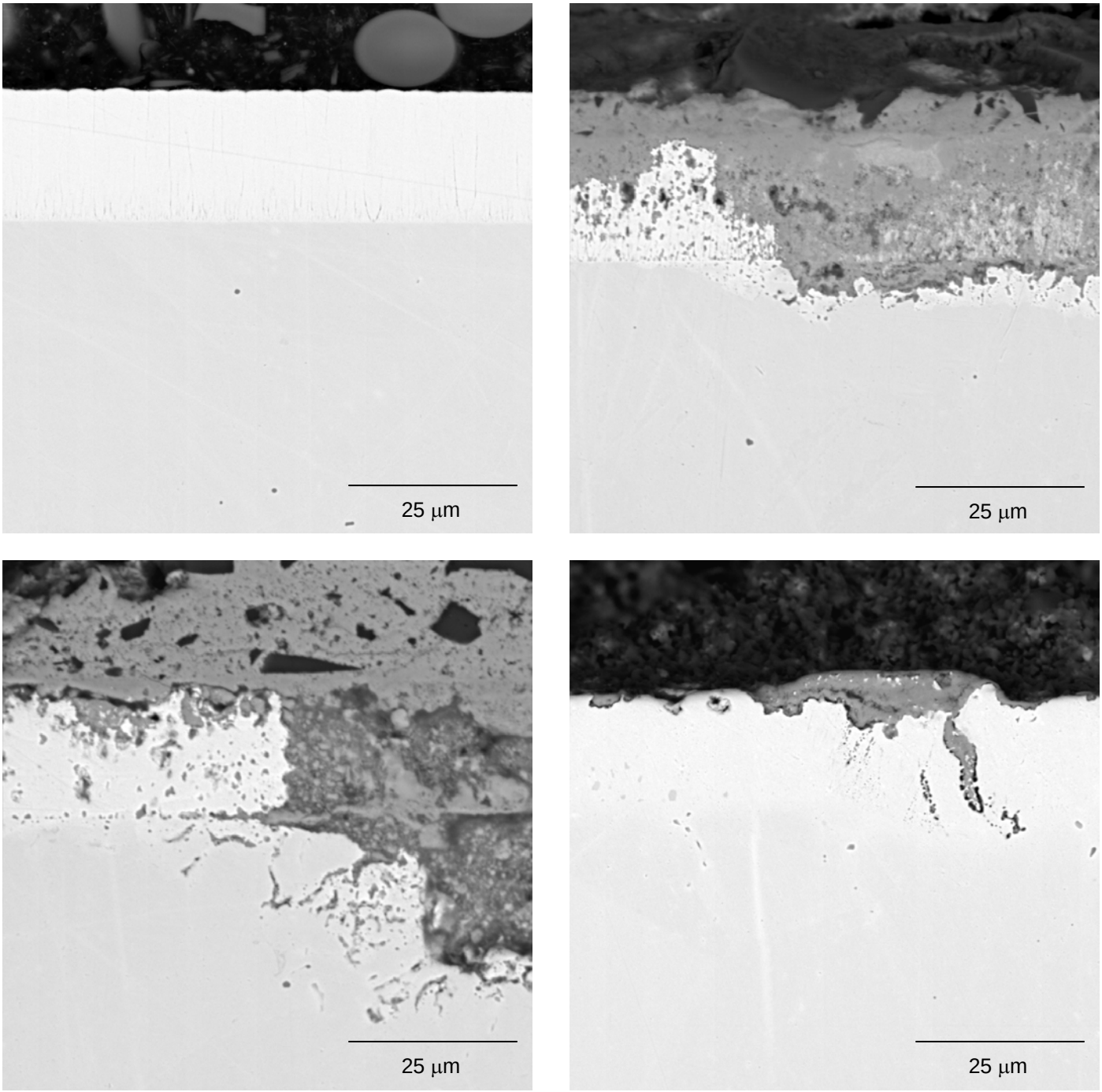

FIGURE 5-18
Representative Backscatter SEM Images of Nanocoating B3 on 304 Substrate Material in the As-received Condition (Top Left); after 600 hrs of Exposure to SH/RH Conditions at 1100ºF (Top Right); after 600 hrs of Exposure to SH/RH Conditions at 1300ºF (Bottom Left); after 600 hrs of Exposure to SH/RH Conditions at 1500ºF (Bottom Right)

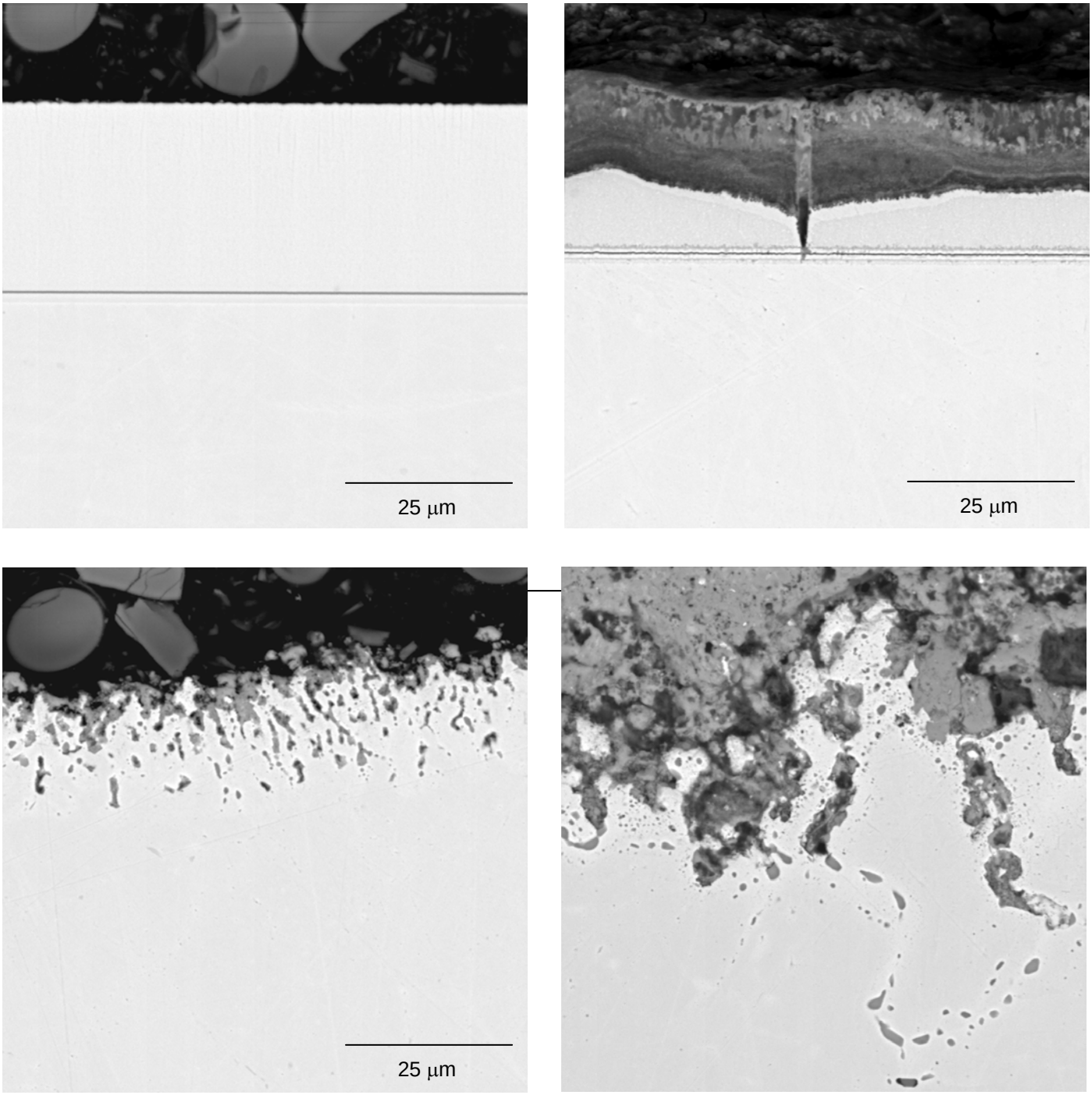

FIGURE 5-19
Representative Backscatter SEM Images of Nanocoating B4 on 304 Substrate Material in the As-received Condition (Top Left); after 600 hrs of Exposure to SH/RH Conditions at 1100ºF (Top Right); after 600 hrs of Exposure to SH/RH Conditions at 1300ºF (Bottom Left); after 600 hrs of Exposure to SH/RH Conditions at 1500ºF (Bottom Right)

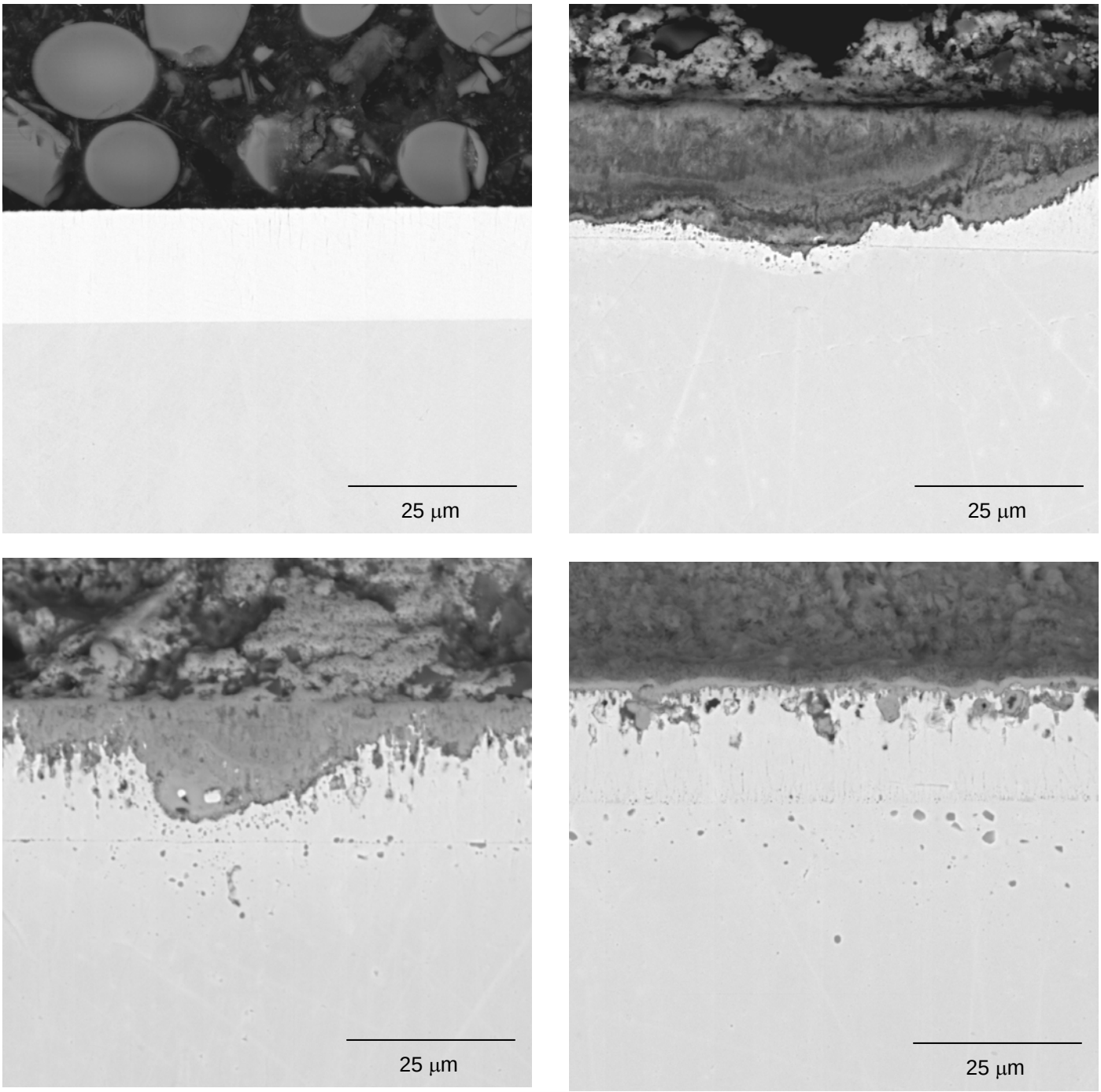

FIGURE 5-20
Representative Backscatter SEM Images of Nanocoating B5 on 304 Substrate Material in the As-received Condition (Top Left); after 600 hrs of Exposure to SH/RH Conditions at 1100ºF (Top Right); after 600 hrs of Exposure to SH/RH Conditions at 1300ºF (Bottom Left); after 600 hrs of Exposure to SH/RH Conditions at 1500ºF (Bottom Right)

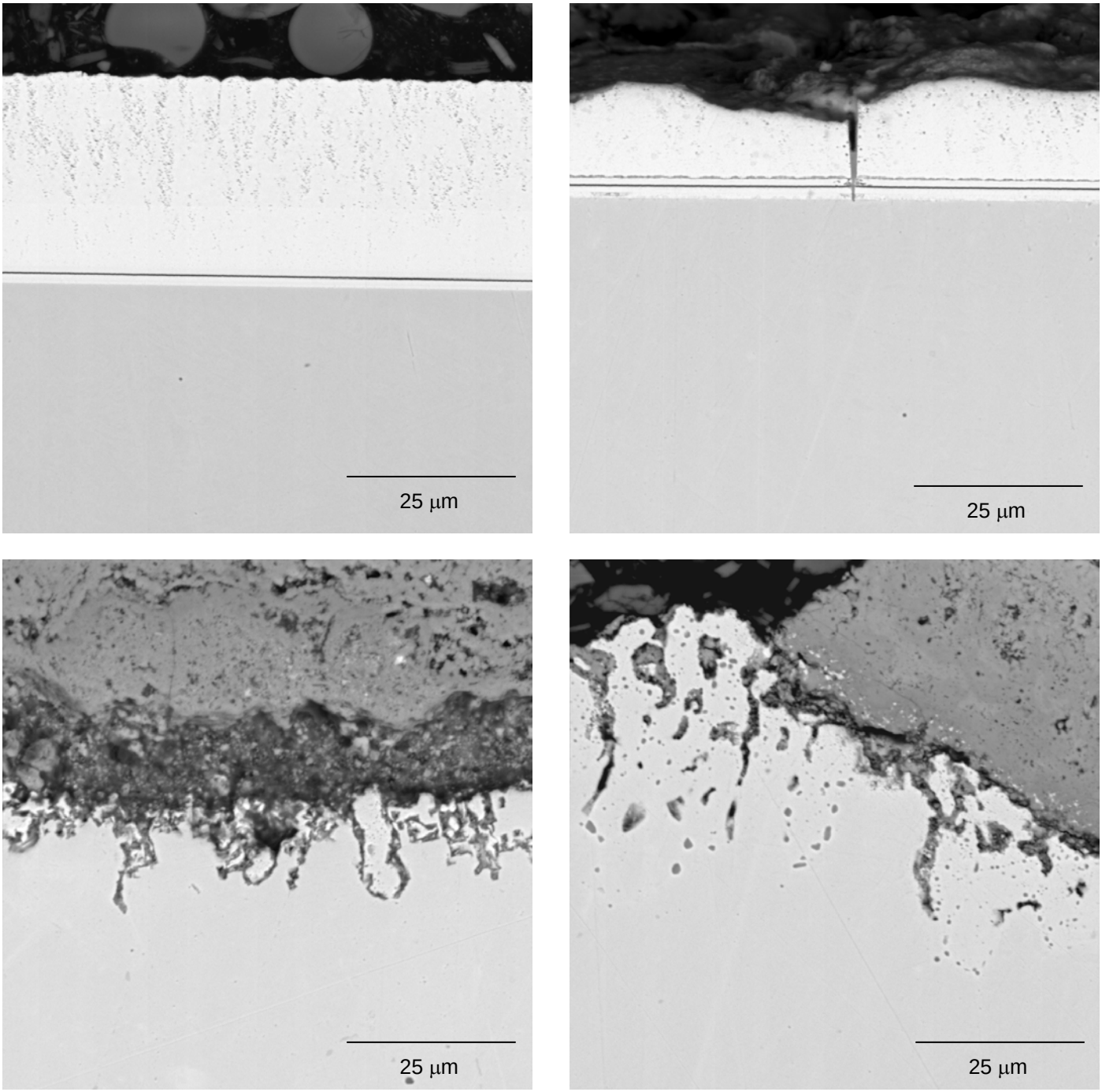

FIGURE 5-21
Representative Backscatter SEM Images of Nanocoating B6 on 304 Substrate Material in the As-received Condition (Top Left); after 600 hrs of Exposure to SH/RH Conditions at 1100ºF (Top Right); after 600 hrs of Exposure to SH/RH Conditions at 1300ºF (Bottom Left); after 600 hrs of Exposure to SH/RH Conditions at 1500ºF (Bottom Right)

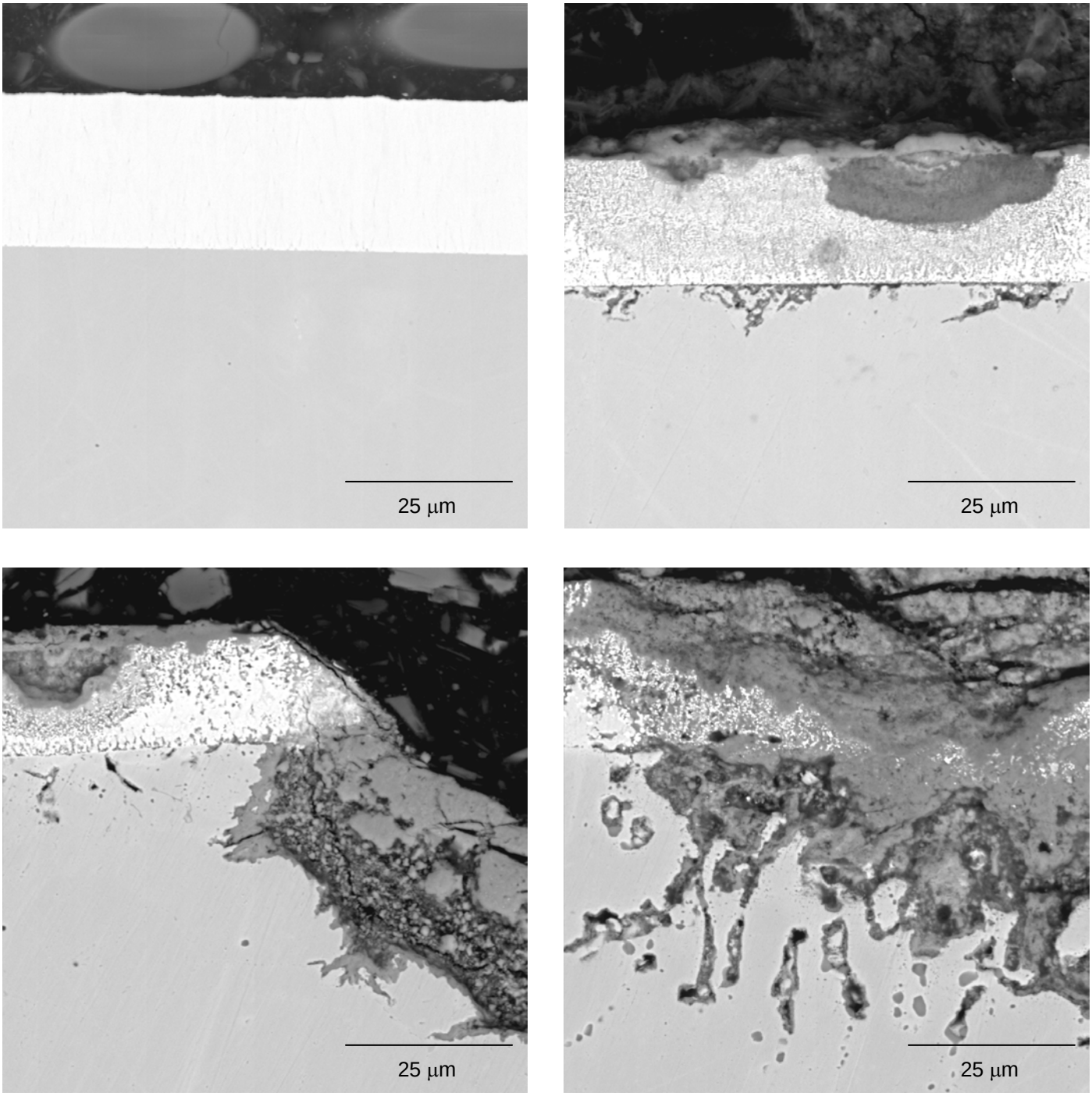

FIGURE 5-22
Representative Backscatter SEM Images of Nanocoating B7 on 304 Substrate Material in the As-received Condition (Top Left); after 600 hrs of Exposure to SH/RH Conditions at 1100ºF (Top Right); after 600 hrs of Exposure to SH/RH Conditions at 1300ºF (Bottom Left); after 600 hrs of Exposure to SH/RH Conditions at 1500ºF (Bottom Right)

6
SUMMARY AND CONCLUSIONS

Laboratory corrosion testing was performed on various nanostructured coating materials in order to qualitatively assess the fireside corrosion resistance of these materials upon exposure to synthetic fireside environments typical of those that will most likely exist in the furnace and heat recovery areas of an A-USC boiler burning moderately aggressive coals. In order to generate a basic understanding of the high temperature corrosion behavior of the nanocoating materials screening tests were initially conducted on select coatings, which were subsequently exposed for 100 hours to aggressive ash deposits at temperature within the range set for the 1000 hour tests. The data obtained was then used to optimize the test parameters (deposit, gas and temperature conditions) for the 1000 hour tests. The less than desirable results obtained from the 100-hour screening tests dictated that the aggressiveness of the deposit compositions needed to be scaled back. Even with a reduction in the aggressiveness of the deposits, visible evidence of distress was noted on many of the nanocoating coupons prior completion of the 1000 hour test, resulting in removal of most of the superheater/reheater coatings and several waterwall coatings after only 600 hours of testing.

Based on the results of the testing program, the following general conclusions can be drawn:

1. From a structural standpoint, most of the nanocoating materials contained a high concentration of columnar grain boundaries and scattered flaws/defects/morphological features, which were revealed in the pre-test examination/characterization. While the vast majority of these "features" did not overtly compromise the integrity of the coating (no cracking was noted in the as-supplied conditions), the extreme thinness coupled with the high number density of columnar grain boundaries and flaws/imperfections most likely provided pathways for corrosive constituents to diffuse to the interface.

2. Coatings tested under waterwall conditions generally exhibited considerably less bulk corrosion/wastage that those tested under superheater/reheater conditions; however, most if not all of the coatings displayed visual evidence of degradation for all test conditions. Coatings exposed to superheater/reheater conditions generally exhibited severe bulk corrosion resulting in complete coating consumption and subsequent attack of the substrate material.

With specific regards to testing under waterwall conditions:

1. Degradation was mainly in the form of cracks and fissures, and to a lesser extent general coating material loss; the cracks/fissures tended to follow along preexisting morphological features such as the columnar grain boundaries and/or globular imperfections.

2. Coatings A1 and A2, which had a mottled appearance, were relatively porous and, as such, provided little to no protection against oxidation/sulfidation of the underlying substarte material, even at the lowest test temperatures.

3. The dense, uniform coatings, specifically those containing more than 20% Cr, such as B1 - B6, generally resisted widespread corrosive attack, but were susceptible to cracking and spallation. On several samples, namely B2, B4, B5, and B6 evidence of oxide and sulfide species was noted along the columnar grain boundaries and gross imperfections.

4. When bulk corrosion was observed, the depth and extent of attack seemingly increased with increasing test temperature.

5. In general, most of the dense coatings (A4, B1 – B6) provided some level of protection to the underlying substrate for the prescribed test conditions, suggesting that they could potentially be considered for waterwall applications where enhanced corrosion protection is required on a short-term basis. However, given that all of these coatings displayed some degree of distress after relatively short exposure times to mildly aggressive ash conditions, and because the coatings are much thinner (compared to conventional coatings such as weld overlays and thermal sprays) and contain pre-existing "flaws", it is unlikely that they would provide continuous long-term protection under A-USC conditions.

With respect to superheater/reheater conditions:

1. All of the nanocoating materials exhibited severe corrosion (complete consumption) and subsequent wastage (gross loss and/or subsurface penetration of oxide and sulfide species) to the underlying substrate.

2. Bulk corrosive loss generally increased with increasing test temperatures; however, some coating materials, such as B3 and B5, resisted attack at the highest test temperature, but were completely consumed in multiple locations upon exposure to the lower test temperatures.

3. Following exposure to 705ºC (1300ºF) and 815ºC (1500ºF), the bulk composition of coating B5 contained higher concentrations of Fe and lesser amounts of Cr and Ni, relative to the initial pre-exposed composition. This indicates that bulk diffusion had occurred between the nanocoating and substrate material. Therefore, use of nanocoatings at temperatures greater than about 705ºC (1300ºF) for long-times may require additional development work to eliminate or reduce diffusion into the substrate.

4. Based on the results of the 100-hour screening tests and 1000-hour corrosion tests, none of the nanocoating materials evaluated in this test program would be acceptable for use as a protective, corrosion-resistant coating for superheater/reheater materials in an A-USC plant. More research and development is clearly needed to provide adequate corrosion protection even at the metal temperatures [595ºC (1100ºF)] routinely expected in a supercritical or high pressure subcritical boiler.

In summary, the commercial nanocoatings evaluated in this work show morphological features which are microscopic in scale. The laboratory tests show that the corrosion resistance of these coatings is relatively poor for both synthetic waterwall and superheater/reheater conditions. The nanocoatings developed as part of this U.S. Department of Energy supported program (B-series)

shows signs of being protective under waterwall conditions but not under superheater/reheater conditions. The major source of attack is attributed to defects and/or columnar structures in the nanocoatings which provide areas for localized corrosion attack. Additionally, at temperatures greater than about 705ºC (1300ºF) for long exposure times, interdiffusion between the nanocoating and the substrate material may cause significant changes in the composition of some of the nanocoatings, thus adversely affecting their corrosion resistance. Further research and development is required to (a) address the sources of defects in the nanocoatings to minimize or eliminate their formation and (b) provide a solution to interdiffusion with the substrate material. Re-testing of crack-free dense adherent defect-free coatings is warranted to assess the applicability of these developed nanocoatings for USC boiler conditions.

7
REFERENCES

1. M.S. Gagliano, H. Hack, G. S. Stanko, *Fireside Corrosion Resistance of Proposed USC Superheater and Reheater Materials: Laboratory and Field Test Results*, The 33rd International Technical Conference on Coal Utilization & Fuel Systems, June 1 - 5, 2008, Clearwater, Florida, USA.
2. M.S. Gagliano, H. Hack, G. S. Stanko, *Update on the Fireside Corrosion Resistance of Proposed Advanced Ultrasupercritical Superheater and Reheater Materials: Laboratory and Field Test Results*", The 34th International Technical Conference on Clean Coal & Fuel Systems, May 31 – June 4, 2009, Clearwater, Florida, USA.
3. *Effect of Iron Sulfide on Furnace Waterwall Corrosion*, EPRI, Palo Alto, CA: 1998. TR111152.
4. *Mitigation of Fireside Corrosion in Low NOx Boilers: A State of the Art Assessment of Materials Solutions,* EPRI, Palo Alto, CA: 1999. TR112823.
5. W. T. Bakker, S. C. Kung, M. Heap, J Valentine, *Waterwall Corrosion in Low NOx Boilers Root Causes and Remedies*, MEGA Symposium, Atlanta, GA, August 1999.
6. *Waterwall Wastage Root Causes: Or How to Predict Wastage Rates from Coal Chemistry,* EPRI, Palo Alto, CA: 2004. TR1004737.
7. *The Effect of Coal Chlorine on Waterwall Wastage in Coal-Fired Boilers with Staged Low NO_x Combustion Systems*, EPRI, Palo Alto, CA; Ameren Corporation, St. Louis, MO; Dairyland Power Cooperative, La Crosse, WI: 2002, TR1004082.
8. W. Nelson and C. Cain, Jr., *Corrosion of Superheaters and Reheaters of Pulverized Coal Fired Boilers,* Transactions of the ASME, Journal of Engineering for Power, July 1960.
9. W. T. Reid, *Formation of Alkali Iron Trisulphates and Other Compounds Causing Corrosion in Boilers and Gas Turbines,* Project Review July 1, 1966, June 30, 1968, prepared by Battelle Memorial Institute, Columbus, OH, June 1968.
10. W. T. Reid, *External Corrosion and Deposits: Boilers and Gas Turbines*, American Elsevier Publishing Company, New York, 1974.
11. G. J. Hills, *Corrosion of Metals by Molten Salts*, Proceedings of the Marchwood Conference: Mechanism of Corrosion by Fuel Impurities, Johnson and Littler, eds., Butterworths, London, 1963.
12. *Superheater Corrosion in Ultra-Supercritical Power Plants: Long-Term Field Exposure at TVA's Gallatin Station*, EPRI, Palo Alto, CA: 1999. TR111239.
13. S. Kihara, K. Nakagawa, A. Ohtomo, H. Aoki, and S. Ando, *Simulating Test Results for Fireside Corrosion of Superheater & Reheater Tubes Operating at Advanced Steam Conditions in Coal-Fired Boilers*, High Temperature Corrosion in Energy Systems, TMS/AIME, M. F. Rothman, ed., 1984, pp. 361-376.
14. *Program of Technology and Innovation State of Knowledge Review of Nanostructured Coatings for Boiler Tube Applications*, EPRI, Palo Alto, CA: 2007. Technical Update 1014805

A
APPENDIX

Macroscopic Appearance of the Pre and Post-Exposed Coupons

FIGURE A-1
Nanocoating Samples Prior to Testing at 455ºC (850ºF) for Waterwall Conditions. The Coupons are Labeled with the Substrate Material Followed by the Coating Designation.

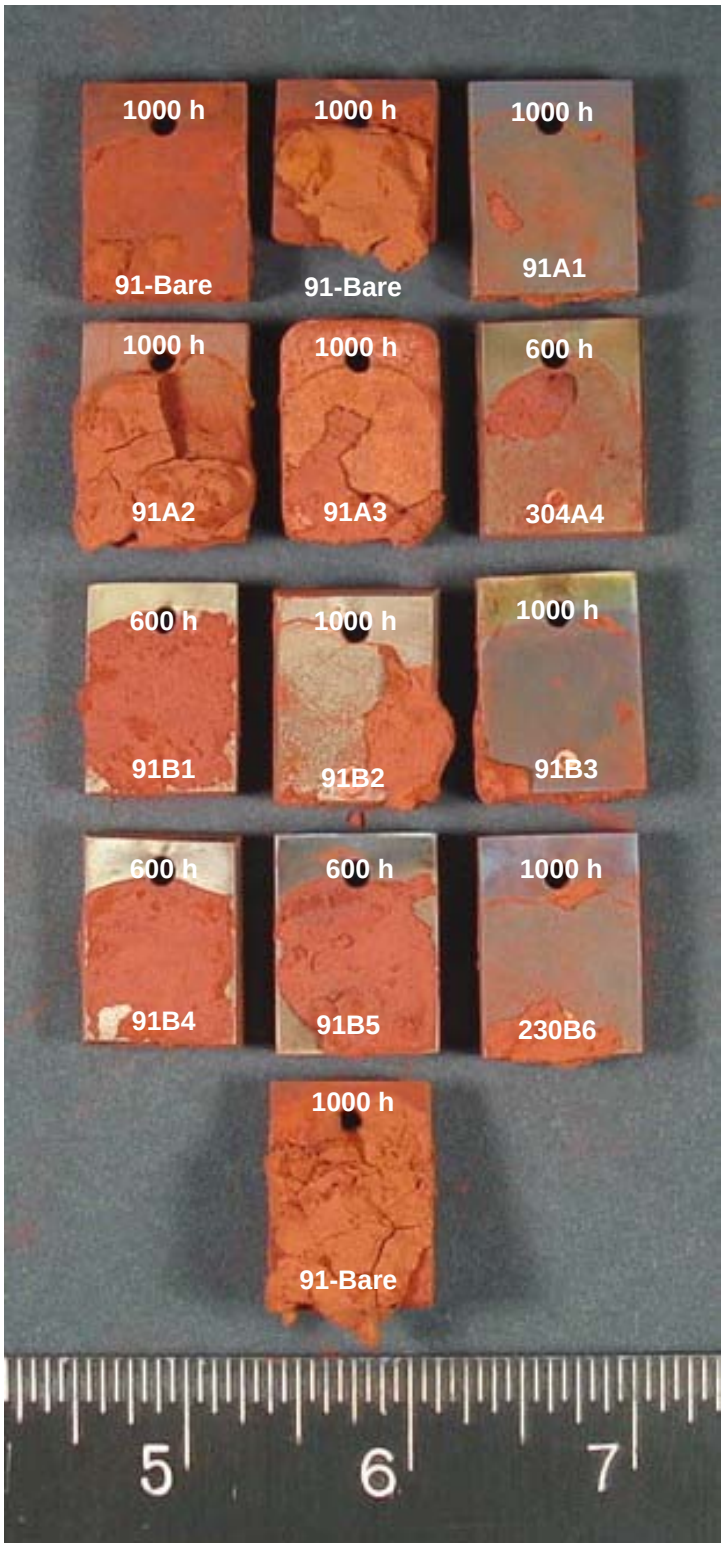

FIGURE A-2
Nanocoating Samples after Testing at 455ºC (850ºF) Under Waterwall Conditions. The Exposure Times are Indicated at the Top of Each Coupon.

FIGURE A-3
Nanocoating Samples Prior to Testing at 525ºC (975ºF) for Waterwall Conditions. The Coupons are Labeled with the Substrate Material Followed by the Coating Designation.

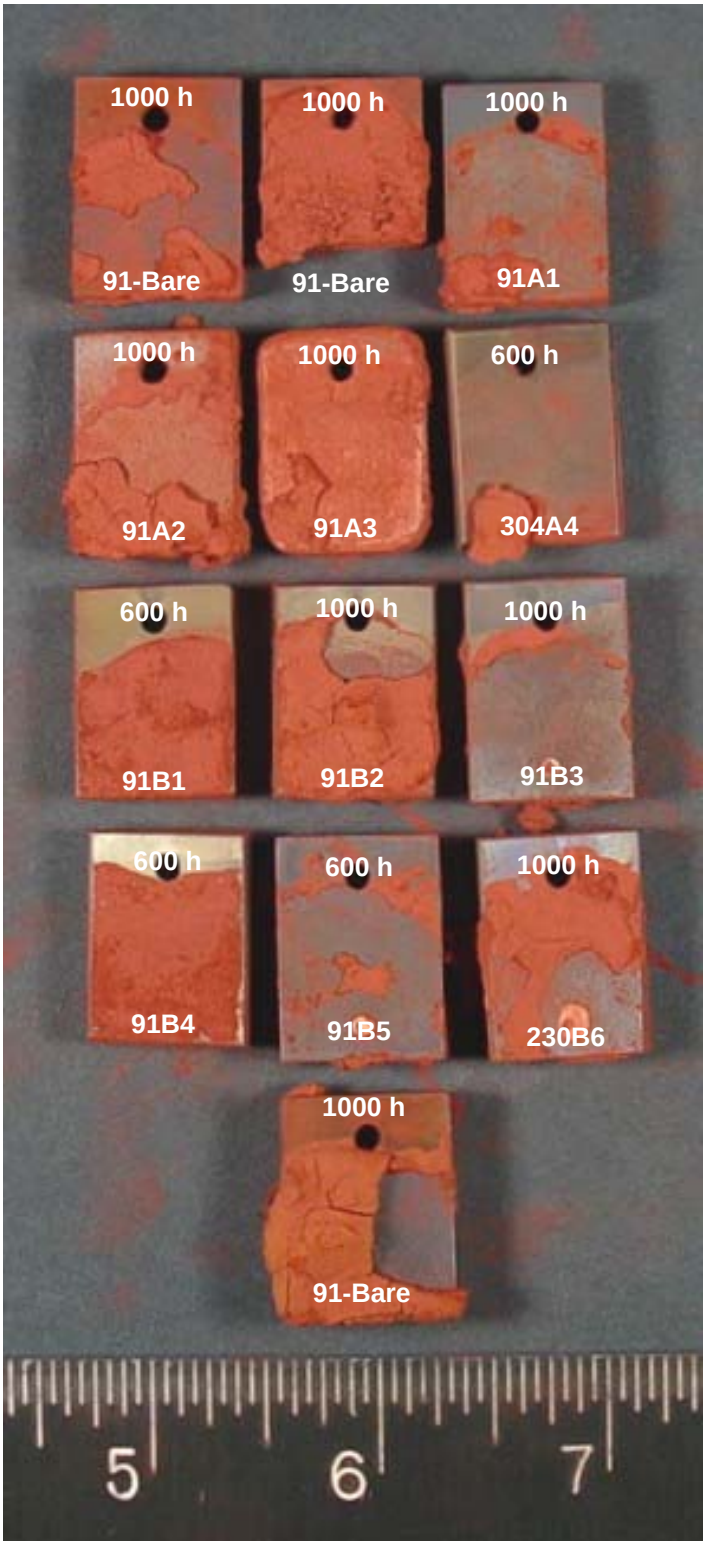

FIGURE A-4
Nanocoating Samples after Testing at 525ºC (975ºF) Under Waterwall Conditions. The Exposure Times are Indicated at the Top of Each Coupon

FIGURE A-5
Nanocoating Samples Prior to Testing at 595ºC (1100ºF) for Waterwall Conditions. The Coupons are Labeled with the Substrate Material Followed by the Coating Designation.

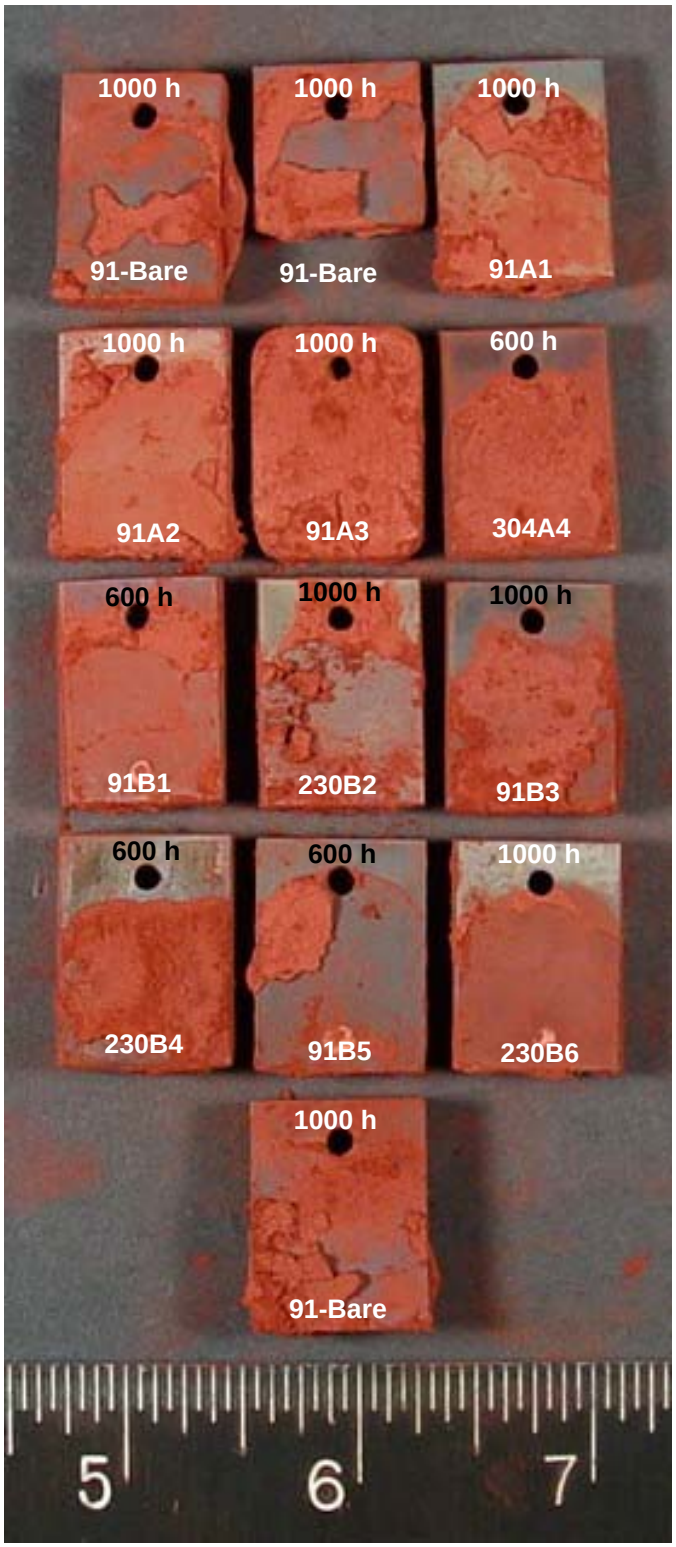

FIGURE A-6
Nanocoating Samples after Testing at 595ºC (1100ºF) Under Waterwall Conditions. The Exposure Times are Indicated at the Top of Each Coupon

FIGURE A-7
Nanocoating Samples Prior to Testing at 595ºC (1100ºF) for Superheater/Reheater Conditions (Board 1). The Coupons are Labeled with the Substrate Material Followed by the Coating Designation.

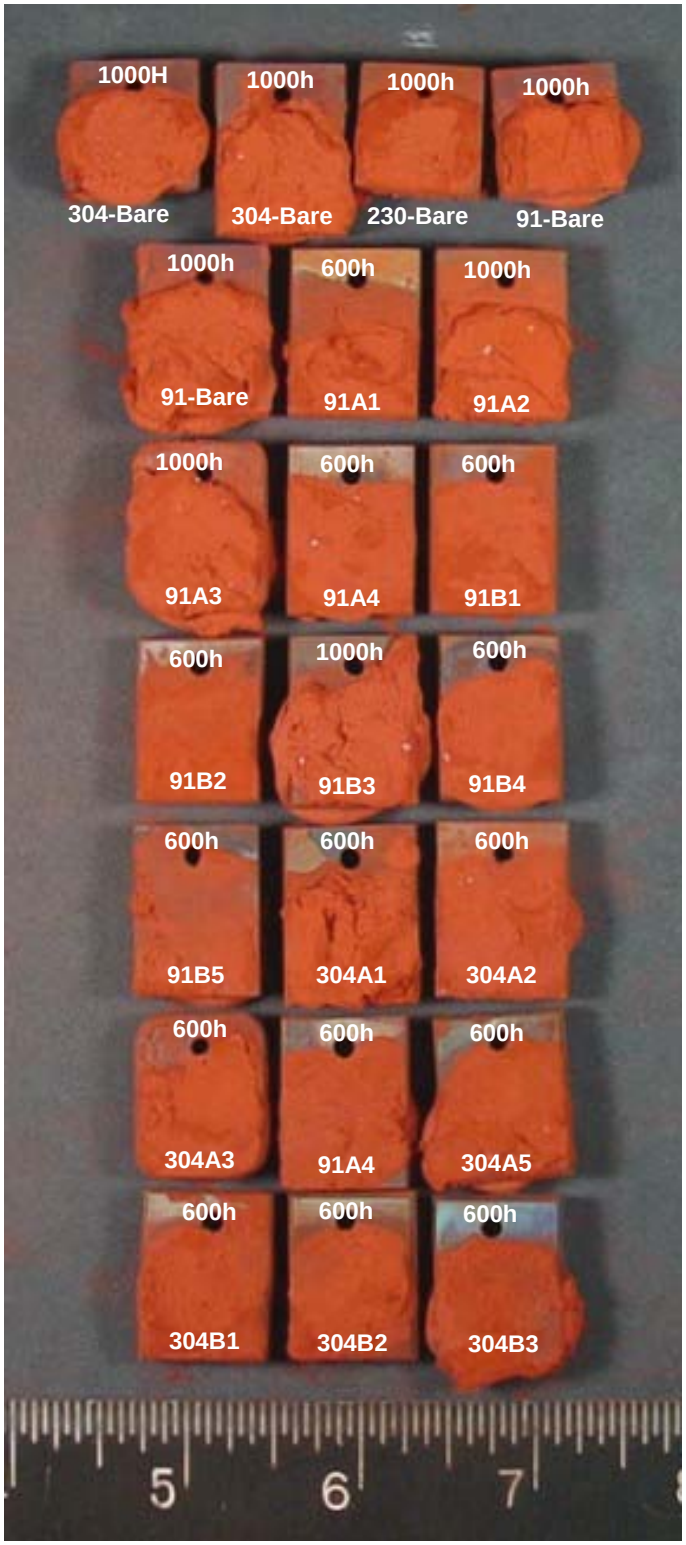

FIGURE A-8
Nanocoating Samples after Testing at 595ºC (1100ºF) for Superheater/Reheater Conditions (Board 1). The Exposure Times are Indicated at the Top of Each Coupon.

FIGURE A-9
Nanocoating Samples Prior to Testing at 595ºC (1100ºF) for Superheater/Reheater Conditions (Board 2). The Coupons are Labeled with the Substrate Material Followed by the Coating Designation

FIGURE A-10
Nanocoating Samples after Testing at 595ºC (1100ºF) for Superheater/Reheater Conditions (Board 2). The Exposure Times are Indicated at the Top of Each Coupon

FIGURE A-11
Nanocoating Samples Prior to Testing at 705ºC (1300ºF) for Superheater/Reheater Conditions (Board 1). The Coupons are Labeled with the Substrate Material Followed by the Coating Designation

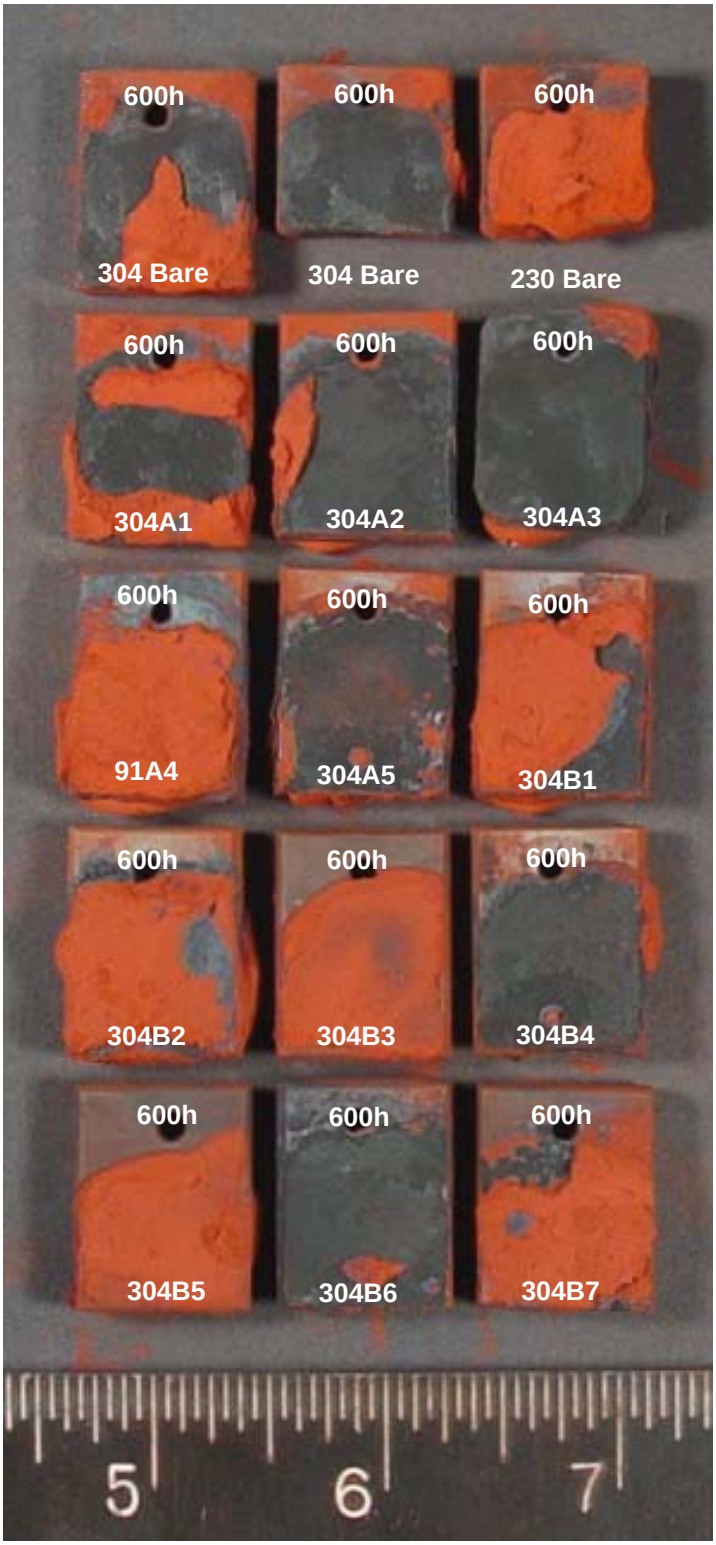

FIGURE A-12
Nanocoating Samples after Testing at 705ºC (1300ºF) for Superheater/Reheater Conditions (Board 1). The Exposure Times are Indicated at the Top of Each Coupon

FI GURE A-13
Nanocoating Samples Prior to Testing at 705ºC (1300ºF) for Superheater/Reheater Conditions (Board 2). The Coupons are Labeled with the Substrate Material Followed by the Coating Designation

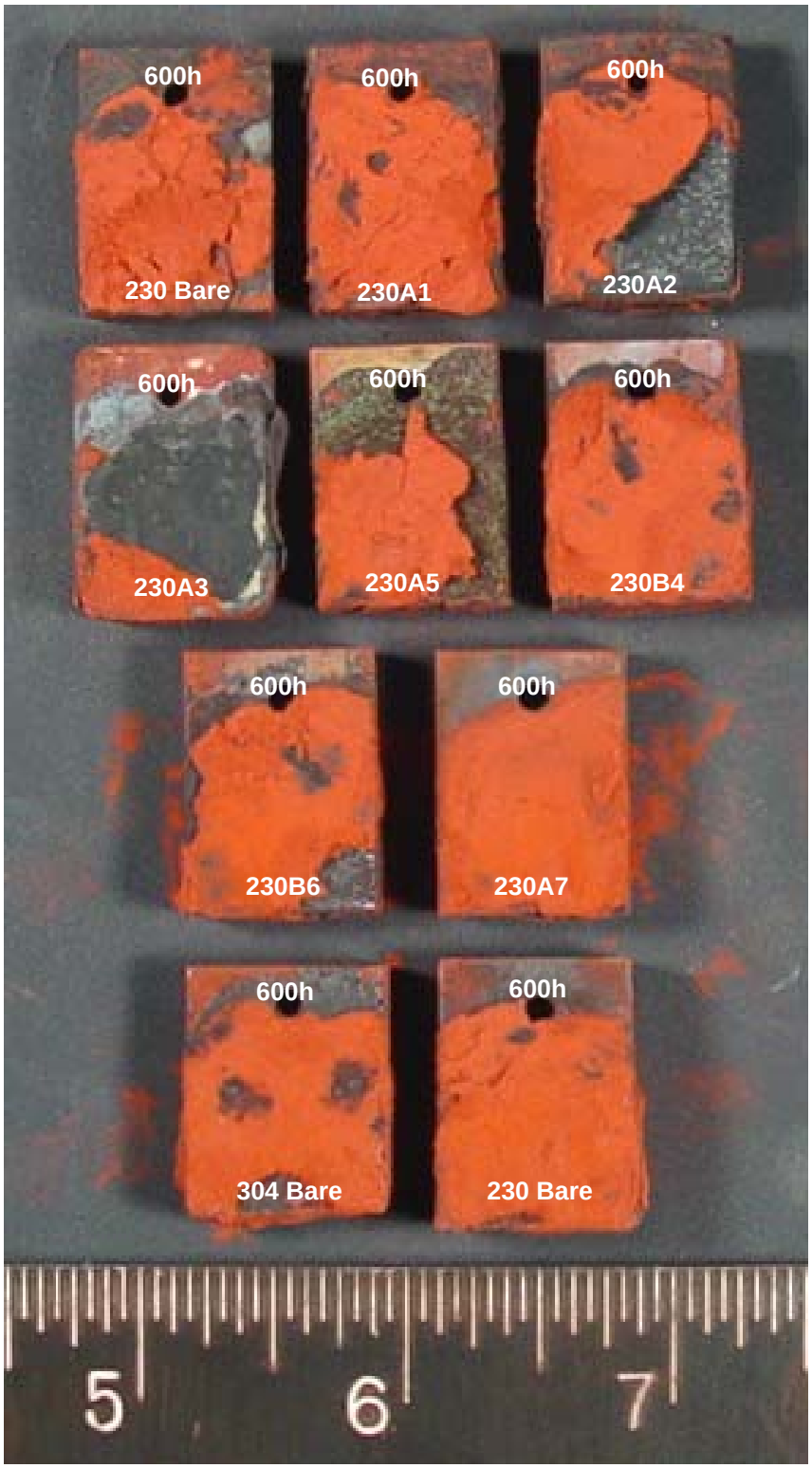

FIGURE A-14
Nanocoating Samples after Testing at 705ºC (1300ºF) for Superheater/Reheater Conditions (Board 2). The Exposure Times are Indicated at the Top of Each Coupon

FIGURE A-15
Nanocoating Samples Prior to Testing at 815ºC (1500ºF) for Superheater/Reheater Conditions (Board 1). The Coupons are Labeled with the Substrate Material Followed by the Coating Designation

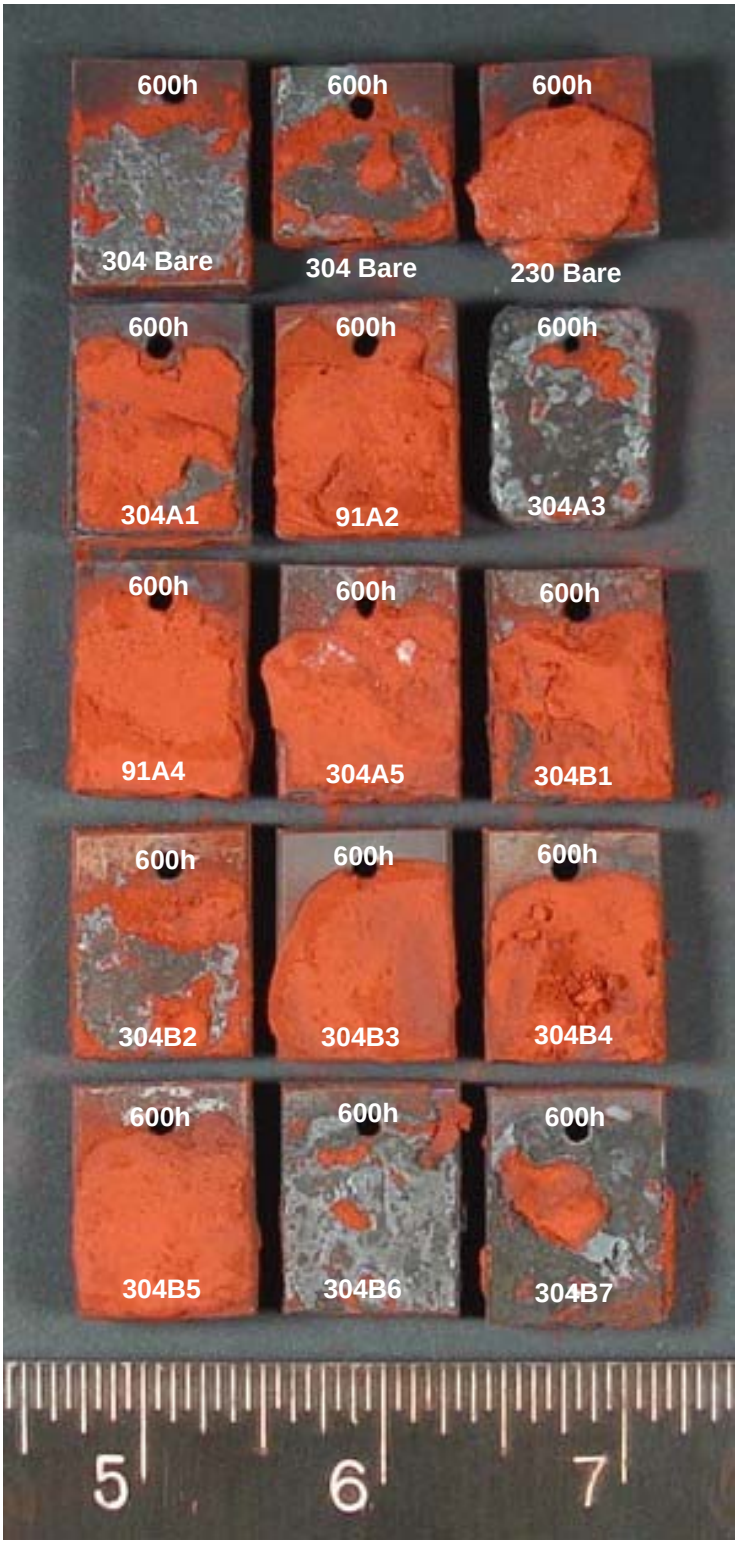

FIGURE A-16
Nanocoating Samples after Testing at 815ºC (1500ºF) for Superheater/Reheater Conditions (Board 1). The Exposure Times are Indicated at the Top of Each Coupon

FIGURE A-17
Nanocoating Samples Prior to Testing at 815ºC (1500ºF) for Superheater/Reheater Conditions (Board 2). The Coupons are Labeled with the Substrate Material Followed by the Coating Designation

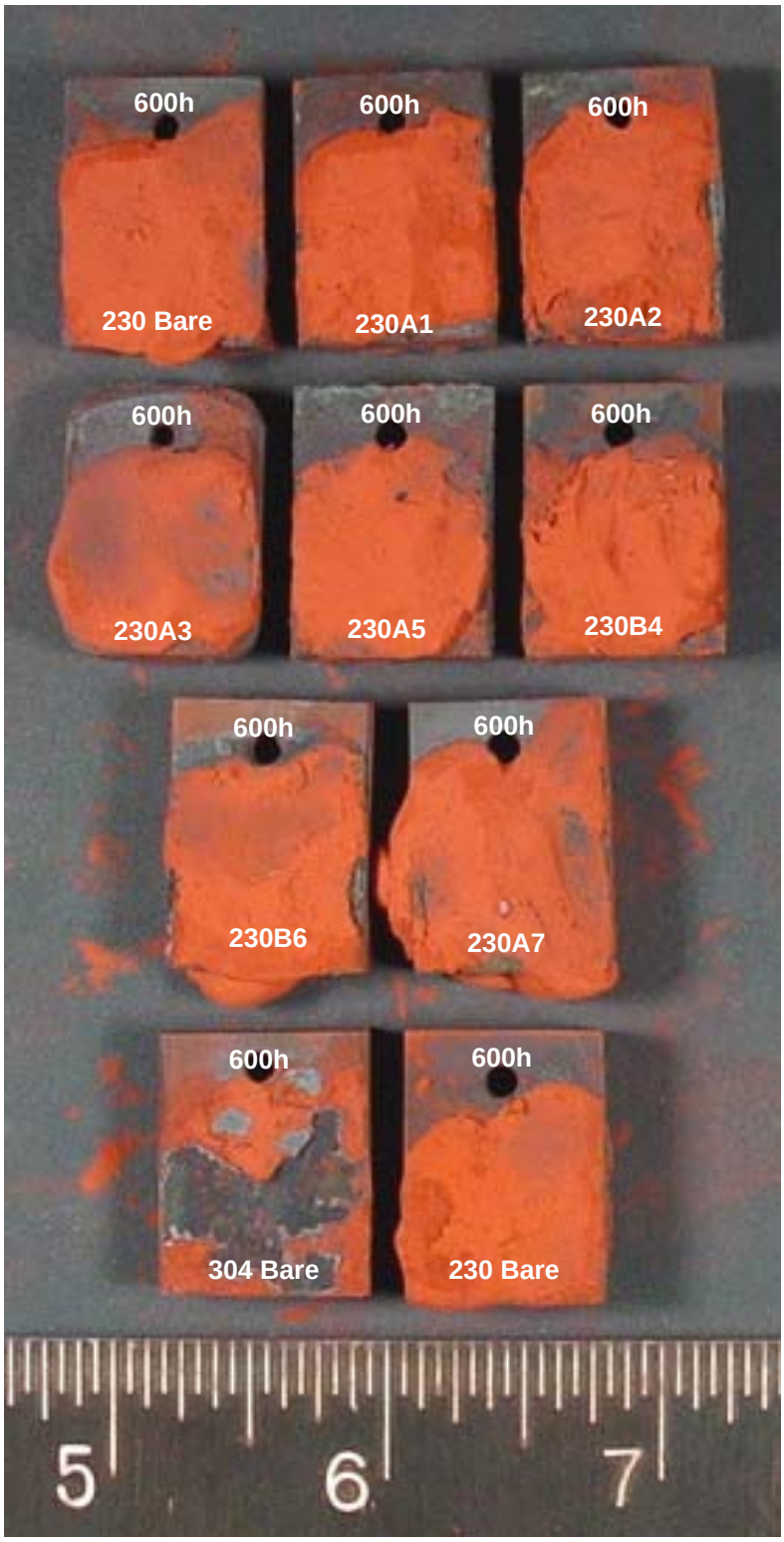

FIGURE A-18
Nanocoating Samples after Testing at 815ºC (1500ºF) for Superheater/Reheater Conditions (Board 2). The Exposure Times are Indicated at the Top of Each Coupon

Electric Power Research Institute
3420 Hillview Avenue, Palo Alto, California 94304-1338 • PO Box 10412, Palo Alto, California 94303-0813 • USA
800.313.3774 • 650.855.2121 • askepri@epri.com • www.epri.com